SUSAK

Environmental reconstruction of a loess island in the Adriatic

Geographical Research Institute
Hungarian Academy of Sciences

SUSAK
ENVIRONMENTAL RECONSTRUCTION OF A LOESS ISLAND
IN THE ADRIATIC

Theory–Methods–Practice

60

GEOGRAPHICAL RESEARCH INSTITUTE
Research Centre for Earth Sciences
Hungarian Academy of Sciences

SUSAK
ENVIRONMENTAL RECONSTRUCTION OF A LOESS ISLAND IN THE ADRIATIC

Edited by

ANDRIJA BOGNAR, FERENC SCHWEITZER and GYULA SZÖŐR

Geographical Research Institute
Research Centre for Earth Sciences
Hungarian Academy of Sciences

Budapest, 2003

Edited by Andrija Bognar, Ferenc Schweitzer and Gyula Szőőr
Revised by György Hahn

English translation: László Bassa, Péter Rózsa, Edina Rudner
Assistant editor: László Bassa
Technical editor: Zoltán Keresztesi
Technical staff: Anikó Kovács, Margit Molnár, István Poór

Desktop editor: Eszter Garai-Édler

Cover design: Anikó Kovács

Cover photo: Aleksander Volarević (Foto Rio • Mali Lošinj)

Supported by National Scientific Research Fund (OTKA) Project No. T 019326

ISBN 963 9545 00 7
ISSN 0139-2875

Published by the Geographical Research Institute HAS
Responsible publisher: Ferenc Schweitzer, director

Printed in Hungary by TIMP Kft.

CONTENTS

INTRODUCTION

This book contains the achievements of the investigations carried out in the framework of a research project launched in 1997 and supported by the Hungarian Academy of Sciences (HAS) and Hungarian National Science Fund (OTKA). The project entitled 'Reconstruction of past changes in global climate and environments through the correlative analysis of type localities of loess in the Mediterranean (Susak Island) and in the Carpathian basins (Paks)' yielded achievements of international interest.

In the work both Hungarian specialists – Gy. SZÖŐR (University of Debrecen), P. SÜMEGI (University of Szeged), E. HERTELENDI (ATOMKI, Debrecen), J. BALOGH, M. di GLERIA, É. KIS, E.Z. RUDNER, F. SCHWEITZER (Geographical Research Institute HAS, Budapest), RINGER, Á. (University of Miskolc) and foreign experts – A. BOGNAR (Zagreb), K. TARNOCAI (Canada) became involved.

The research project has been aimed at an overview of paleoecological and paleogeomorphological transformation in the Carpathian Basin and its southern surroundings as a result of climatic change during the Pliocene and Pleistocene epochs. The research primarily focused on those events in the physical environment, which

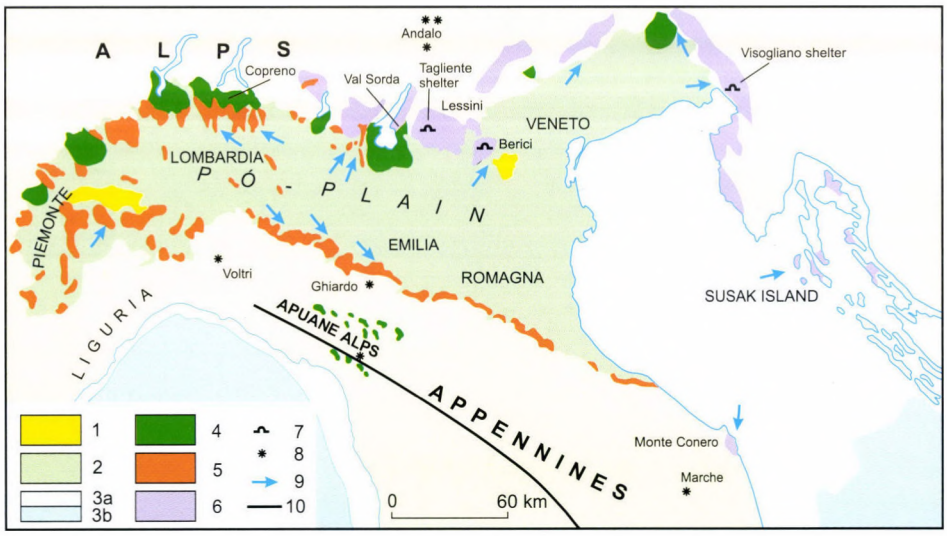

Fig. 1. The distribution of loess deposits in Northern Italy (CREMASCHI, M. 1987b modified by CREMASCHI, M. 1991). – 1 = Pre-Quaternary rocks; 2 = Late Pleistocene and Holocene alluvial plain; 3 = present day sea extent: a<100 m; b>100 m; 4 = Pre-Alpine and Appennine moraine system; 5 = loess deposits on fluviatile, fluvioglacial terraces and moraine ridges; 6 = loess deposits on karstic plateaus; 7 = loess in caves or shelters; 8 = loess on erosional surfaces; 9 = directions of dominant winds during loess sedimentation; 10 = possible south–west boundary of loess sedimentation during Upper Pleistocene

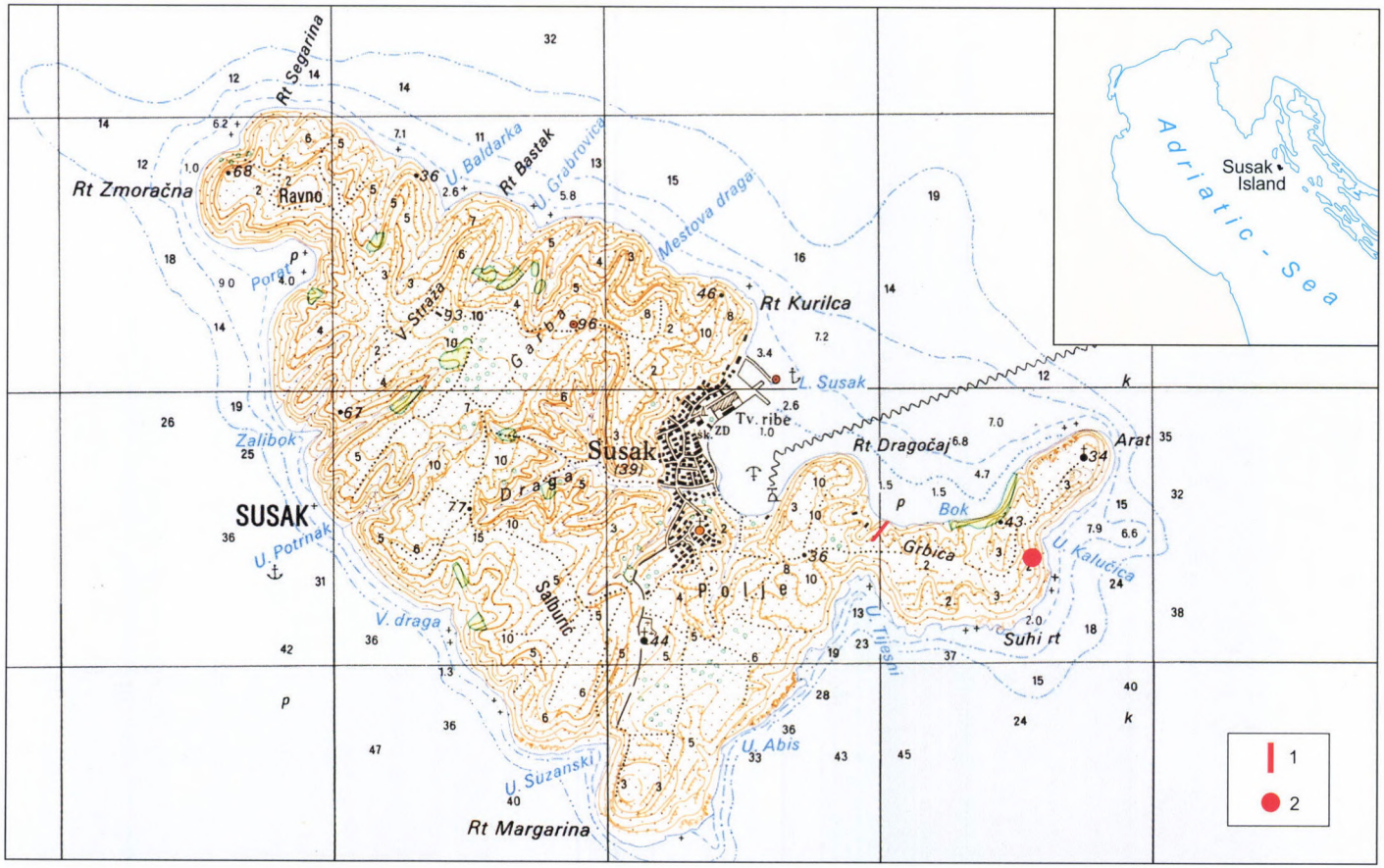

Fig. 2. Geographical setting and topographic map of Susak Island. – 1 = Position of Susak 1997 profile; 2 = Traces of Paleolithic fireplace

Photo 1. A panoramic view of Susak Island (Photo by É. Kis)

controlled geomorphic evolution leading to the emergence of landforms and sediments over the time period in concern.

One of the fundamental tasks of geomorphological research in the region of the Alps and in the Carpathian Basin is clearing up Pliocene landform evolution and the time scales involved. The Quaternary sequence of the Alps and of the Po Plain were studied by M. CREMASCHI (1987/b) in detail. He has dealt with loess-like sediments of the Mediterranean; their distribution and types were identified in a map (*Fig. 1*). The author classified genetically the sediments on Susak Island (*Fig. 2, Photo 1*) studied by our team in detail into the category of loesses developed on karst plateaus and their deposition he put in late Pleistocene. He draws attention to the variability of Quaternary formations on Susak: apart from loess pockets of eolian origin fossil sand dunes and terraces of marine abrasion could be traced, based on previous investigations.

Results of complex mineralogical, lithological, geochemical, geological and geomorphological analyses were published by A. BOGNAR (1979), BOGNAR, A. *et al.* (1989), further by A. BOGNAR and L. ZÁMBÓ (1992), A. BOGNAR *et al.* (2002), according to which the most important stratigraphical features are the followings.

– Red clay as infillings in cracks of Cretaceous limestone of so called rudist facies could have formed in Csarnótan (4 to 3 million years BP); it should be considered the weathering product of subtropical karstification. Reddish clay covering this

rudist facies (with a marked reversal in paleomagnetism) might have formed in Villanyian–Villafranchian (3 to 1.8 million years BP).

– Formation of various sandy silts, sandy loesses and sands overlying red clays reaches back to the second half of Middle Pleistocene and Late Pleistocene, when several phases of sedimentation can be traced. These deposits bear character of flood plains and/or alluvial cones. Typical loess is completely missing from the island.

– Based on the occurrence of paleosols and semipedolites superimposing red clays three humid-warm intervals can be identified, while the occurrence of loessy sand, sandy loess and wind-blown sand refers to drier and warmer climatic phases.

– Micromineralogical studies revealed a similarity between the heavy metal spectrum of the sediments overlying red clays on Susak and that of Middle and Upper Pleistocene fluvial and fluvioglacial sequences of the Po Plain, which suggests a common source of origin.

– It should be stated that only pilot studies were carried out concerning carbonate and clay mineral paragenesis of sediments. As far as their carbonate content is concerned, deposits on Susak Island and in the Po Plain differ between one another.

1. GEOCHRONOLOGICAL OVERVIEW

1.1. Origin and description of the samples

Bay of Bok was designated as the place of the establishment of profiles and sampling for subsequent analyses (*Fig. 2, Photo 2*).

Exposures including a complete sequence of loess and loess-like sediments overlying reddish clays (SAV) were cut with soil steps, followed by a general description of the profile and collection of samples (*Photos 3 and 4*).

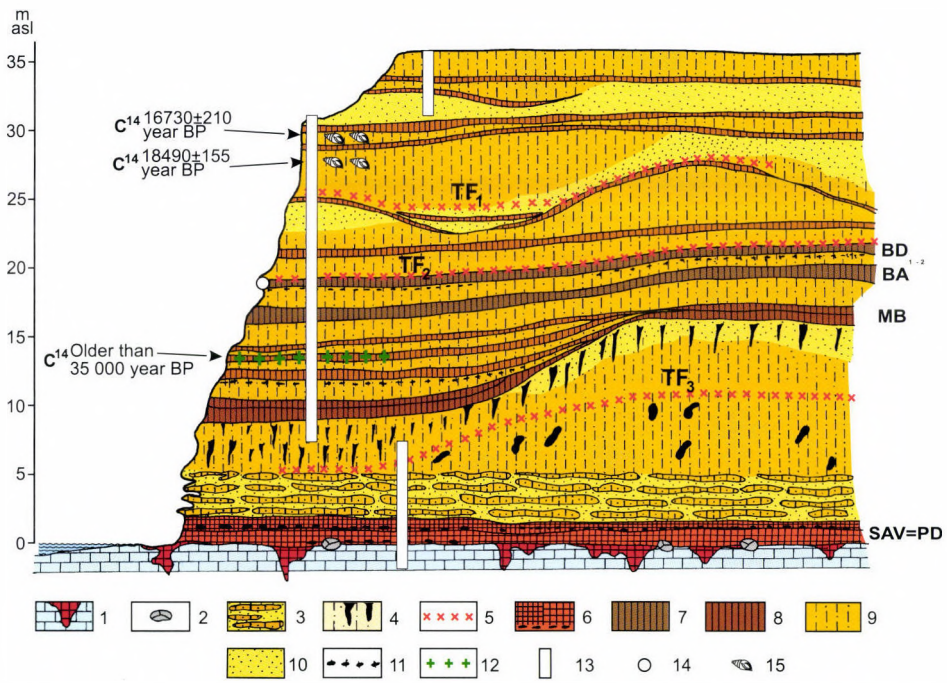

Fig. 3. A geomorphological cross-section of Susak (Compiled by SCHWEITZER, F. 2000). – 1 = Mesozoic (rudist) limestone, with infillings of typical red clay in the karstic depressions (*Photo 6*); 2 = ventifact (*Photo 10*); 3 = sandstone bench; 4 = old loess with loess dolls; 5 = tephra horizons (TF_1, TF_2, TF_3); 6 = reddish clays with horizons of $CaCO_3$ accumulation; 7 = chernozem paleosols; 8 = reddish brown forest soil; 9 = sandy loess; 10 = sand; 11 = charcoal horizon; 12 = charcoal horizon with ^{14}C dating; 13 = sampling sites along the Susak 1997 profile; 14 = Paleolithic artefact finds; 15 = ^{14}C datings of Mollusc fauna

Photo 2. Bay of Bok at Susak Island (Photo by É. Kis)

Photo 3. Upper part of the loess exposure with Bay of Bok in the background (Photo by F. Schweitzer)

Photo 4. Lower part of the loess exposure at Susak (Photo by É. Kis)

Field works and laboratory analyses permitted to compile a geomorphological cross-section (*Fig. 3*) also making possible identification of the set of samples using data of depth from the sea level. A generalised profile Susak 1997 is shown on *Fig. 4.*

1.2. Chronological issues

The Pliocene spans a time interval with duration of 2.5–3 million years; during this period a 200–700 m thick sequence of series was deposited in the innermost

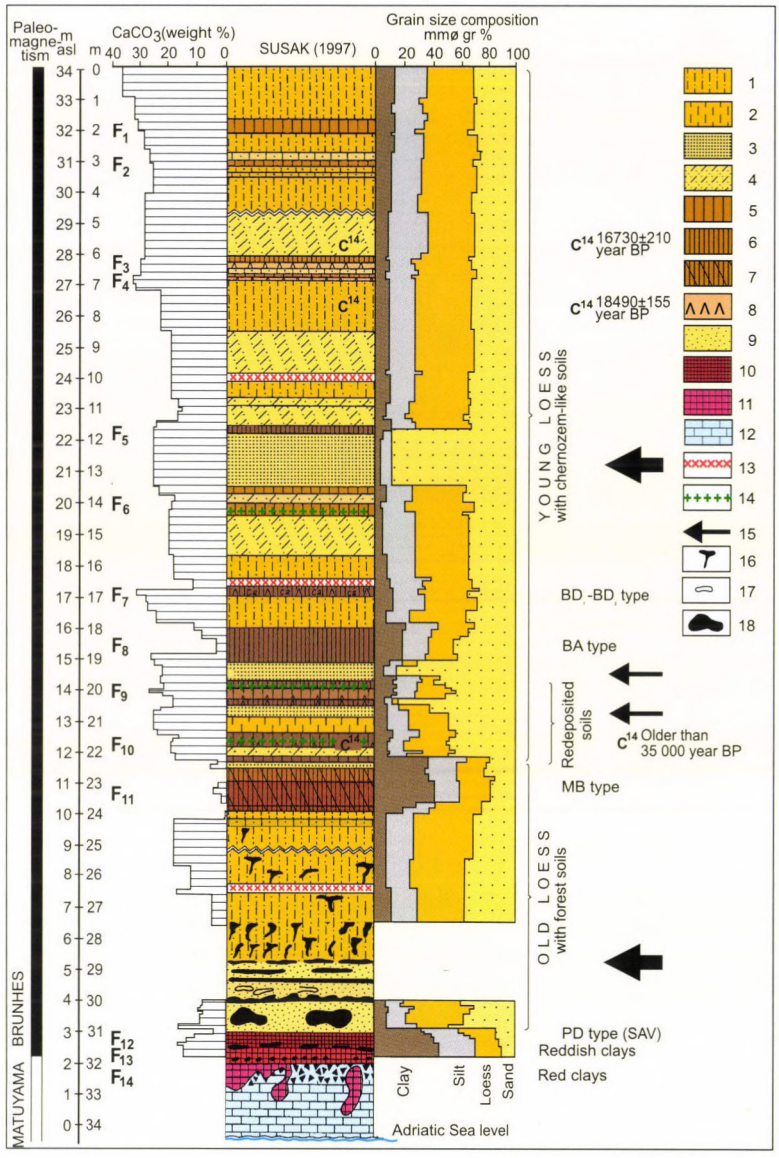

Fig. 4. The generalised Susak (1997) profile with carbonate content and grain size distribution (SCHWEITZER, F., BOGNAR, A., SZÖÖR, GY., KIS, É., BALOGH, J., DI GLERIA M., 1997.). – 1 = sandy loess; 2 = unstratified loess; 3 = sand; 4 = loessy sand; 5 = slightly humified horizon; 6 = chernozem paleosols; 7 = reddish brown forest soil (MB); 8 = horizon of calcium carbonate accumulation; 9 = fine-grained loessy sand formed on sandstone bench; 10 = reddish clay ; 11 = red clay; 12 = rudist limestone 13 = tephra horizon; 14 = charcoal horizon; 15 = erosional hiatus; 16 =loess doll; 17 = rhyzolith; 18 = sandstone bench

Table 1. Correlation of the Central and Eastern paratethys (KRETZOI, M. 1987)

Approximate age (m yr)	Mediterranean biochronology			European terrestrial biochronology[2]								Central Paratethys	
	Codes					MN Zone-Codes						Lithostratigraphy	
												Carpathian Basin	
	Foraminifer zones	Nannoplankton zones	Stage[1]	Group	Age / Stage*	POMEL 1853	GANDRY 1878	CRUSAFONT 1971	C-F-F 1972	CRUSAFONT 1974	MEIN 1975	KM[3]	RB[4]
5		NN-13	(Tabianium-Zancleum)	Barótium	Ruscinium		14	22	11	23	MN 14	Danubian	Transdanubian
	N-18	MN-12	Messinium	Battaváriu*(=Turolium etc.)	Bérbaltaváriu*						MN 13		
6					Hatvanium*								
7	N-17		Tortonium (s. Str.)				13	21	10		NN 12		
8		MN-11			Sümegium	6				22		Pannonian	
9	N-16				Csákvárium						MN 11		
10		MN-10		Eppelcheimium* (=Vallesium)	Rhenohassium*		12	20b	9	21b	NN 10		Premartonian
11	N-15	NN-9	Serravallium		Bodvaium*			20a		21a	MN 9		
12	N-14				Monacium*								
13	N-13	NN-8			(Oeningium)*	5	11	19b	8	20b	MN 8	(Mediter-ranean)	(Sarma-tian)

[1] Traditional, so called mixed (bio-litho) taxa; [2] Biochronological units; of them* with lithostratigraphic significance as well; [3] Author's proposal (KRETZOI, M. 1979). [4] Recommendation of the Pliocene Subcommission of Hungarian Commission on Stratigraphy

areas of the Carpathian Basin. At the same time the basin margins and less peripheral areas became covered by terrestrial sediments of 10–250 m thickness (constituting formations such as the so called Gödöllő sand, red clays, travertines of considerable thickness, the oldest terraces etc.).

One of the sediments formed in the Pliocene is a terrestrial sequence figuring in the literature as the Levantan stage. Its further subdivision (Piacenzan, Astian), however, was carried out using data from the Mediterranean. Perhaps this is the reason why *Pliocene sediments from the Carpathian Basin cannot be correlated completely with the originally described Levantan sediments and levels.*

That is why the denomination 'Levantan' has been abandoned recently and this interval initially became called Upper Pliocene (with the Miocene–Pliocene boundary placed between the Sarmatian and Pannonian stages), later it was simply referred to as *Pliocene stage* (with the *Miocene–Pliocene boundary drawn at 5.5 million yr BP*).

These figures point to highly *diverse* and controversial *concepts* on landform evolution during the Pliocene. Formation of sediments and landforms belonging to various stages was assigned to this epoch by the different authors.

In the Hungarian stratigraphical practice the *lower and upper boundaries of Pliocene vary, therefore it is necessary to specify in what a sense they will be used below.*

The *lower boundary* is drawn, in accordance with the international recommendations, between the Messinian and Zanclean at *5.3 million yr*, which corresponds to the limit between zones MN 13 and MN 14 in the mammal scale by Mein (*Table 1.*).

This was the time of a considerable drop of the level of the Pannonian brackish inland sea considered to be a remnant of the Paratethys.

This in turn can be correlated with the lowering level of the Mediterranean Sea during the Messinian (6.8–5.3 million yr) with the formation of evaporites in that basin ('Messinian Salinity Crisis').

The triggers of this intense evaporite formation have not been cleared yet. At that time there was a change in faunal succession and ecosystems in the Carpathian Basin. Pannonian inland sea had dried out; warm-dry and hot-dry climatic conditions prevailed evidenced by desert pan and varnish.

The upper boundary of the Pliocene does not coincide with the internationally accepted 1.8 million yr BP.

In the present paper the boundary between the Matuyama and Gauss paleomagnetic epochs, i.e. ca *2.4 million yr is adopted* as the Pliocene/Pleistocene boundary–in accordance with the recommendation of the Hungarian Commission on Stratigraphy from 1988.

The middle phase of Pliocene in the Carpathian Basin was characterised by a warm-humid climate between 4 and 3 million yr BP (Csarnotan), in some places with south and southeast Asian faunal elements. This environment changed into a grassy steppe ecotype between 3 and 1.7 million yr BP (Villanyian).

In the present publication Pliocene is subdivided into three time intervals. MN zones are taken for the basis with a tripartite Pliocene with lower (MN 14), middle (MN 15) and upper (MN 16) sections.

Table 2. Fauna of the classic site Polgárdi (N2) evidencig to the regression the Pannonian Lake (Kormos, T. 1911, Kretzoi M. 1952, Kordos, L. 1993), at least in this region of the Transdanubium. According to Kordos (1993) vertebrate fauna at Polgárdi can be correlated with vertebrate fossils found in terrestrial deposits at Crevillente N6 site (Spain) where Messinian marine and terrestrial sediments are intercalated

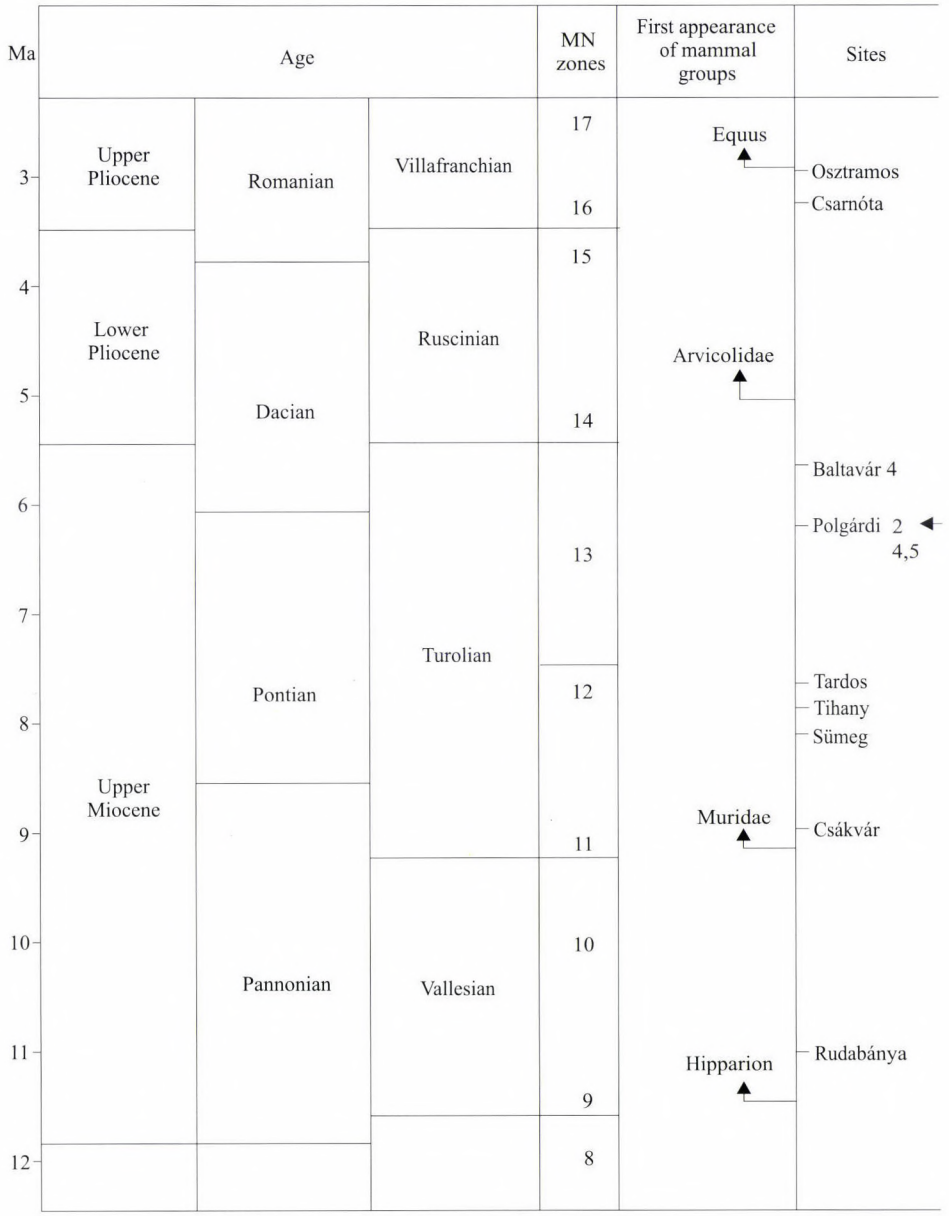

1.3. Pliocene events

1.3.1. Lower Pliocene; possibilities for the correlation of Bérbaltavarian with Messinian

The end of Upper Miocene and the advent of Lower Pliocene were marked by the end of Messinian Salinity Crisis which culminated in an almost total desiccation of the Mediterranean Sea (RÖGL, E.–STEININGER, F. 1978).

In the area what is now the Carpathian Basin it was the era when the Pannonian inland sea was filling up gradually, indicated by carbonate evaporites, sand formations and desert varnish (SCHWEITZER, F. 1993, SCHWEITZER, F.–SZÖŐR, GY. 1993).

The expansion of mainland in the Carpathian Basin toward the end of Pannonian is also supported by borehole and geophysical data (POGÁCSÁS, GY. *et al.* 1989), sand sequences locally reaching 100–200 m (e.g. Gödöllő sand) and indicated by pediment formation as geomorphic features (PÉCSI, M. 1969, SCHWEITZER, F. 1993).

Pedimentation was an active factor in landform evolution during dry and warm periods in the foreland of Hungarian Mountains; pediment surfaces formed along the Dalmatian shore of the Adriatic (e.g. Velebit Mountains), starting with Sümegium and lasted until Ruscinium–Csarnótánum, when it was succeeded by red clay formation. For the latter Bérbaltavarian was an essential phase (*Table 2.*).

1.3.2. Geomorphological position and age of typical red clays and reddish clays

Typical red clays and reddish clays have a high relevance for the identification of paleogeographic periods and phases of tectonic movements. However, no adequate attention has been paid so far to the main interval of their formation.

There is a controversy about the age and formation of red clays proper, which are younger than Upper Miocene formation (previously referred as Upper Pannonian) and superimpose them. They were put in the Pliocene (KRETZOI, M.–PÉCSI, M. 1982; PÉCSI, M. 1985; De BRUIJN, H. 1984; LIU, T.–AN, Z. 1982) or in early Pleistocene (HALMAI, J.–JÁMBOR, Á. *et al.* 1982). Based on the recent geomorphological investigations and sedimentological and paleomagnetic analyses of deep boreholes it can be stated that the appearance of typical red clays is confined to the time interval following pediment formation in the late Miocene (Pontian) and early Pliocene. The oldest generation of red clays can be found on foothills of Bérbaltavarian age situated in a higher position than the Pleistocene terraces, in karstic dolines or on abrasional terraces. In certain partial basins of the Great Hungarian Plain however (e.g. in the Vésztő and Dévaványa boreholes in the Körös Basin) several red clay horizons occur at a depth of 800–1100 m (RÓNAI, A. 1983); they evidence to their character as sediment traps.

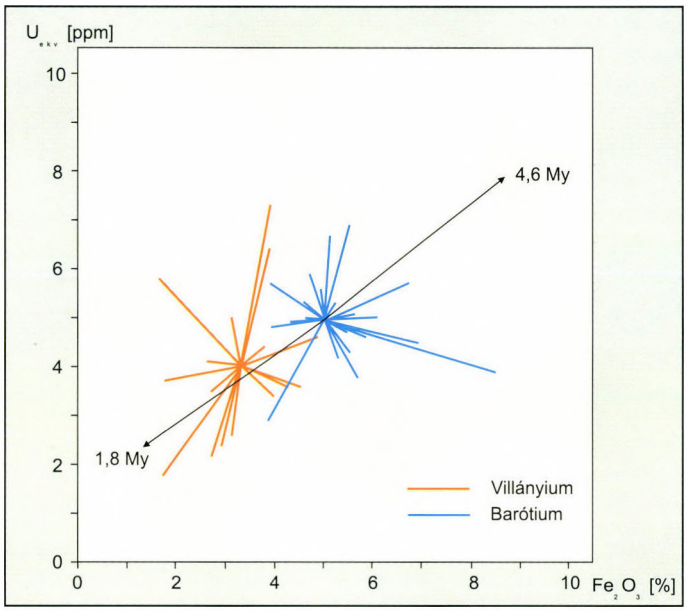

Fig. 5. Chemostratigraphic characteristics of Villányium with changing content of uranium, thorium (U_{ekv}) and ferric oxide. (SCHWEITZER, F., SZŐR, GY., 1993).

1.3.2.1. Typical red clays

Typical red clays (based on an analogy with Csarnóta–2 site) are chemostratigraphic markers of the Pliocene (Ruscinium and Csarnótánum), while fossil reddish clay (terra rossa), sediments and lime tuffs (based on the sample from the Villány–3 type locality) are markers of the lower Pleistocene (Villanyian). Their distinct mineral paragenesis is an indication of varied climatic conditions. The product of weathering under warm (subtropical) and humid climate is kaolinite–halloysite, whereas moderately warm, humid and arid climates had resulted in formation of illite–montmorillonite and various carbonate paragenesis. These two sediments of distinct type might be separated along several geochemical parameters. A good example is the total amount of uranium and thorium (U_{ekv}) and changes in the rate of ferric oxide (Fe_2O_3) (*Fig. 5*). This regularity can be associated with weathering and solution processes influencing mineral paragenesis.

The age of typical red clays – apart from some exceptions – cannot be identified exactly by radiometric and paleomagnetic measurements for the time being. Nevertheless, an indirect correlation with paleontological finds seems to be possible. Based on faunistic evidence provided by M. KRETZOI (1969), D. JÁNOSSY (1972),

L. KORDOS (1988), H. De BRUIJN (1984) and especially on fossils of the European Pliocene *Spalax* (*Micro spalax*), it is considered probable by L. KORDOS (1992) that material of red clay site Csarnóta I (*Photo 5*) and that of red clay site Maritsa I formed between 3 and 4 million yr BP, while red clay containing Odessa *Spalax* is somewhat older (ca. 4 m yr, PEVZNER, M.A., *ex verbis* 1989). (In China red clay formation span the period between 5–2.4 million yr BP.) Red clays found on Susak Island in cavities of karstified Mesozoic limestone are supposed to be of the same age (*Photo 6*).

The occurrence of warm periods necessary for the formation of red clays are corroborated by paleoclimatic reconstructions by Zs. KOPPÁNY (1997) covering the time interval between 4 and 2 million yr BP. It is well known that a decisive factor in fluctuations of global climate is the variation of solar irradiation as a result of secular oscillations of the Earth orbit.

Based on values of total insolation obtained through calculations the following phases could be identified during the 2 million years in concern:

$2.00\ 10^6 - 2.16\ 10^6$ yr WARM
$2.16\ 10^6 - 2.26\ 10^6$ yr COLD
$2.26\ 10^6 - 2.50\ 10^6$ yr WARM
$2.50\ 10^6 - 2.66\ 10^6$ yr COLD
$2.66\ 10^6 - 2.90\ 10^6$ yr WARM
$2.90\ 10^6 - 3.04\ 10^6$ yr COLD
$3.04\ 10^6 - 3.14\ 10^6$ yr WARM
$3.14\ 10^6 - 3.17\ 10^6$ yr COLD
$3.17\ 10^6 - 3.51\ 10^6$ yr WARM
$3.51\ 10^6 - 3.61\ 10^6$ yr COLD
$3.61\ 10^6 - 3.96\ 10^6$ yr WARM

Such an exact delimitation of boundaries is purely theoretical and it serves only for fixing the dominant climate type during the studied period.

Between 3 and 2 m yr BP:
WARM ca 640 thousand yr;
COLD ca 360 thousand yr;

Between 4 and 3 m yr BP:
WARM ca 790 thousand yr;
COLD ca 210 thousand yr;

Over the two periods combined (ca 2 million yr):
WARM ca 1430 thousand yr (72%);
COLD ca 570 thousand yr (28%).

Photo 5. Type locality of Csarnotan fossil fauna in south Hungary (Photo by F. SCHWEITZER)

Photo 6. Infillings of typical red clay in karstic depressions of Mesozoic limestone on Susak (Photo by F. SCHWEITZER)

These results corroborate information gained from other (paleontological, paleobotanic, sedimentological, geological and geomorphological) sources that this interval of 2 million yr duration was predominantly warm but, due to possible miscalculations nothing else can be concluded.

1.3.2.2. Reddish clays

The other group of formations is highly varied genetically. Fossil soils and pedosediments of purplish and reddish colour, and silty clays and clayey silts of pink tint are classified here. Reddish clays are as a rule intercalated in old loesses. None of them is typical red clay; rather they are steppe soils formed under warm and dry or subhumid climates. They have a lower plasticity than red clays proper and a higher carbonate content (between 10 and 70 %), frequently with carbonate veins and grains. Samples are characterised with clay mineral of illite–montmorillonite (smectite) type and the carbonate association is highly varied: calcite, dolomite calcite (magnesite calcite) and dolomite occur. In the samples quartzite reoccurs frequently.

Formation of reddish clays is put to the Villanyian, Villafranchian, sometimes to Calabrian; they represent lower or the lowermost Pleistocene (*Photos 7 and 8*). They might have formed between 3 and 1.7 million yr BP.

1.3.2.3. Ventifacts polished by wind

These gravels are frequently encountered in the central part of the Carpathian Basin. They occur in alluvial fans and in clastic sediments. Along with its transportation function, polishing and scouring are also typical of wind action. In areas with frequent sand storms even the hardest rocks are being worn down. Desert and semidesert landforms bear traces of this process and this is the case with Susak Island as well. Here surfaces with ventifact occurrences in sediments transported by torrents and cemented by calcium carbonate are overlain by reddish clays (*Photos 9 and 10*). In the Carpathian Basin they can be found both in older alluvial fans and debris and on younger (mainly Pleistocene) terrace surfaces.

1.4. The problem of Tertiary/Quaternary boundary and of other possible boundaries

As far as the Neogene/Quaternary boundary is concerned, experts on late Neogene and Quaternary have always been strongly divided. According to the recommendations of the International Geological Congress (London, 1948) the Pliocene/Pleistocene boundary should be drawn at the bottom of the Calabrian layers where

Photo 7. Displacements along faults in Mesozoic (rudist) limestone with thermal spring occurrences (Photo by F. SCHWEITZER)

Photo 8. Crater of a thermal spring breaking through rudist limestone occurring in several places on Susak (Photo by F. SCHWEITZER)

Photo 9. 10–30 cm thick debris cemented by carbonate on the surface of Mesozoic limestone and covered by reddish clay with ventifact occurrences, on Susak (Photo by É. Kis)

Photo 10. Ventifacts embedded in reddish clay on Susak (Photo by F. Schweitzer)

Photo 11. 0.5–1 m wide fissures formed as a result of tectonic displacement filled with minutely broken limestone and reddish clay on Susak (Photo by F. SCHWEITZER)

Photo 12. Reddish clay filling up tectonic fissures in Villányi Mountains (Hungary) and containing Villanyian fossil fauna (Photo by F. SCHWEITZER)

cold tolerant foraminifers appear in marine sediments. Later these layers were dated ca 2 million yr BP by ARIAS, C. *et al.* (1980) with paleomagnetic analyses.

Earlier the Neogene/Quaternary boundary was drawn at 600 thousand yr BP based on the climatic calendar by MILANKOVIĆ, M. (1930) and BACSÁK, Gy (1942)* and on the Alpine glaciation stages by Penck and Bruckner and coincided with the first significant glacial as the advent of the Ice Age proper. However, through the study of the Günz glacial several previous stages (such as Donau /Eburon/, Biber / Praeteigelen) were traced, consequently the duration of the Pleistocene was extended (initially back to 1.8 million, then by some to 2.4 and even to 3 million yr BP).

This extension of the Quaternary was corroborated by the tendency to correlate the appearance of Early Man with the advent of this epoch. The sites at Olduvai are 1.7–1.8 million yr old and the age of Coobi Forai (sites on the eastern shore of Lake Turkana) is 2.2–2.0 million yr BP.

The arid and warm steppe fauna of the Villafranchian (3.0–2.5 million yr) had deteriorated (KORDOS, L. 1992, JÁNOSSY, D. 1979, KRETZOI, M. 1954, 1969) then disappeared and between 2.4 and 2.0 million yr a new faunistic event followed with an enrichment of fauna.

Probably this event starting from 2.4 million yr could be an adequate boundary between the Pliocene and Pleistocene in the Carpathian Basin. According to RÓNAI, A. (1972, 1985) the borehole sediments in the Great Hungarian Plain evidence to a climatic change that had a general trend to cool down but not continuously. Beside an uneven deterioration of climate the alternation of arid and humid phases was a typical feature of fluctuations. Borehole samples from the Hungarian Great Plain have revealed five longer cycles between 2.4 and 1.8 million yr BP.

There are, however, several authors (RUGGIERI 1977, SPROVIERI 1983, AZZAROLI 1983, De GIULI *et al.* 1983, SHACKLETON and OPDYKE 1973, EVANS, P. 1971, NIKIFOROVA, K:V: 1977) suggesting the *lowermost boundary* of the Pleistocene to be drawn at the 22nd stage of the oxygen-isotope scale. This coincides with the coldest peak of the Pleistocene with an age of 0.8 million yr BP. In the Russian Quaternary literature this is the Pleistocene/Eopleistocene boundary.

In Hungary the Pleistocene–Pliocene boundary coincides with the Matuyama/ Gauss paleomagnetic boundary (2.4 m yr) while in the Mediterranean this is 1.8–1.7 m yr.

The former is associated with significant structural, paleogeographic and environmental changes in the Carpathian Basin.

---

* As it is known global climate change is regulated by solar radiation. The impact of fluctuations in cycles of insolation during the Pleistocene first was calculated by MILANKOVIĆ, M. (1920, 1930). Later this theory on the relationship between glaciations and solar irradiation was criticised repeatedly but recently it has come to the fore again. The calculations by MILANKOVIĆ were checked by several experts and found correct within a time period back to 1 million yr BP.

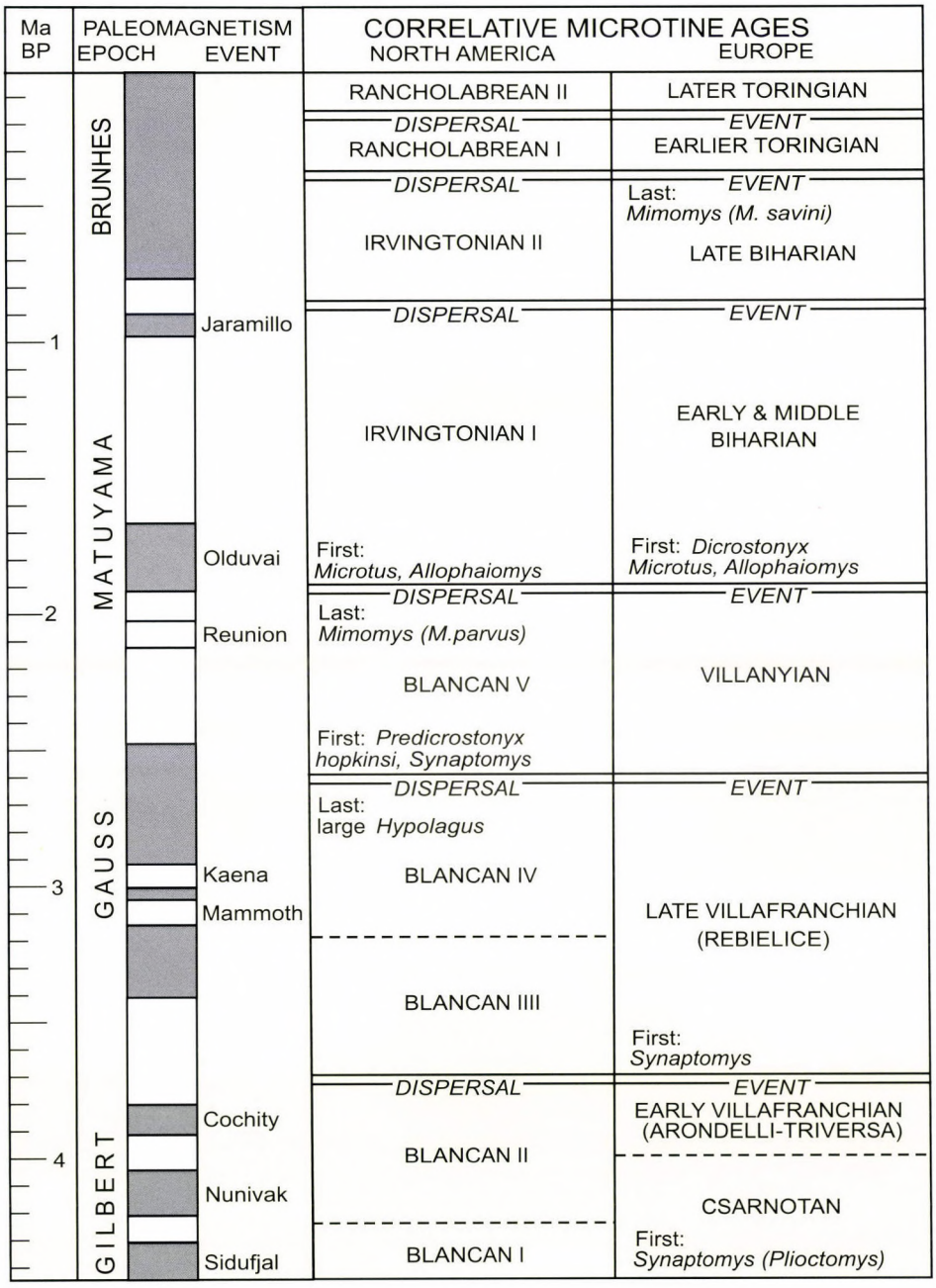

Fig. 6. Correlation of Late Pliocene events in North America and Europe (after REPENNING 1987)

1.5. Quaternary events

When overviewing the geological events over the past 4 million years, five cycles of climatic fluctuations can be distinguished that had brought about significant geomorphic–lithological changes in the Carpathian Basin and in northern Adriatic (Susak and Krk islands).

1. The time interval between 4 and 3 million yr BP was a period of humid and warm climate with a high diversity of species of mammal fauna. As a result red clays formed in considerable thickness and there was a significant karstification in the limestone regions. It was a period of formation of typical red clays in the Carpathian Basin (*Photo 5*) and also on Susak Island (*Photo 6*). Tectonic events induced activities of thermal springs (*Photos 11 and 12*).

2. The second climatic cycle started ca 3 million yr ago, when a warm and humid environment had been succeeded by a warm and drier climate lasting between 3 and 1.8 million yr BP. The contemporary rivers deposited coarser sediments. Pediment surfaces in lower position were formed at that time. Based on marine stratigraphy the 1.8 million yr BP marker is considered the boundary both between the Pliocene and Pleistocene and between the Neogene and Quaternary in the northern Mediterranean, contrary to the Matuyama–Gauss paleomagnetic boundary of 2.4 million yr adopted as the Plio/Pleistocene boundary in Hungary.

3. The third significant change started between 1.8–1.7 million yr and terminated at ca 700 thousand yr BP when, after a nearly 1 million year of relative stability, a considerable subsidence started in the area what is now the Great Hungarian Plain and in the northern Adriatic. The first spell of cooling occurred at that time but it had not resulted in tundra environment over these regions. Stratigraphically this is the Lower Biharian stage (*Fig. 6).*

4. In the beginning of the fourth phase (ca 1 million–800 thousand yr BP) the expansion of Alpine mountain glaciation and of the advancement of European inland ice sheet could be felt for the first time. Eastern and northern faunal species penetrated in the Carpathian Basin and proceeding through the desiccated northern Adriatic they reached the the Appennine Peninsula. Under dry and cold climate loess formation started and subsequently it had become general during the cold periods of the Pleistocene (*Fig. 1*).

5. The last regional climatic event took place ca 400 thousand years ago as a consequence of a glacial stage of long duration. The vertebrate fauna had changed fundamentally and a process of the emergence of the present-day species began. In the Adriatic sandy loess accumulated in a vast thickness whereas in the Carpathian Basin typical loess developed. Generally it is held that continental drift was primarily responsible for changes in the global climate and for the recurrence of glaciations, but rhythmic oscillations of the latter probably were controlled by cosmic factors.

2. GEOMORPHOLOGICAL CONDITIONS

2.1. General features

Susak Island together with the neighbouring islands Vele and Male Srakane and Unije Island form a distinct subgeomorphic regional unit. These islands constitute part of the island group in the Kvarner Bay considered as a mesogeomorphic region. All of them are small islands, their area being as follows: Susak – 3.76 km^2, Vele Srakane – 1.17 km^2, Male Srakane – 0.60 km^2 and the largest Unije – 16.8 km^2. The islands are of continental type and had become isolated from the mainland during transgressions following glacial stages.

Susak Island has all characteristics of a dissected loess plateau developed on an isometric block. It is a relatively low-lying island with maximum height of 98 m above sea level. The hypsometric levels have a belt-arch outline. They follow one another from the sea towards the interior part of the island. A characteristic feature of Susak is that its summit level coincides with the relatively flat part of the loess plateau.

Relief dissection is in conformity with the hilly orographic structure. The maximum vertical dissection of terrain is 98 m/km^2. The relative relief on the top of the loess plateau is between 0–2 m/km^2. However, because of the small extension of the island, unit of measure (m/km^2) and presence of the characteristic steep loess bluffs at the seaside, categories from 3–4 to 30–100 m/km^2 prevail. The same applies to the slopes angles: on the top of the loess plateau they vary between 0–2° to 2–5°, whereas the loess bluffs and sides of gullies have inclination of 32 to 55° and even steeper.

Susak has an isometric outline, its main orographic axis shows a north-west–south-east Dinaric spreading direction. Towards north-west this axis continues into a shallow and narrow submarine plateau in the form of a reef, with sea depths ranging between 5 and 15 m. Along the north-eastern and south-western coasts of the island and this submarine reef, condensing isobaths of 20, 30 and 40 m indicate the presence of steep submarine slopes, which separate the belt of a shallower submarine relief along the coast from an almost flat sea bottom (40–50 m) lying further. The steepest part of the island is the south-eastern coastal belt, represented by a flooded slope of north-west–south-east orientation. It continues on a lower a south-eastern part of the island. The higher north-western loess bluffs, however, continue into a shallower and flatter submarine relief. This altogether points to a specific asymmetry of Susak Island.

The steep submarine coastal sections of Susak probably have fault characteristics (*Fig. 7*). It can be also said about the curving north-east–south-west direction which is stretching from Vela Draga towards the south-western open-sea side of the island. The fault divides the island (*Photo 13*). into a higher (60–98 m a.s.l.), and larger north-western part (and a lower (30–50 m a.s.l.), and smaller south-eastern part (*Photo 14*), Morphologically, it is characterised by an intensive cutting of the Vela Draga system of gullies.

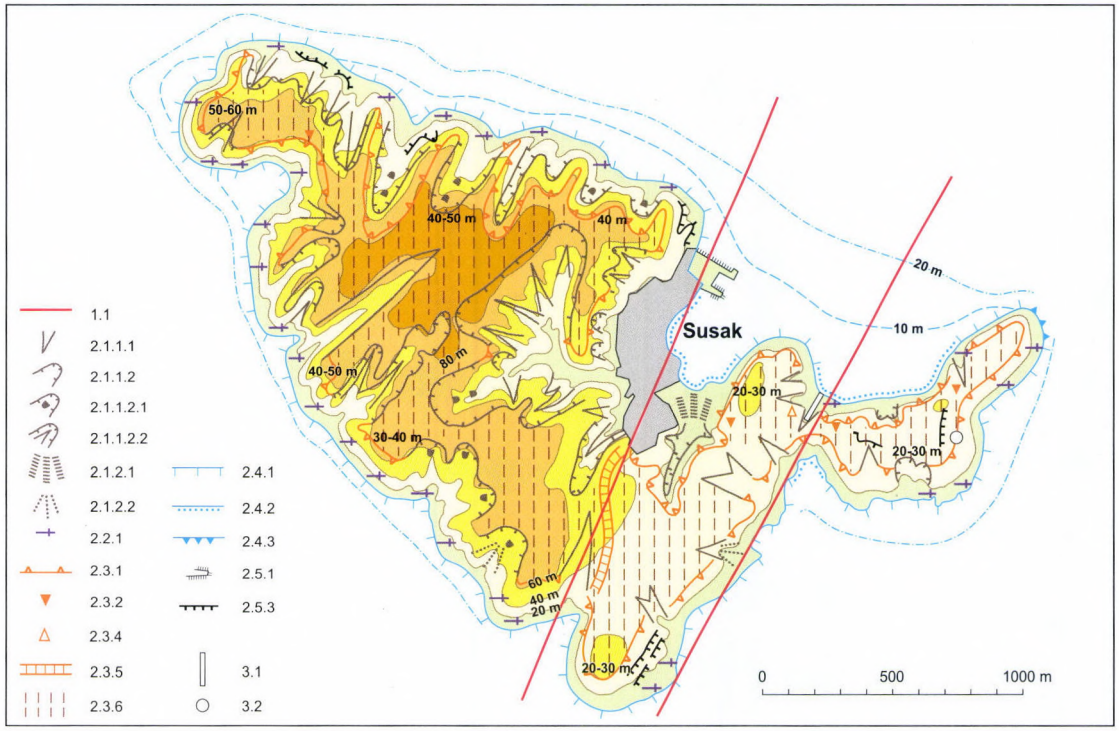

Fig. 7. Geomorphological map of Susak Island. (A. BOGNAR 1999). – 1 = Endogeneous relief; 1.1. = faults; 2 = Exogeneous relief; 2.1. = Slope landforms; 2.1.1. = derasional landforms; 2.1.1.1. = gullies; 2.1.1.2. = derasional valleys; 2.1.1.2.1. = derasional valleys of sliding origin; 2.1.1.2.2. = derasional valleys as remodelled gullies; 2.1.2. = Accumulational landforms; 2.1.2.1. = proluvial fans; 2.1.2.2. = colluvial fans; 2.2. Karst landforms; 2.2.1. = bare karst; 2.3. = Suffosional landforms; 2.3.1. = loess bluffs; 2.3.2. = loess wells; 2.3.3. = gaps; 2.3.4. = loess pyramids; 2.3.5. = anthropogeneous loess gullies; 2.3.6. = loess plateau; 2.4. = Coastal landforms; 2.4.1. = flat shore built of limestone; 2.4.2. = flat shore built of mud; 2.4.3. = headland, spur; 2.5. = Man-made landforms; 2.5.1. = pier; 2.5.2. = human settlement; 2.5.3. = slope steps of farming origin; 3.1. = Position of Susak 1997 profile; 3.2 = Traces of Paleolithic fireplace

Photo 13. The loess plateau is subdivided by a marked step into a higher level (60–98 m a.s.l., in the background) and a lower level (30–50 m a.s.l., in the foreground). (Photo by É. Kis)

Photo 14. The lower level of the loess plateau with heavily degrading bluff featuring slumps and slides (Photo by É. Kis)

Regarding the spatial relationship between the shape of the island corresponding to the submarine relief around it, it can be seen that not only the terrestrial and submarine parts of the island form a single morphological unit but, due to marine transgression, Susak happens to be a hidden morphostructural unit of horst type. Its neotectonic and morphological features have also contributed to a fairly good conservation of the existing loess and loess-like deposits.

2.2. The importance of geotectonic factors

According to the geotectonic division of the submarine Adriatic (KUDINA, A. 1980), Susak is a part of para-autochton of the Outer Dinarides, boundary line or transition zone of imbricated structures, bordering on the Adriatic, respectively on the Istrian platform (autochton). General morphological properties of the island, especially the planation of a carbonate plateau underlying loess, loess-like and sand sediments, affected by corrosion processes, point to Susak being an integral part of the Istrian platform. This is also indicated by the relief conditions in the wider surroundings of the island.

The planated plateau-like relief forms, so characteristic for the Istrian Peninsula also dominate Susak, and in the south-western part of the Unije Island, while they are missing from the other areas of the para-autochton. This implies, at least in the geomorphological sense, that Susak Island and the south-western part of Unije are parts of the Istrian autochton of the Northern Adriatic platform. The fault towards north-west–south-east which divides the Istrian autochthon from the mountain system Ćićarija and mountain range Učka, follows the line of the islands Cres – Unije – Susak – Dugi otok – Kornati towards the south-east. In fact, this fault represents the border between the Adriatic microplate and the Dinarides; just within the fault zone, where the former is submerged under the latter. The process has collision characteristics reflected by seismotectonics i.e. by the arrangement of the hypocentres. North and north-east of the mentioned fault, the hypocentres are located deeper (*Figs. 8 and 9*). This border fault between the two large geotectonic units has caused the arch bending of the neighbouring Unije Island and microtectonic dissection of both islands.

Recent structural- geomorphological studies of the relief in the north-western part of the Outer Dinarides in the neotectonic stage (MIHLJEVIČ, D. 1995) also confirm this hypothesis. Namely, the kinematic mechanism in the most recent phase, as the consequence of the shift of stress direction from north-east–south-west to north–south, has modified striking of the orographic structures of the mountain ranges and islands. It is the consequence of a specific kinematics of deformation developed in the most recent and tectonically active phase, marked by a retrograde rotation of structures. It is primarily expressed by an arch-convex outline of the relief forms. It also caused the arch bending of the range of the central and southern parts of the islands of Cres and Lošinj and arch shaping of the reverse fault limited by the geotectonic

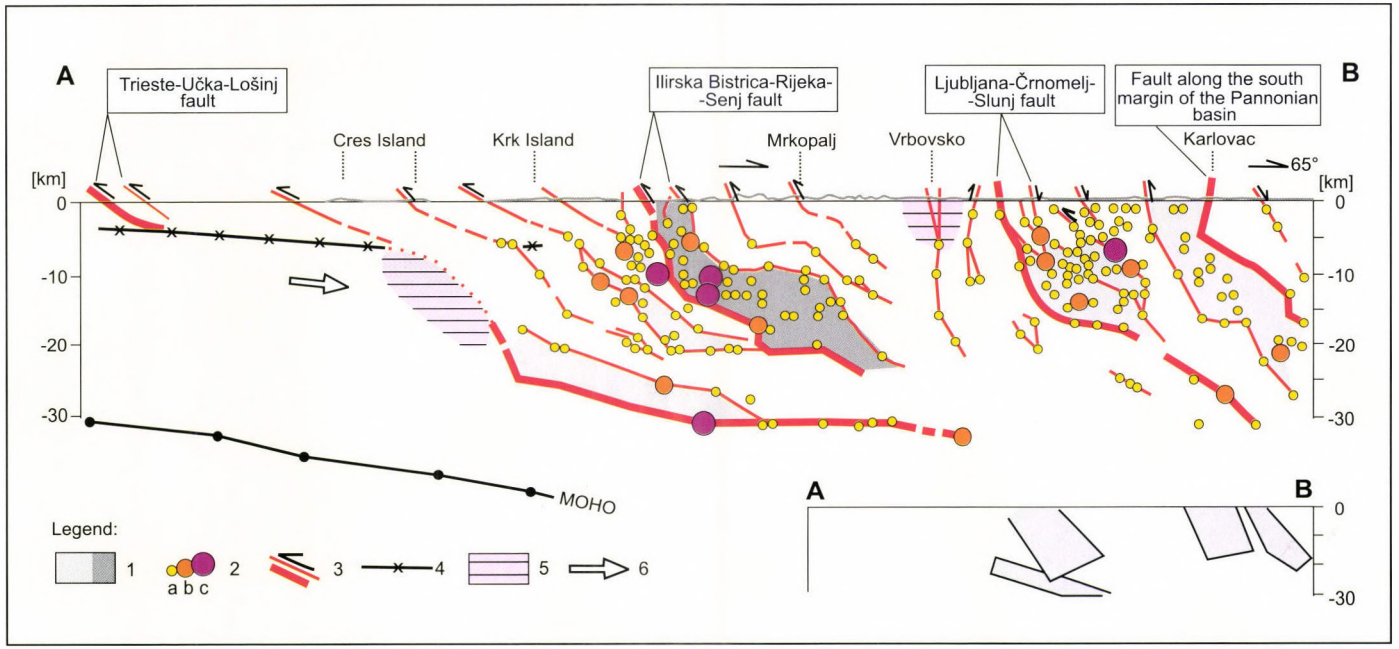

Fig. 8. Seismotectonic cross-section A–B, Cres Island – Karlovac. – 1 = seismotectonically active zones; 2 = earthquake epicentres with magnitudes: a) <4, b) 4 –5, c) >5; 3 = faults; 4 = inferred contact between carbonates and underlying rocks; 5 = zones of higher gravimetric gradients; 6 = direction of displacement of the Adriatic microplate (according to KUK, V. PRELOGOVIĆ, E. and DRAGIČEVIĆ, I. 2000)

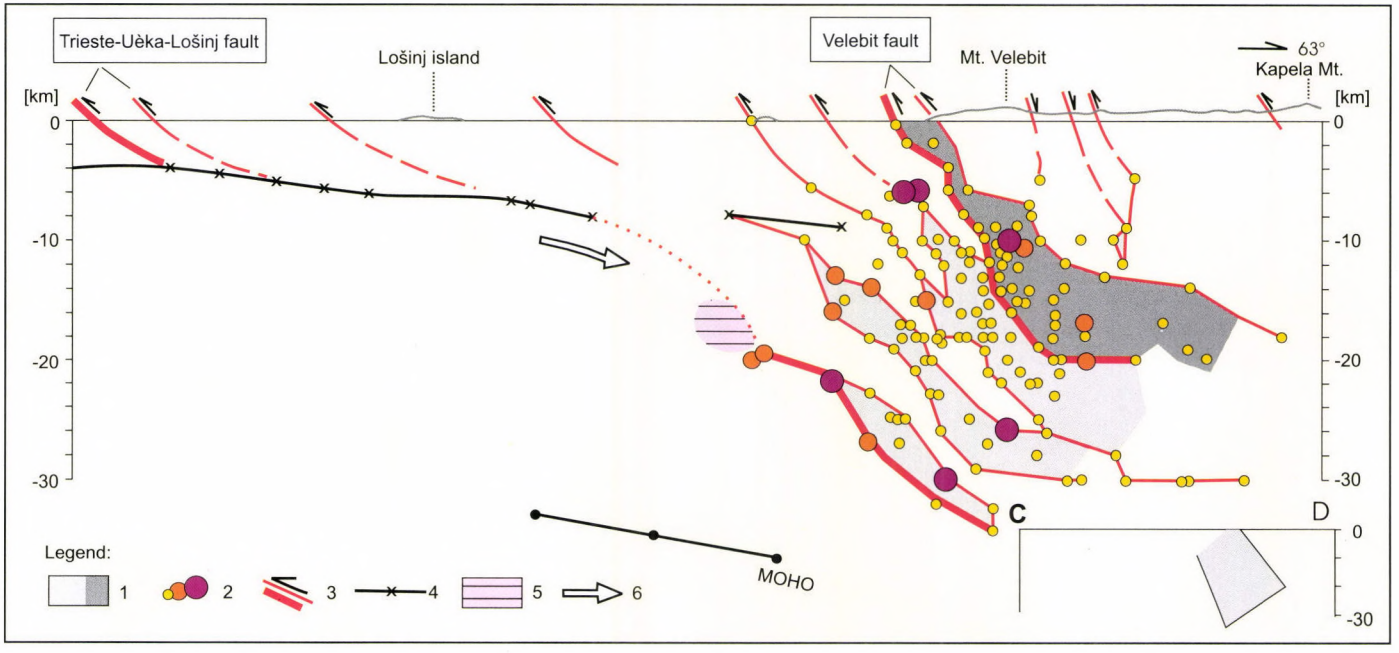

Fig. 9. Seismotectonic cross-section C–D, Lošinj Island – Mt. Kapela (for explanation see *Fig. 8*)

units of Istria and Outer Dinarides. That fault was the trigger to the arch bending of Unije and its microtectonic fractures. Besides, it is confirmed by the above assumption, based on a geomorphological analysis, that the island Susak and the south-western part of the island Unije are parts of the Istrian platform, i.e. of the para-autochton.

2.3. Landform evolution

Besides endogeneous factors, exogeneous forces and processes also take part in relief formation. The most important of them are past eolian processes and recent corrosive-suffosive, slope karst and abrasional phenomena. A heavy influence of human activities on the geomorphological evolution during historical times must also be mentioned.

2.3.1. Corrosive-suffosive processes and relief forms

As for the landforms on loess and loess-like sediments on Susak, there are two basic relief types: those developed by accumulation and others shaped by denudation processes. Loess cover of the plateaus with concave surface represents accumulation forms. As a rule, denudation forms are smaller landforms, however at present they are the prevailing morphological features of the island. In their morphogenesis denudational relief forms are influenced by lithological characteristics of loess and loess-like deposits, slope processes, neotectonic and actual tectonic movements, climate, vegetation cover and by human activity.

Corrosive-suffosive processes (*Photo 15*) are most important for morphological modelling where loess deposits are the thickest. These processes are responsible for the accumulation relief characteristics of the island. Depending on the distribution of $CaCO_3$ claystones, tectonic predisposition and degree of the porosity of rocks underlying loess (sands and limestones), ground water circulation, denudation processes and influenced by marine abrasion, mainly heterogeneous pseudokarstic suffosive relief forms, such as loess wells, loess gaps, loess solution flutes, loess gorges and steep loess bluffs were formed.

Development of the loess plateaus and *loess wells* is related to the steep loess bluffs. They are of complex origin. Intermittent streams (torrents) caused by intense rainfalls run along the loess bluffs developing a massive erosional activity. A hole is formed, and it is further widened by corrosion and suffosion. The capillary fissures are being widened by leaching out $CaCO_3$, and by washing out of the particles, so the loess loses its vertical stability, and forms a vertical semi-circular hole with the shape of a well. The loess wells are not stable formations because their outer wall falls in time by time under the influence of a strong erosional activity of the water stream. Vertical development of the loess wells can be remarkable and often spans the whole

Photo 15. Corrosional-suffosional relief forms (Photo by É. Kis)

loess bluff profile (20–30 m). According to their origin, *the loess gaps* are also connected with the margin of the loess bluffs. Their vertical development corresponds to the thickness of the layers beneath the relict pedological horizon, which necessarily points to the fact that the development of the loess gaps is conditioned by the position of the impermeable layer and the circulation of underground waters. Infiltrated precipitation waters, flowing off along the impermeable layer, combining the activities of corrosion and suffosion, make a fracture inside the loess deposits which is being widened gradually. Finally, it cracks along the underground fracture because of the poorer vertical stability of loess. Stability of a loess gap developed this way highly depends on the thickness of the loess deposits beneath the impermeable layer with

a thickness of 5–10 m and even more. Loess gaps are unstable landforms, because during showers and thunderstorms the cracks are being widened by the activity of the torrents and their sides collapse. Most often they become *gullies* with very steep sides. *Loess gorges* are shaped by the combined impact of human activities, corrosive-suffosive processes and floods. They are very deep and narrow features partly serving as dirt roads leading from the coast to the plateau (*Photo 16*), partly being found atop the Susak plateau. A constant traffic flow of people and animals has dissected the surface of loess, subsequently being washed out. Rainwater percolating into loess solves the carbonate shells out of the quartz grains and widens the capillary fissures finally causing collapse in loess. These processes deepen the gorge. During intense

Photo 16. Dirt road cut into loess in the eastern part of the island (Photo by É. Kis)

rainfalls water drains towards the sea coast in the form of mud flows. On Susak, due to a high sand content of the loess deposits, the gorges on the margin of the plateau towards the coast change their configuration very quickly (a process started in the past and having been intensified by human activity) being transformed into gullies. All this leads to the deterioration of hydrogeological properties of loess, and eventually intensifies mass movements along the steep *loess bluffs* (20–50 m). There are smaller forms of different kind related to loess bluffs, the morphological characteristics of which highly affect the degree of stability of the latter. Three basic types of steep bluffs can be identified:

– steep loess bluffs as a direct product of marine abrasion;
– loess bluffs with landslide and rock-fall material in their base;
– loess bluffs terraced by humans.

Directly abraded loess bluffs are frequently encountered. They are characterised by slope angles generally exceeding 55°.

Waves of abrasion break against the loess wall, so they latter periodically collapses and retreats. There are frequent collapses provoked by landslides. Because of that, and in conformity with the physical characteristics of loess, being unstable due to a chiefly vertical orientation of the capillary fissures, development of the slice-slides is characteristic for Susak. They are especially widespread in places where loess deposits are most exposed to abrasion.

As to the loess bluffs with their base constituted of rockfall and/or landslide material (Bay of Bok and the bay of the settlement Susak) abrasion appears as a trigger, as the rockfall–landslide material is permanently exposed to the impact of the waves and of the intermittent water courses, which eventually degrade the stability of the steep loess bluffs.

Man-made terraces essentially induce changes in hydrogeological situation of the loess deposits. Most often they exert a negative impact on vertical stability of loess. The loess base denudation speeds up slope-wash, but also enhances an uncontrolled spread of vertical capillary fissures through the processes of corrosion and suffosion. It facilitates the subsidence of loess deposits or development of landslides and mass movements along the steep loess bluffs.

2.3.2. Slope processes and forms

The slope processes and forms are characteristic for the slopes of the island, but there are considerable differences in their appearance and intensity of activity. As a rule, they are most remarkable on loess and loess-like deposits, especially on the steep loess bluffs. The most important are: slope-wash, colluvial process, rockfall, rockfall–landslide movements and gullying.

Slope-wash is present on island plateaus whether they are formed on limestones or loess. Heavy warming up in summer and corrosion of limestone are the ba-

sic causes of a relatively intense mechanical weathering of the rock complexes. Slope-wash reaches its maximum intensity on loess and loess-like sediments. Atmospheric precipitation is relatively low – 825 mm anually. Maximum of daily precipitation on the island Susak amounts to 110,8 mm. Annually only on 28 days rains in excess of 10 mm have been recorded. However, strong man-made impact like viticulture, accelerates the processes of slope-wash and *gullying*. Loess deposits of the island Susak form a row of deep gullies, which are in steady retreat. Therefore, the loess plateau is densely dissected and there are planated loess areas. The best example is retroactive cutting in of the gully is formed by a transversal fault *(Fig. 6),* but in its „source" part there is its fingers-like widening to develop a row of new gullies. During heavy rainfalls the streams transport massive portions of „eroded" loess and sand forming a proluvial fan in the area of the lower part of the settlement Susak causing this way silting up of the most part of the bay. Gullies develop rapidly. Their steep sides collapse, and eventually they evolve into so called derasional valleys (*Photo 17*) with a trough-shaped transversal profile. Numerous derasional valleys are formed by processes of gullying or by the sliding-colluvial movements, with the development of slice-slides (*Photo 18*). Cut into the carbonate base, gullies are being widened by slope-wash and colluvial process. The result is formation of deep dry derasional valleys. In the case of slice-slides, which most often have shape of amphitheatre. Loess and sandy layers deformed by movements are affected by a combined impact of sliding, collu-

Photo 17. Retreating derasional valley running toward the middle part of Bay of Bok (Photo by É. Kis)

Photo 18. Slice-slides in the south-eastern part of the island (Photo by F. SCHWEITZER)

vial process, slope-wash and gullying. Oval and trough-shaped dry derasional valleys are also being formed in that way.

Intensive out-migration from the island after 1945 has led to an old and ever ageing population. As a consequence, labour-intensive vine-growing has been neglected and vinyards abandoned (*Photo 19*), which has essentially reduced destructive effects of slope-wash and gullying. Abandonment of vine-growing has stimulated the spreading of grass vegetation (*Imperata cylindrica*), which covers today an overwhelming part of the island. The latest attempts aimed at the revival of vine-growing on Susak, east of the local cemetery, have led to an intensive deterioration of the loess deposits by slope-wash.

As it was mentioned before, the processes of colluvial process, slumps, landslide and rockfall movements are primarily confined to the steep loess bluffs of the loess plateau along its contact with the sea, and also to the steep sides of deep gullies. Colluvial process and rockfall are the processes present everywhere on the island, while landslide and rockfall movements are typical of those parts of Susak where at the base of the loess and sand deposits there is concentration of the underground waters i.e. very probably along tectonically predisposed fissure systems. The underground water of atmospheric origin washes out smaller particles of loess (suffosion) and wets the underlying clay, and also of those vertically oriented inside the loess deposits, falling in of the latter and sliding upon the wet clayey plane (examples: Vela Draga and Uvala Bok).

Photo 19. Once a mainstay of the economy at Susak, vine-growing has become a rare phenomenon on the artificial terraces (Photo by F. SCHWEITZER)

2.3.3. Processes and forms of marine abrasion: coasts

The sea-coast represents a remarkable element of topography. A greater section of the coast has been formed by processes of abrasion and only its smaller portion built by accumulation processes. That formation was essentially influenced by lithological structure, bedrock, tectonic movements, recent glacio-eustatic changes of the sea level and by exposure to the prevailing winds. Low and high coasts are distinguished, with a prevalence of the former. They are mainly formed in the limestone layers of monoclinal bedding. Over 95% of the low coasts belong to the category of rocky coasts. A strong influence of abrasion combined with corrosion resulted in „rough" microrelief, with the occurrence of abrasion solution flutes, blocks of rock etc. They are most typical of the southern margin of the island overlooking the open sea.

The low coasts built of clastic sediments are characteristic for Vela Draga (bay) and the Bay of Bok. They have been formed by the collapsed and transformed material or by streams redepositing loessy and sandy sediments eventually turned into mud. Part of the coast along Vela Draga is rocky.

2.3.4. Man-induced processes and man-made landforms

During the historical period, humans and their social-economic activities had a remarkable influence on landform evolution and transformation. The anthropogeneous relief forms are mainly related to farming once flourishing on the island. Terraced slopes appear frequently and dominate the landscape and relief. On the island 13 000 parcels used to be cultivated, a figure that suggests a high number of artificial terraces (WEIN, N. 1976).

Beside the mentioned forms we must quote buildings in human settlements and karstic projects which due to their constructive function (paved roads, filled up areas etc.) have, influenced the rate and intensity of the natural morphological processes, especially of those of marine abrasion and mass movements.

3. FORMATION OF LOESS AND LOESS-LIKE SEDIMENTS

According to G. COUDÉ-GAUSSEN (1991) loesses in northern Mediterranean are to be considered the local facies of European periglacial loesses in contrast to loesses of southern Mediterranean. The latter are desert loesses flanking the Sahara margin. Susak loess belongs to the loess region of the northern Mediterranean. The loess-paleosol sequence on Susak Island is one of the best examples of eolian loess formations on the Dalmatian islands (*Fig. 4*).

Formation of loess and loess-like sediments near the northern and southern coasts of the Mediterranean Sea is as a rule put to late Pleistocene. In the north sediments were repeatedly formed in periglacial environments whereas loess material in North Africa accumulated along desert margins during the pluvial phases (*Fig. 10*).

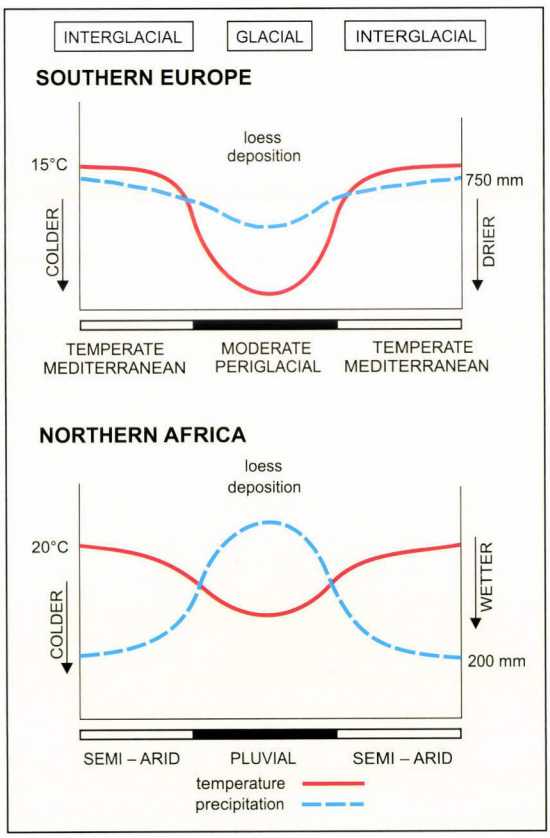

Fig. 10. Comparison of the loess deposition conditions during a theoretical glacial/interglacial cycle, between southern Europe and North Africa (COUDÉ-GAUSSEN, G. 1991)

3.1. Northern Mediterranean loess region

1. In the Po Plain and in the foreland of the Alps and Appennines (FRÄNZLE, O. 1969, CREMASCHI, M. 1987a, 1988, 1991) loesses mantle fluvial and fluvioglacial terraces and moraine ridges. East of Verona, in Friuli and on the Istrian Peninsula and along the Dalmatian coast they cover karstic plateaus and are settled in caves and shelters (G. COUDÉ-GAUSSEN 1991) .

2. In Mediterranean France loesses are cover sediments on the alluvial terraces in the south-eastern part of that country (DUBAR, M. 1979) in the Durance, Var and Hueaume valleys.

3. In other regions of southern Europe: in the northern areas of Spain redeposited loess is to be found in the vicinities of Tarragona, Lerida and Gerona (BRUNNACKER, K. 1969 a,b, MÜCHER H.J. *et al.* 1988) whereas in the Ebro valley eolian silt of gypsum (BOMER, B. 1978) occur. In the southern parts of Spain similar sediments can be met in Andaluzia, in the Piedmont and in the coastal plains in the east (BRUNNACKER, K. and LOŽEK, V. 1969, BRUNNACKER, K. 1969 a,b, 1980, DUMAS, B. 1977). In the Balkans loesses occur along the Adriatic coastline, on the Dalmatian islands, in the vicinity of Zadar (MARKOVIĆ-MARJANOVIĆ, J. 1969, CREMASCHI, M. 1987b), along the lower stretches of Neretva (BRUNNACKER, K. and BASLER, D. 1969), in Macedonia and northern Greece.

3.2. Southern Mediterranean loess region

In Tunesia loessial sediments occur in the valleys of the Matmata limestone plateau (BRUNNACKER, K. 1979, 1980, BROSHE, K. and MOLLE, H.G. 1975, COUDÉ-GAUSSEN, G. and ROGNON, G. 1988b). In situ loess covers hilltops and is found redeposited by colluvial processes on the slopes and on vadi terraces by fluviatile processes (COUDÉ-GAUSSEN, G. 1991). Three superimposing loess formations were identified in a profile in south Tunesia:

a. The uppermost part is a brown coloured clayey slope loess;

b. The middle part is a sequence of paleosols;

c. The lower part is a series of red coloured old loess.

Other silty deposits of eolian origin mantle the Sahara Atlas piedmont. There is redeposited loess at Tripoli, Lybia (HEY R.W. 1972) in the eastern part of Matmata plateau.

3.3. Differences in the origin of loess and loess-like sediments in the Mediterranean

1. On the northern periphery of the Mediterranean the emergence of initial material for loess formation is often attributed to pyroclastic processes. According to

this hypothesis, sediments were transported by the wind and deposited in the foreland regions. Here glacial and fluvioglacial deposits have been sources of loess material subsequently affected by eolian sedimentation e.g. in the Po Plain and in Provence (valleys of Durance and Var rivers), as evidenced by studies on heavy mineral and clay mineral composition). (G. COUDÉ-GAUSSEN 1991.)

2. In North Africa the Matmata loess formed from the deflated material of sand dunes of Eastern Great Erg as it has been proven by analogous heavy mineral and clay material composition. Quartz grains are of red colour. Initial material of loess was fine fraction blown out of the dune; the lowermost old loess of reddish colour formed in this way. The loess is composed by relatively coarse fractions because fine dust had been transported toward the Bay of Gabes.

3.4. Origin of loess

According to G. Coudé-Gaussen (1991) loess of the Po Plain is of fluvial and fluvioglacial origin, Material of the Dalmatian loessial sediments (including that of the Susak loess) has been transported from the Po Plain to the Adriatic during the Pleistocene glacio-eustatic marine regression. Eolian deposits in eastern Spain originate from the continental shelf, whereas similar sediments in Tunesia from the Eastern Great Erg.

Most of the material of the Po Plain accumulated during two pleniglacials of Upper Pleistocene. The initial material formed in Middle Pleistocene and was subsequently transported from the Alps and Appennines.

In France there are Upper Pleistocene loesses (constituting a major part of those in the Durance valley) and Middle Pleistocene loesses (Var valley).

Loesses in the Neretva valley and northern Greece are considered to be of Upper Pleistocene age.

According to Cremaschi, M. (1988) loess formation took place in the cold–dry phases of Pleistocene. In the cold phases glaciers descended over the southern ridges of the Alps. As a result of the glacio-eustatic regression of the Adriatic Sea, continental climatic conditions of Pannonian type prevailed (CREMASCHI, M. 1988) that had led to intense sedimentation.

Marine molluscs could not be recognised on Susak, hence the initially eolian material is not littoral but of fluvial origin (CREMASCHI, M. 1991). As it is shown by *Fig. 11.* (MELIK, A. 1952) marine sediments did not form here even in Miocene and early Pliocene. Coast line and drainage system of the Adriatic during the glacial stages of Pleistocene is represented on *Fig. 12.* The sea level was well below the present day one.

In the opinion of DE MARCHI (1922), due to the drop of the sea level, the Po Plain extended several hundred kilometers south-east of present day coastline (CREMASCHI, M. 1991, *Fig. 13*) including an area what is now Susak Island.

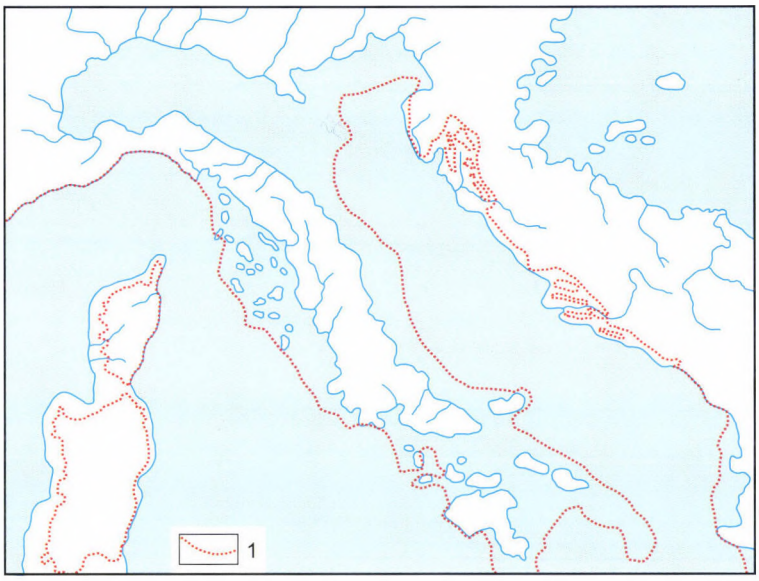

Fig. 11. Adriatic Sea during the Miocene and early Pliocene (after MELIK, A. 1952). It should be noted that previously the Miocene/Pliocene boundary was the end of Sarmatian. – 1 = present day coastline

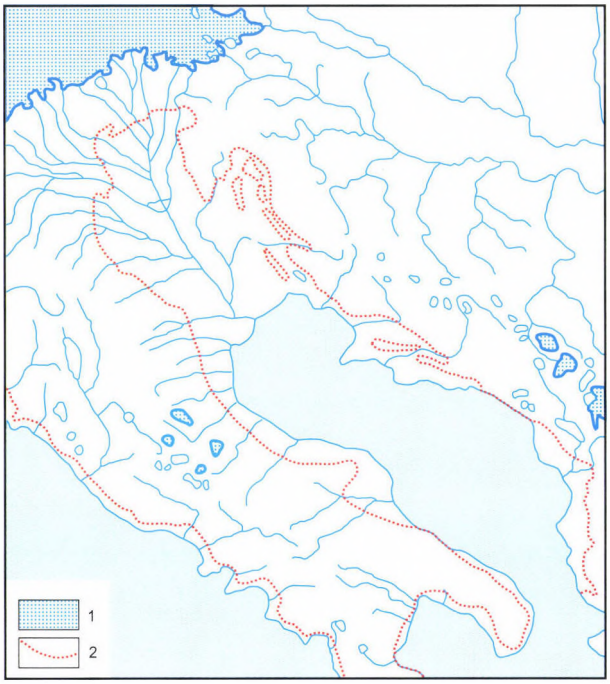

Fig. 12. Adriatic Sea during the Pleistocene (after MELIK, A. 1952). – 1 = glaciated areas; 2 = present day coastline

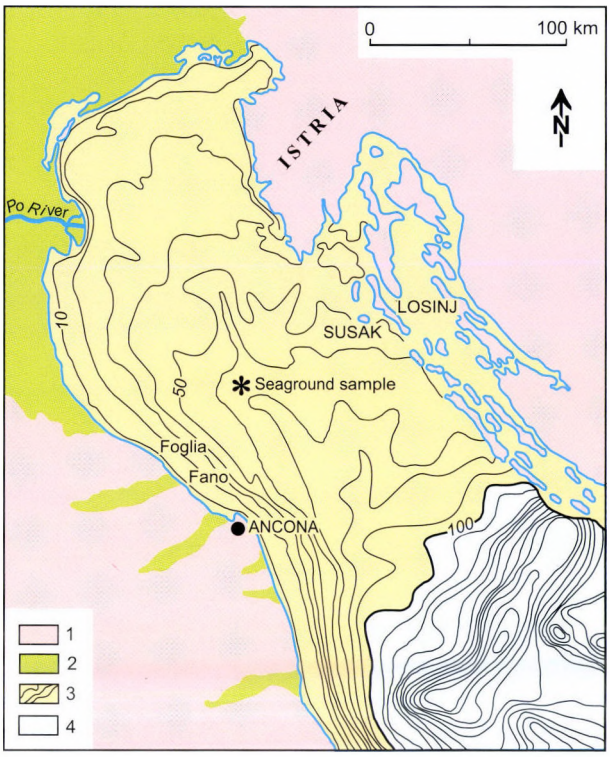

Fig. 13. Relationship between Susak Island and the Po Plain during the Last Glacial. – 1 = pre-Quaternary rocks; 2 = present day alluvial deposits; 3 = part of the Po Plain now submerged by the Adriatic Sea; 4 = extension of the sea during the Last Glacial (after CREMASCHI, M. 1991).

CREMASCHI, M. (1987b, 1991) holds that material of loesses in Dalmatia was blown out from the sediments of the Po Plain. Composition of loess in the Po Plain and that in Dalmatia was compared in relation to amounts of zircon–tourmaline, amphibole–epidote and garnet. Susak loess is more compact than loessial sediments of the Adriatic coast in Italy (Fano and Foglia). The material was transported toward the island by winds blowing in south-east direction (GAZZI *et al.* 1973, CREMASCHI, M. 1991). Mineralogical analyses of grains deflated from the Adriatic alluvial level have shown present day submerged level was an accumulation level during the last glacial (CREMASCHI, M. 1991).

The loess sequence at Susak can be correlated lithostratigraphically with the series of Val Sorda (Northern Italy) and Crispiero (Central Italy). There are loessial deposits interbedding between the last interglacial soil and isohumic soils. They probably formed during the interpleniglacial (Hengelo–Arcy interval).

Upper Pleistocene sequence at Susak can be correlated chronostratigraphically with series of Lessini Plateau (CREMASCHI, M. 1990) and with those in the vicinity of Rivoli (CREMASCHI, M. *et al.* 1987, CREMASCHI, M. (ed.) 1991).

In Cremaschi's opinion (1990) loess has polygenetic origin, its material has been redeposited repeatedly by fluvioglacial, fluvial and eolian processes, eventually reaching the Po Plain. Then it was transported by western winds across the dry basin of the Adriatic. During glacial maxima the sea level was ca 100 m lower than nowadays. Watercourses were longer flowing in the basin and the glaciers in the Alps extended far south (CREMASCHI, M. 1991). Due to circumstances of their origin loesses of the northern Adriatic are much more weathered than e.g. similar sediments in the Carpathian Basin and fall short of classical loess criteria.

3.5. Occurrence of loess sediments in the northern Adriatic basin

1. In the Alpine foreland (Lombardy and Venice provinces) and at Monte Conera (a human settlement on the western coast of the Adriatic Sea overlooking Susak Island), on Istria and Dalmatian islands *loess superimposes soils of terra rossa type, it covers surfaces denuded by periglacial processes. Loess redeposited by mass movements also forms slope sediments on valley sides* (CREMASCHI, M. 1987b modified by CREMASCHI, M. 1991).

2. On Susak and other islands of Dalmatia loess overlies *fossil sand dunes and abrasional terraces*. Eolian dust penetrated into shelters and caves where hunting tribes lived during the Paleolithic. These sites are rich in paleontological and paleobotanic findings.

3. On the margin of the Appennines, from Piemonte to Marche, loess has settled on fluvial terraces. Its thickness varies from some decimetres to several metres, thinning out from northwest toward southeast. Loess is intercalated within thick soil complexes over the plains of Lombardy and Piemonte and in the Mugello Basin.

4. On the glacial and erosional surfaces (from Liguria to Marche) loess (often heavily weathered) ovelies different kind of bedrock (e.g. Tertiary flisch).

5. On glacial drift and fluvioglacial surfaces, in the Alpine foreland (from Piemonte to Tagliamento Valley) loesses formed presumably during the penultimate glaciation.

4. THE SEQUENCE OF THE SUSAK LOESS PROFILE

Samples from the Susak section (*Fig. 4, Photo 20*) were collected in 1997 and since then it has been revisited by our team on several occasions. In the course of these field observations control samplings were performed. Previously stratigraphic sequences were studied by M. Cremaschi (1991) in three profiles (Margarina, Arat and Harbour sequences (*Fig. 14*) and by BOGNAR, A. *et al.* (1999) in one (Bay of Bok sequence).

Photo 20. Lower and middle part of the sequence at the Bay of Bok, overlying Mesozoic limestone (Photo by F. SCHWEITZER)

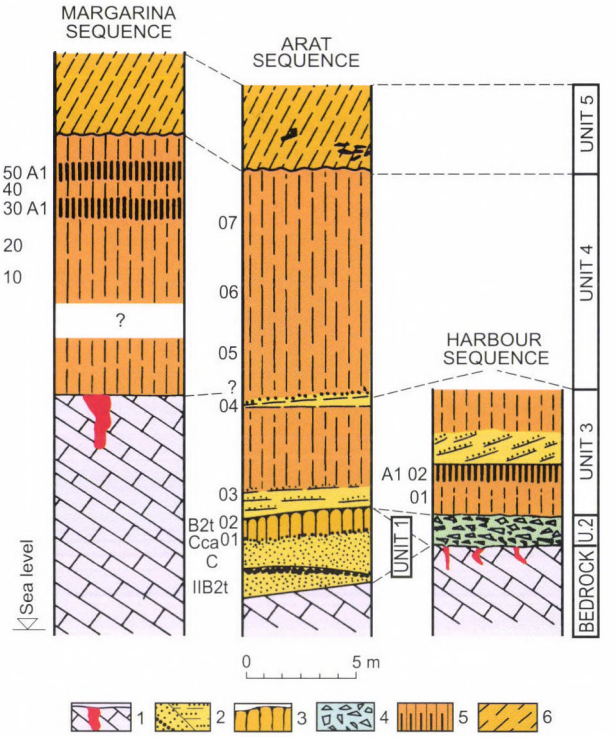

Fig. 14. The observed stratigraphic sections and position of the studied samples on Susak Island (CREMASCHI, M. 1991) – 1 = terra rossa in karstic pits; 2 = eolian sand including $CaCO_3$ horizon and lamination; 3 = alfisol; 4 = breccia; 5 = loess and intercalated chernozem; 6 = reworked loess

4.1. Granulometric parameters of loess

On the basis of *granulometric parameters (Fig. 15, Table 3)* several cycles of sedimentation which differ markedly from each other and associated with distinctly different physical environments can be distinguished along the Susak profile. To specify our knowledge of the profile four traditional granulometric parameters: *sorting, kurtosis, asymmetry, median* (*So*, *K*, S_k, M_d respectively) were applied together with two newly introduced indices of environmental discrimination: *fineness grade* (*FG*) and *degree of weathering* (K_d). $CaCO_3$ content, and variations in the percentage of clay, silt, loess and sand fractions were also obtained.

The recognition of the applicability of fineness grade to environmental discrimination of sediments was first noted by SMIDT, G.D. (1942) in his study of the Peorian loesses in the USA. The formula was established by SCHÖNHALS, E. (1955)

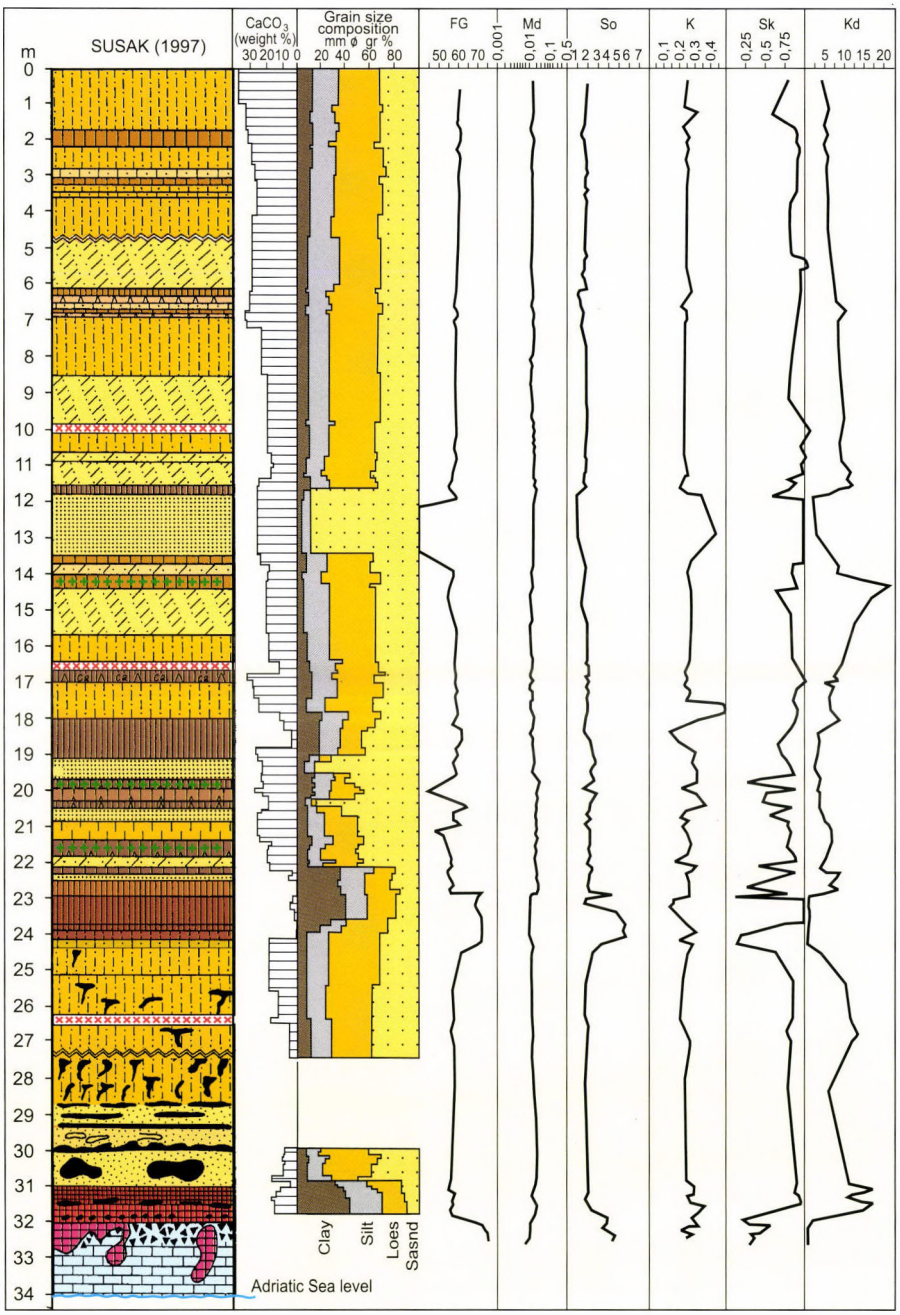

Fig. 15. Granulometric parameter values of the Susak 1997 profile (KIS, É. 1999, stratigraphical analysis by SCHWEITZER, F., BOGNAR, A., KIS, É., SZÖŐR, Gy., BALOGH, J., di GLERIA, M.)

Table 3. Granulometric parameters of the Susak 1997 profile (KIS, É. 1999)

Depth of layer, m	Fineness grade (FG)		Degree of weathering (K_d)		Sorting (So)		Kurtosis (K)		Asymmetry (S_k)	
	value	sediment	value	sediment	value	origin	value	sediment	value	formation
0.00–1.75	58.58–59.47	loess	4.72–5.87	loess	1.66–1.87	eolian	0.22–0.31	–	0.59–0.84	in situ
2.05–2.15	57.06	weak humus	5.28	weak humus	1.57	–	0.24	–	0.92	redeposited
2.15–6.10	58.20–59.38	loess	4.4–7.14	loess	1.61–1.74	eolian	0.23–0.25	–	081–1.37	redeposited
6.10–6.55	56.48–57.06	weak humus	7.47–7.33	weak humus	1.53–1.66	eolian	0.23–0.27	–	0.86–1.03	redeposited
6.55–9.78	56.69–57.20	loess	8.00–8.83	loess	1.46–1.54	eolian	0.21–0.24	–	0.83–0.95	redeposited
9.78–9.85	57.68	upper tephra	9.56	upper tephra	1.61	eolian	0.26	–	1.1	redeposited
9.85–10.95	56.52–56.67	loess	7.83–8.26	loess	1.47–1.61	eolian	0.23–0.27	–	0.91–1.02	redeposited
10.95–11.35	54.91–55.6	loess	11.1–11.94	loess	1.43–1.49	eolian	0.22–0.26	–	0.83–0.97	redeposited
11.35–11.70	56.53–57.34	soil	6.86–7.83	soil	1.47–1.48	–	0.2–0.23	–	0.7–0.77	in situ
11.70–13.50	31.46–31.53	coarse grained sand	2.1–2.76	coarse grained sand	0.84–0.85	eolian	0.36–0.43	–	2.5–2.52	redeposited
13.50–14.00	55.84–56.00	loess	7.9–8.65	loess	1.53–1.56	eolian	0.25–0.27	–	0.84–0.87	redeposited
14.00–14.35	54.13–54.23	soil	16.82–22.8	soil	1.25–1.49	–	0.27–0.28	–	0.64–0.9	in situ
14.35–16.45	56.09–56.37	sandy loess	9.75–12.4	sandy loess	1.53–1.62	eolian	0.27–0.28	–	0.88–0.9	redeposited
16.50–16.52	57.79	middle tephra	7.95	middle tephra	1.66	eolian	0.23	–	1	in situ
16.52–17.50	57.00–59.24	soil	4.59.24	soil	1.68–1.72	–	0.23–1.2	–	1.91–0.96	in situ
17.50–17.90	55.57	loess	8.95	loess	1.56	eolian	0.31	–	0.5	redeposited
17.90–19.10	56.53–60.79	soil	2.49–2.94	soil	1.32–2.15	–	0.14–0.32	–	0.69–0.86	in situ
19.10–19.60	43.90–49.60	fine grained sand	2.59–3.08	fine grained sand	1.28–2.21	eolian	0.2–0.32		0.32–0.91	in situ
19.60–20.33	54.44–64.82	soil	2.77–4.23	soil	1.53–2.42	–	0.2–0.34	–	0.51–0.84	in situ
20.33–20.55	45.9	fine grained sand	5.09	fine grained sand	1.37	eolian	0.21	–	0.79	in situ
20.55–21.40	51.59–53.68	loess	6.01–6.58	loess	1.48–1.65	–	0.24–0.27	–	0.8–0.84	in situ
21.40–21.75	53.03–54.6	soil	3.76–4.73	soil	1.68–2.03	–	0.16–0.32	–	0.46–0.89	in situ
21.75–22.10	53.16	loess	8.05	loess	1.93	eolian	0.24	–	0.88	in situ
22.10–22.18	53.16–55.19	skeletal soil	6.18	skeletal soil	1.7	–	0.24	–	0.24	in situ
22.18–22.23	52.59	loess	7.8	loess	1.62	eolian	0.25	–	0.78	in situ
22.23–24.10	60.08–70.87	soil	1.1–2.98	soil	1.1–5.48	–	0.14–0.23	–	0.1–25	in situ
24.10–26.40	54.73–56.03	loess-like sediment	10.5–12.9	loess-like sediment	1.39–1.51	eolian	0.21–0.23	–	0.78–0.84	in situ
26.40–26.43	55.09	lower tephra	11.32	lower tephra	1.53	eolian	0.27	–	0.84	in situ
26.43–28.70	56.72	loess-like sediment	6	loess-like sediment	1.57	eolian	0.25	–	0.81	redeposited
30.10–31.00	53.44–56.58	fine grained sand	10.27–	fine grained sand	1.39–1.84	eolian	0.24–0.36	–	0.72–0.93	redeposited
31.00–31.66	69.19–74.61	reddish clay	1.03–1.71	reddish clay	2.86–4.42	–	0.19–0.33	–	0.27–0.62	redeposited

on the example of the loesses along the Rhein River and it was first employed for the characterisation of grain size distribution by SIEBERTS, H. (1980) during a study of eolian sediments of Vistulian glaciation in the Lower Rhein–Westphalen. The K_d index was first applied in China by LIU TUNGSHENG *et al.* (1965, 1966), AN ZHISHENG and WEI LANYING (1979, 1980), LU YANCHOU and AN ZHISHENG (1979) and LU YANCHOU (1981). The characteristics of these six parameters were determined for the sediments from Susak in order to facilitate a better understanding of the changes in the dynamics of sedimentation during the Pleistocene. Grain size variations were used to recognise major lithological units and sedimentation gaps and to identify mutations within a seemingly homogeneous horizon and to distinguish between layers of apparently similar genesis.

In a summary table characterising the profile by layers *(Table 3)* the values of two newly added parameters, fineness grade (*FG*) and degree of weathering (K_d) are presented. FG is used to distinguish between sediments and for the reconstruction of paleotopography. The origin of dust and wind direction and velocity during dust transportation and deposition can be deduced from the decrease and increase of the FG percentage value. The K_d index allows periods of warming and cooling within the profiles. Of the traditional granulometric parameters sorting (*So*) serves to reconstruct the environment of deposition, kurtosis (*K*) identifies loess and paleosol boundaries, whereas asymmetry (S_k) helps identify areas of accumulation and denudation. (M_d values were not specified in the table for *FG* values present richer and more reliable information on grain size variations.) Also interpretation possibilities are offered by layers for the respective parameter values together with geographical characteristics: FG: value, sediment; K_d: value, sediment; So: value, origin; K: value, loess/paleosol boundary; S_k: value, formation (*in situ* or redeposited); comment: sedimentation gaps.

The determination of the granulometric parameters of the deposits on Susak Island allows both vertical and horizontal correlation of the sedimentary sequences. The parameter values for the most important sequences can be obtained from a database which contains all the granulometric data for 93 samples.

Of the newly introduced indices FG shows maxima in soils and minima in sands *(Fig. 15, Table 3)*. Thus, from its maximum values can be used to identify the paleosol layers, values less than median indicate young loesses, whereas old loesses display fineness maxima. Minima fineness grade can be identified within sands and the layers containing higher values indicate silt interbedding. Consequently FG values can be used to help delimit boundaries between horizons. An increase or decrease of the values indicate either finer or coarser granulometry, and help make distinction between young and old loesses and identify inhomogeneities within paleosols.

Apart from the identification and separation of sediments the K_d *index* enables conclusions to be drawn about climatic conditions that prevailed during the period of sedimentation. Its minima coincide with a period of warming and paleosol formation (their exact depth in the paleosol layer can be determined) whereas maxima refer to

a period of cooling and loess formation (their exact depth in the loess layer can be determined) and gaps in sedimentation can be identified.

The use of both the FG and K_d index values and the traditional parameters makes it easier to distinguish more clearly between sediments within the stratigraphic sequence based on their sedimentary characteristics, and to draw some conclusions about the environmental conditions during deposition, including hiatuses of deposition.

Eolian (*So*>2.5) and fluvial (*So*=2.5–3.0) deposits can be distinguished on the basis of *sorting (So)* (TRASK 1931). Values of 3–5.59 (along some profiles values up to *So*=10) indicate a mixture of sediments of eolian and fluvial origin, and in almost all cases represent paleosols.

Kurtosis (K) allows a precise determination of the boundaries between loesses and paleosols, with extreme values indicating mixing of these two kinds of deposits (KELLEY 1951).

Asymmetry (S_k) demonstrates a relative rate of sedimentation in accumulation area. Determination of asymmetry allows a distinction to be made between *in situ* and redeposited sediments (FOLK and WARD 1957). S_k values higher than 0.80 represent redeposited material.

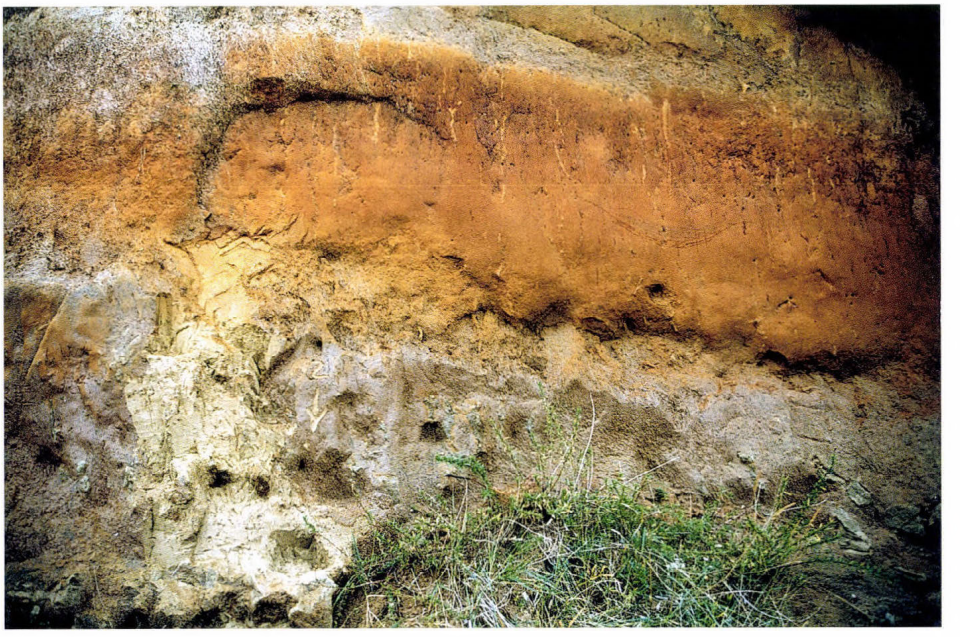

Photo 21. Reddish clay (double, locally tripartite) superimposing rudist limestone with carbonate concretions of 5–15 cm diameter size forming $CaCO_3$ horizon (lower part). Reddish clay is overlain by a sandstone bench of 0.5–1.5 m, cemented by carbonates (upper part) (Photo by É. Kis)

Photo 22. Reddish brown soil of MB type (double, locally tripartite) on Susak. It is frequently encountered in the key loess-paleosol sections of the Carpathian Basin. Upward in the profile there is a chernozem-like paleosol which can be correlated with soil of BA type in the Carpathian Basin (Photo by É. Kis)

4.2. Loess stratigraphy

Using the granulometric parameters described above 31 layers could be distinguished along the section *(Fig. 15, Table 3, Photo 20)*:

I. *11 paleosol layers*:
– 1 double, sometimes triple reddish clay *(Photo 21)*;
– 1 double reddish brown soil labelled Susak soil of MB type *(Photo 22)*;

– 6 chocolate brown chernozem-type soils in some cases with fire places resembling paleolithic sites i.e. horizons with charcoal remains *(Photos 23–24)*;

– 3 weak humous horizons (index values show less of them than found during sampling) with a thickness of 20–40 cm containing gypsum.

II. *4 sand layers*:

– 1 coarse grained sand (11.70–13.50 m);

– 2 fine grained sands superimposing young loess (19.10–19.60 and 20.33–20.55 m);

– 1 fine grained sand superimposing reddish clay (30.10–31.00 m) *(Photos 25–26)*.

III. *13 layers of loess and loess-like deposits*:

– 11 loess layers (*Photo 27*);

– 2 loess-like layers;

IV. *3 tephra horizons*:

– upper tephra horizon (9.78–9.85 m): a reddish brown layer in loess with fine sand redeposited in several places;

Photo 23. Slope of a fossil derasional valley with soil of MB type, constituting the older loess sequence (left side). A loess with intercalated paleosols represents a younger, predominantly Würm sequence (right side) (Photo by F. SCHWEITZER)

Photo 24. Above the soil of MB type there is a chernozem-like paleosol with two charcoal horizons of more than 35,000 yr BP radiocarbon age (Photo by F. SCHWEITZER)

– middle tephra horizon (16.50–16.52 m): a yellow layer superimposing a chocolate brown fossil soil (*Photo 28*);

– lower tephra horizon (26.40–26.43 m): a grey layer overlying silty sand (*Photo 29*);

Boundaries of the layers within the section can be localised from *Table 3* and *Fig. 15.*

Denuded horizons between loess and paleosols can be assumed by the occurrence of *extreme values of* K_d. It is especially useful in cases, when only this parameter provides distinct values and the other indicators show average figures: e.g. at a depth

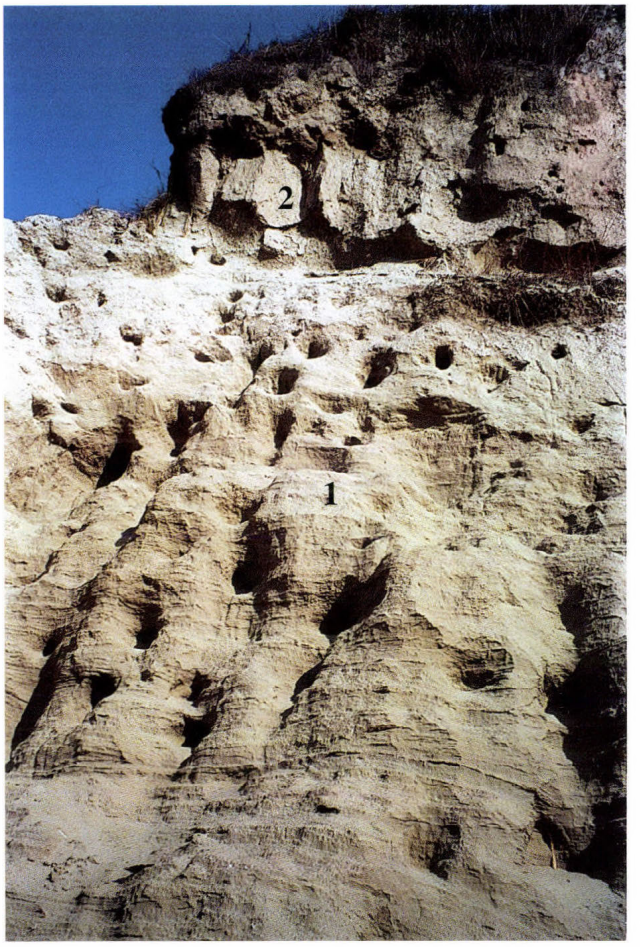

Photo 25. A wind blown sand horizon of 4–5 m thickness (1) with the superimposing sandy loess (2) in the eastern part of the island (Photo by F. SCHWEITZER)

of 17.40 m a denuded soil layer can be detected. Similarly, K_d shows a strikingly high value (22.80) within a paleosol between 14.00–14.35 m. A hiatus in loess deposition can be assumed to have occurred here.

Sands of three fineness grades are of interest in relation to the origin of the sediments.

1. coarse grained sand (FG=31.46–35.53)
2. fine grained sand superimposing young loess (FG=43.90–49.60; 49.90)
3. fine grained sand superimposing reddish clay (FG=53.44–56.58)

Asymmetry (S_k) value of the first of these sands is three times greater than the average (2.50–2.52) whereas its sorting (*So*) is half of the median value (0.84–0.85). Plot-

ting the values on average grain size versus its standard derivation diagrams, upon asymmetry versus standard derivation diagrams and upon asymmetry-kurtosis diagrams we arrive at fluvial origin of sand. This seems to be quite possible, as during Pleistocene marine regressions the river channels had become longer. At that time the Isonzo delta to the Adriatic was located 70 km west of Mali Lošinj whereas its tributary Raša stretched up to Susak (MELIK, A. 1952). It is probable that the sand was blown out of the latter's bed and a dune of 2 m height i.e. a cross-bedded sand had been built of it.

The granulometric parameter values obtained from the tephras which are superimposed on the loesses, loess-like sediments or paleosols (1: upper /redeposited/ tephra /*So*=1.61/; 2: middle /in situ/ tephra (*So*=1.66; 3: lower /in situ/ tephra on loess-like sediments /*So*=1.53/) appear to have an eolian origin.

Photo 26. A sandy skeletal soil on fossil wind blown sand in the upper part of the profile (Photo by É. KIS)

Photo 27. Loess horizon of more than 35,000 yr BP radiocarbon age in the middle part of the profile (Photo by É. Kis)

Based on asymmetry parameters the uppermost loess (with the interbedded middle tephra), which overlies the middle paleosol complex appears to represent a reworked deposit, except for the loess layers between 0.00–0.75 and 16.52–17.50 m depths, paleosols between 11.35–11.70 and 14.00–14.35 m and middle tephra between 16.50–16.52. Below this soil *in situ* formed sediments are found (17.90–19.10 m). A notable case is that of loess-like sediments (24.10–28.70 m) and fine grained sand (30.10–31.00 m).

Based on the *variations displayed FG* values by the *young and old loess pockets and paleosols are singled out.* In general, over the Carpathian Basin values 60.98–68.38 indicate young loesses, whilst values 65.34–73.59 refer to old loesses.

Photo 28. Tephra horizon of yellow colour with a thickness of 2–3 cm in the middle part of the profile TF_2 (Photo by F. SCHWEITZER)

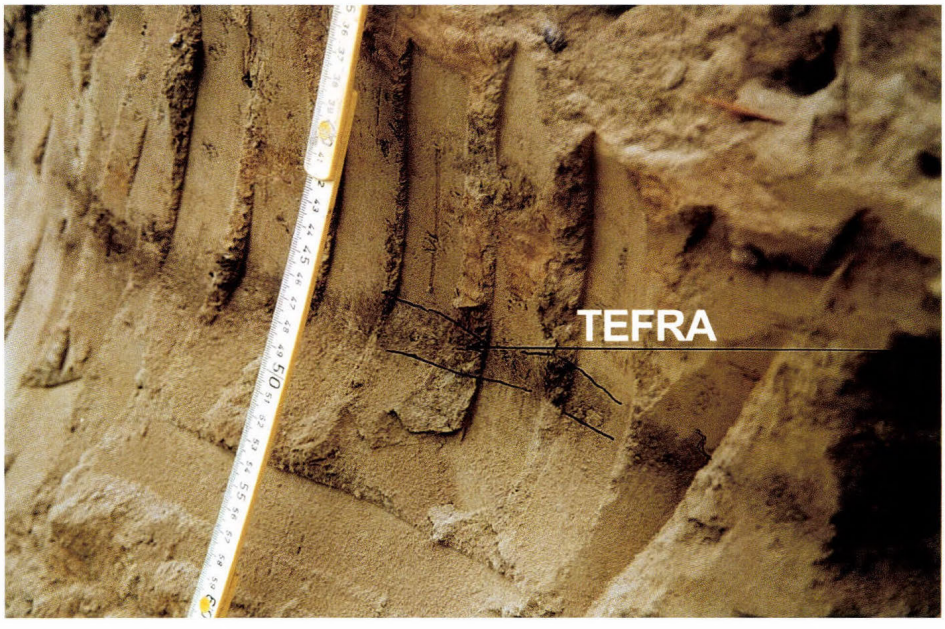

Photo 29. Tephra horizon of grey colour in the lower part of the profile TF_3 (Photo by É. KIS)

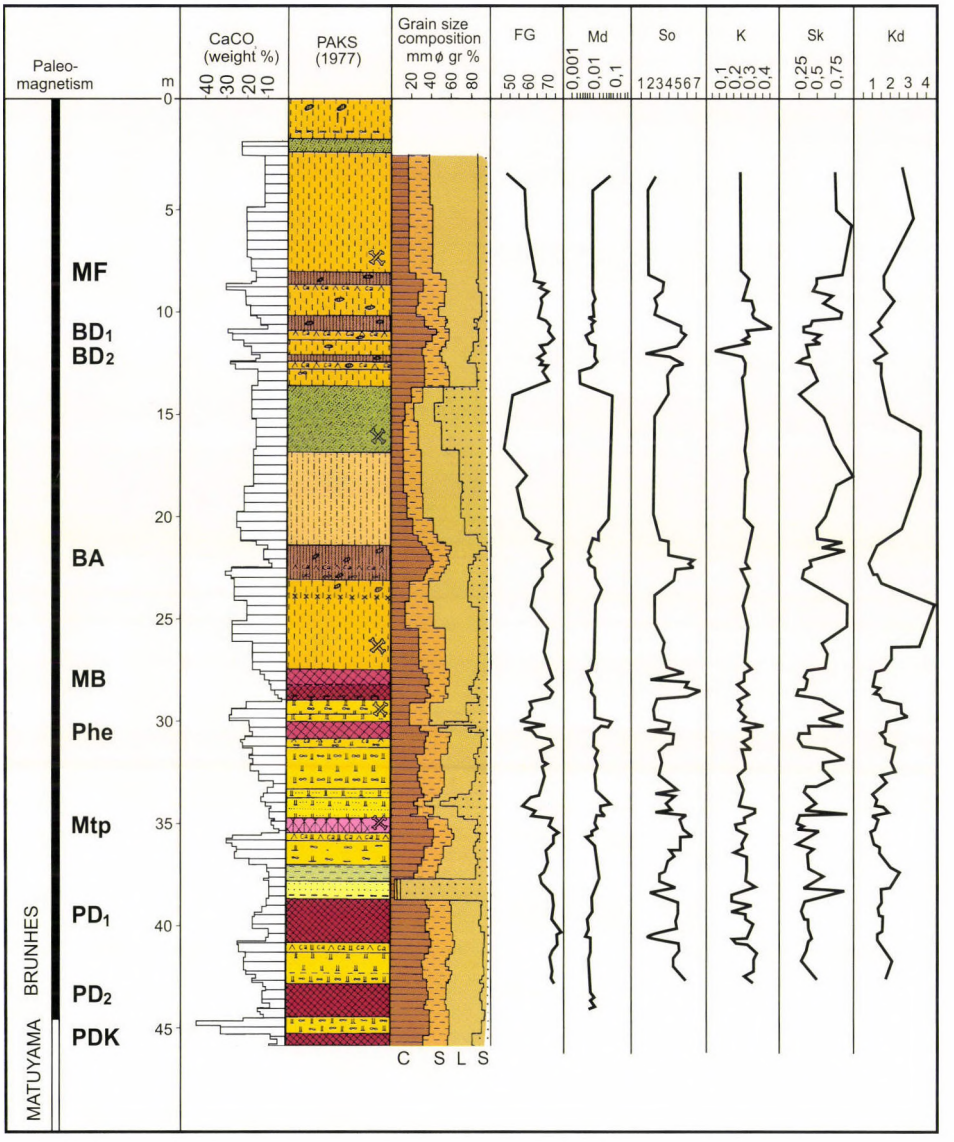

Fig. 16. Granulometric parameter values of the Paks 1977 North profile (KIS, É. 1996, stratigraphic analysis by PÉCSI, M., SZEBÉNYI, E. *et al.* 1978)

Along the Susak profile loess is represented by a variety with high sand content. Values 55.57–59.47 are typical of young loesses. Below 20.55 m, loess the sand content becomes even higher and *FG* decreases to 52.59, which is almost sand. In the lower-

most part of the profile loess-like material prevails (54.73–56.03 and 53.44–56.58) contrasting with loesses of higher parameter values. Variations in granulometric parameter values can be compared visually from the two stratigraphic diagrams (Susak: *Fig. 15,* Paks: *Fig. 16*).

Using the method described above information on the granulometry of the Susak profile allows paleogeographic conclusions to be obtained directly from the database, from the summary table containing the parameter values for the individual layers *(Table 1)* and from the stratigraphic diagrams.

5. SEDIMENTOLOGICAL ANALYSES OF THE LOESS PROFILE

One of the important parameters in the lithological classification of sedimentary rocks and of loess and loess-like deposits among them is granulometric composition. Grain size and weight percentage (wt %) distribution of particles by the individual size categories plays a significant part in identification of typical loess and its varieties and of loess-like deposits.

In the course of the mechanical analyses of loesses, loess like and other sediments and of fossil soils (paleosols) and incipient soils, nine grain-size categories were distinguished (*Table 4*).

Separation of the finer fractions is based on the law of STOKES stating that in a water-column at rest, solid particles of different grain size settle within various duration of time (KLIMES-SZMIK, A 1962). Based on this and on $CaCO_3$ content it can be judged about whether a sediment having similar or nearly similar physical properties is loess or some other formation and what kind of its further variations can be distinguished. The layered, redeposited sediments otherwise dominated by the loess fraction are not considered 'typical' loess (SZILÁRD, J. 1983). Also a sediment with similar to loess features* cannot be labelled loess if it contains loess fraction only in a subordinate amount. Particle size analysis can be instrumental in the solution of similar questions. Naturally the above analyses should be completed with field observations and identification of genetic features.

The complete Quaternary sequence of the Susak Island key section of 1997 (with a thickness of 32 m) was studied in a generalised profile (*Fig. 4*). When performing sedimentological analyses there were used categories applied by PÉCSI, M. and colleagues and internationally accepted (PÉCSI, M. 1967). Samples were taken from each layer, more frequent from the soils and in a less frequent pattern from loess of considerable thickness. Altogether 93 samples were collected from the whole profile. The results are shown in *(Table 4)*.

Of the routine analyses $CaCO_3$ and humus content and pH by distilled water were determined. After merging some of the nine categories the following classes were established: clay (< 0.005), silt (0.005–0.02), loess (0.02–0.05), sand (> 0.05). Grain size distribution in wt % was indicated along the right side of the profile whereas percentage $CaCO_3$ content was marked along its left side (*Fig. 4*).

* Including properties such as layered or unstratified character, porosity, colour

Table 4. Physical and chemical properties of sediments in Susak 1997 profile

Depth. m	$CaC0_3$ %	H %	pH d. water	<0.002	0.002–0.005	0.005–0.01	0.01–0.02	0.02–0.05	0.05–0.1	0.1–0.2	0.2–0.5	>0.5	Clay %	Silt %	Loess %	Sand %
				mm Ø gr %												
0.00–1.00	32.6	–	7.4	8.4	3.7	5.6	14.0	37.9	27.5	1.8	0.2	0.9	12.1	19.6	37.9	30.4
1.00–1.75	29.4	–	7.6	6.6	3.1	5.2	11.8	45.1	26.4	1.4	0.2	0.2	9.7	17.0	45.1	28.2
1.25–1.50	30.1	–	8.0	7.4	3.9	3.6	12.7	42.9	27.0	1.4	0.2	0.9	11.3	16.3	42.9	29.5
1.75–2.05	27.6	0.43	7.5	7.9	3.8	4.5	14.4	40.8	26.7	1.5	0.1	0.3	11.7	18.9	40.8	28.6
2.05–2.15	27.8	0.43	7.7	6.3	3.7	3.8	11.1	41.7	29.3	1.9	0.4	1.8	10.0	14.9	41.7	33.4
2.15–2.75	26.2	–	7.7	7.3	5.0	4.9	12.3	41.8	26.7	1.3	0.2	0.5	12.3	17.2	41.8	28.7
2.75–3.00	24.3	–	7.8	7.2	3.4	4.3	14.1	45.4	24.0	0.9	0.2	0.5	10.6	18.4	45.4	25.6
3.00–3.15	23.9	0.21	7.8	7.1	3.7	4.1	13.7	40.4	29.2	1.3	0.1	0.4	10.8	17.8	40.4	31.0
3.15–4.10	22.9	–	7.4	7.0	3.5	3.9	12.7	44.6	26.7	1.0	0.1	0.5	10.5	16.6	44.6	28.3
4.10–4.70	25.5	–	7.3	6.7	3.7	3.8	12.6	41.4	30.5	1.1	0.1	0.1	10.4	16.4	41.4	31.8
Profile interruption																
4.70–6.10	25.5	0.21	7.4	5.2	2.8	4.0	20.0	37.1	29.2	1.2	0.2	0.3	8.0	24.0	37.1	30.9
6.10–6.20	25.6	0.43	7.5	4.9	2.6	4.2	18.0	37.0	31.7	1.3	0.2	0.1	7.5	22.2	37.0	33.3
6.20–6.35	26.7	0.11	7.4	5.1	2.4 .	3.3	12.1	43.9	30.2	1.9	0.4	0.7	7.5	15.4	43.9	33.2
6.35–6.55	27.0	0.11	7.5	5.0	2.5	3.4	13.0	43.5	30.4	1.7	0.2	0.3	7.5	16.4	43.5	32.6
6.55–6.70	27.2	0.21	7.2	4.8	2.1	3.6	15.4	45.5	26.0	1.4	0.3	0.9	6.9	19.0	45.5	28.6
6.70–6.85	29.7	–	7.2	3.9	2.0	3.4	13.0	49.4	26.6	1.0	0.2	0.5	5.9	16.4	49.4	28.3
6.85–7.20	28.5	–	7.3	4.9	2.3	3.5	13.9	43.7	29.7	1.1	0.4	0.5	7.2	17.4	43.7	31.7
7.20–8.50	20.3	–	7.3	5.0	2.1	3.4	12.8	44.5	30.5	1.2	0.2	0.3	7.1	16.2	44.5	32.2
8.50–9.78	17.5	0.21	7.4	4.8	2.4	3.3	14.1	45.1	28.0	1.4	0.3	0.6	7.2	17.4	45.1	30.3
9.78–9.85	17.0	–	7.4	4.7	1.7	3.4	18.8	42.4	27.9	0.9	0.1	0.1	6.4	22.2	42.4	29.0
9.85–10.70	17.4	–	7.4	5.0	2.1	3.3	13.0	42.6	32.3	1.1	0.2	0.4	7.1	16.3	42.6	34.0
10.70–10.$5	15.3	–	7.3	4.8	2.3	3.4	12.8	44.1	30.8	1.0	0.3	0.5	7.1	16.2	44.1	32.6
10.85–10.95	14.5	–	7.4	4.7	2.2	3.3	13.5	43.5	30.6	1.1	0.4	0.7	6.9	16.8	43.5	32.8
10.95–11.10	13.8	0.43	7.5	4.0	1.2	2.1	13.2	45.3	32.4	1.4	0.2	0.2	5.2	15.3	45.3	34.2
11.10–11.25	15.4	0.43	7.5	3.9	1.3	2.2	12.8	44.9	33.0	1.3	0.2	0.4	5.2	15.0	44.9	34.9

Table 4. (Continuation)

Depth. m	$CaC0_3$ %	H %	pH d. water	<0.002	0.002–0.005	0.005–0.01	0.01–0.02	0.02–0.05	0.05–0.1	0.1–0.2	0.2–0.5	>0.5	Clay %	Silt %	Loess %	Sand %
				mm Ø gr %												
11.25–11.35	15.7	0.43	7.6	3.5	1.2	2.1	11.8	44.3	35.5	1.2	0.1	0.3	4.7	13.9	44.3	37.1
11.35–11.50	23.6	0.43	7.0	4.3	2.8	3.5	11.9	43.7	32.4	1.1	0.1	0.2	7.1	15.4	43.7	33.8
11.50–11.70	23.7	0.43	7.5	4.7	3.3	4.8	11.6	43.3	31.1	1.0	0.1	0.1	8.0	16.4	43.3	32.3
11.70–12.00	22.8	0.21	7.5	1.8	1.3	1.1	4.2	2.3	45.0	43.3	0.9	0.1	3.1	5.3	2.3	89.3
12.00–13.50	22.4	0.21	7.4	1.4	1.1	1.2	4.4	2.5	47.4	40.8	1.1	0.1	2.5	5.6	2.5	89.4
13.50–13.70	21.2	0.21	7.2	4.1	2.1	3.5	12.1	41.5	34.9	1.3	0.2	0.3	6.2	15.6	41.5	36.7
13.70–14.00	15.8	0.21	7.3	3.9	2.8	3.8	11.9	41.0	35.1	1.1	0.2	0.2	6.7	15.7	41.0	36.6
14.00–14.25	16.9	0.32	7.2	1.7	0.7	3.4	13.1	41.6	38.0	1.3	0.1	0.1	2.4	16.5	41.6	39.5
14.25–14.35	17.1	0.32	7.7	2.0	1.4	1.6	12.5	44.7	36.3	1.2	0.1	0.2	3.4	14.1	44.7	37.8
14.35–15.70	18.6	0.21	7.8	3.4	1.1	5.2	13.7	42.1	33.2	1.0	0.2	0.1	4.5	18.9	42.1	34.5
15.70–16.45	16.8	0.21	7.8	4.2	1.5	4.1	14.5	41.1	33.1	1.1	0.2	0.2	5.7	18.6	41.1	34.8
16.45–16.50	16.2	0.97	7.8	5.0	2.7	5.4	21.5	34.5	28.3	1.8	0.3	0.5	7;7	26.9	34.5	30.9
16.50–16.52	9.6	0.97	7.6	4.3	3.2	4.2	15.5	44.1	27.1	1.4	0.1	0.1	7.5	19.7	44.1	28.7
16.52–16.75	10.1	0.32	7.7	6.5	3.5	3.9	15.1	39.8	29.4	1.5	0.2	0.1	10.0	19.0	39.8	31.2
16.75–16.85	21.4	0.32	7.8	7.3	3.6	3.7	14.8	43.7	25.0	1.4	0.2	0.3	10.9	18.5	43.7	26.9
16.85–17.02	29.6	0.21	7.5	6.5	2.1	2.1	14.6	39.1	33.7	1.6	0.1	0.2	8.6	16.7	39.1	35.6
17.02–17.16	25.8	0.43	7.6	6.9	3.4	4.0	14.9	42.1	27.0	1.3	0.2	0.2	10.3	18.9	42.1	28.7
17.16–17.50	24.9	0.21	7.7	7.0	3.5	3.9	15.3	44.1	24.4	1.5	0.2	0.1	10.5	19.2	44.1	26.2
17.50–17.90	22.1	0.32	7.7	4.2	2.1	1.7	12.7	43.7	33.5	1.3	0.2	0.6	6.3	14.4	43.7	35.6
17.90–18.10	9.6	0.75	7.4	12.6	5.5	6.0	14.5	30.0	21.2	4.5	4.3	0.8	18.1	20.5	30.6	30.8
18.10–18.40	7.6	0.75	8.0	11.5	4.5	2.2	15.5	31.5	26.2	5.6	0.8	2.2	16.0	17.7	31.5	34.8
18.40–18.60	4.2	0.43	8.1	12.4	3.1	1.7	14.0	28.7	28.0	9.6	0.9	1.6	15.5	15.7	28.7	40.1
18.60–18.90	3.8	0.54	7.7	6.9	8.1	2.3	14.2	23.5	30.5	12.8	1.0	0.7	15.0	16.5	23.5	45.0
18.90–19.10	24.7	0.43	7.7	10.9	4.4	1.2	13.2	28.4	33.0	7.7	0.7	0.5	15.3	14.4	28.4	41.9
19.10–19.25	22.6	0.21	7.6	5.8	1.9	1.2	7.1	16.6	44.6	21.6	0.9	0.3	7.7	8.3	16.6	67.4
19.25–19.60	20.3	0.11	7.6	3.4	0.8	0.7	6.3	4.6	41.8	40.6	1.6	0.2	4.2	7.0	4.6	84.2

Table 4. (Continuation)

Depth. m	$CaC0_3$ %	H %	pH d. water	<0.002	0.002–0.005	0.005–0.01	0.01–0.02	0.02–0.05	0.05–0.1	0.1–0.2	0.2–0.5	>0.5	Clay %	Silt %	Loess %	Sand %
				mm Ø gr %												
19.60–19.75	21.1	0.43	7.3	8.7	3.3	1.0	12.6	20.6	39.9	12.5	12.0	2.0	12.0	13.6	20.6	53.8
19.75–19.92	20.5	0.43	7.5	8.6	1.9	3.6	14.2	14.9	45.7	10.1	0.6	0.4	10.5	17.8	14.9	56.8
19.92–20.05	26.9	0.43	7.5	7.5	3.8	3.6	9.9	25.1	40.4	7.1	1.7	0.9	11.3	13.5	25.1	50.1
20.05–20.13	24.2	0.32	7.5	6.8	2.6	4.8	10.3	28.7	39.6	4.9	1.2	1.1	9.4	15.1	28.7	46.8
20.13–20.23	20.5	0.32	7.5	8.4	2.9	5.2	9.1	31.5	37.4	3.7	0.9	0.9	11.3	14.3	31.5	42.9
20.23–20.33	17.2	0.21	7.3	6.7	2.2	3.9	9.1	28.6	42.2	4.2	0.8	2.3	8.9	13.0	28.6	49.5
20.33–20.55	16.8	0.11	7.2	2.6	0.7	0.7	3.3	13.5	56.5	20.8	1.6	0.3	3.3	4.0	13.5	79.2
20.55–20.75	21.0	0.21	7.3	4.5	0.9	2.1	5.9	26.6	54.6	4.6	0.5	0.3	5.4	8.0	26.6	60.0
20.75–21.40	24.0	0.21	7.4	3.9	2.5	3.9	10.1	32.0	41.8	3.2	0.7	1.9	6.4	14.0	32.0	47.6
21.40–21.50	22.9	0.32	7.5	7.1	3.0	3.6	11.5	33.4	31.3	2.6	1.8	5.7	10.1	15.1	33.4	41.4
21.50–21.65	15.2	0.32	7.4	8.1	2.5	5.6	10.2	29.5	33.1	3.9	1.2	5.9	10.6	15.8	29.5	44.1
21.65–21.75	18.7	0.32	7.4	5.5	2.5	3.9	8.4	29.4	40.5	5.0	1.3	3.5	8.0	12.3	29.4	50.3
21.75–22.10	18.6	0.32	7.3	3.9	1.6	2.3	7.7	36.6	43.5	3.1	0.6	0.7	5.5	10.0	36.6	47.9
22.10–22.18	15.5	0.32	7.4	5.3	1.9	4.0	16.1	28.7	37.5	4.2	0.8	1.5	7.2	20.1	28.7	44.0
22.18–22.23	15.2	0.32	7.5	3.3	2.3	2.5	9.4	34.3	40.9	4.1	0.7	2.5	5.6	11.9	34.3	48.2
22.23–22.45	3.4	0.21	7.6	26.1	5.7	7.6	17.7	22.6	15.3	2.6	1.1	1.3	31.8	25.3	22.6	20.3
22.45–22.65	5.4	0.21	7.6	25.4	4.9	6.9	12.8	28.1	15.7	2.3	1.1	2.8	30.3	19.7	28.1	21.9
22.65–22.90	0.0	0.11	7.6	25.3	4.4	7.0	12.9	27.2	16.2	2.2	0.9	3.9	29.7	19.9	27.2	23.2
22.90–23.05	2.8	0.11	7.6	28.6	3.5	6.8	10.8	32.2	14.6	1.7	0..5	1.3	32.1	17.6	32.2	18.1
23.05–23.35	3.6	0.21	7.5	31.1	4.5	5.8	11.0	28.5	15.2	1.5	0.4	2.0	35.6	16.8	28.5	19.1
23.35–23.65	1.8	0.21	7.4	30.9	4.8	5.6	11.6	27.6	17.3	1.4	0.3	0.5	35.7	17.2	27.6	19.5
23.65–23.75	0.6	0.11	7.2	30.4	4.6	5.7	11.5	26.9	18.1	1.2	0.4	1.2	35.0	17.2	26.9	20.9
23.75–23.90	0.0	–	7.1	19.0	4.2	4.6	11.0	35.8	22.7	1.3	0.3	1.1	23.2	15.6	35.8	25.4
23.90–24.10	2.6	–	7.2	11.9	5.2	5.1	11.6	39.3	22.5	1.1	0.3	3.0	17.1	16.7	39.3	26.9
24.10–25.60	17.5	–	7.7	2.9	2.7	3.5	13.1	45.8	28.5	1.2	0.4	1.9	5.6	16.6	45.8	32.0
Profile interruption																

Table 4. (Continuation)

Depth. m	$CaC0_3$ %	H %	pH d. water	<0.002	0.002–0.005	0.005–0.01	0.01–0.02	0.02–0.05	0.05–0.1	0.1–0.2	0.2–0.5	>0.5	Clay %	Silt %	Loess %	Sand %
				mm Ø gr %												
25.60–26.10	12.3	–	7.7	2.7	2.2	2.8	15.4	44.3	31.4	1.0	0.1	0.1	4.9	18.2	44.3	32.6
26.10–26.40	11.2	–	7.6	2.6	1.6	3.3	12.7	41.5	36.3	1.1	0.2	0.7	4.2	16.0	41.5	38.3
26.40–26.43	16.1	–	7.4	2.8	1.9	4.3	11.2	42.0	35.8	1.3	0.3	0.4	4.7	15.5	42.0	37.8
26.43–28.70	4.8	–	7.4	5.9	2.5	3.8	10.9	39.5	36.0	1.2	0.1	0.1	8.4	14.7	39.5	37.4
Sandstone bench (without sample)																
30.10–30.20	8.2	–	8.1	2.8	1.9	3.6	7.9	43.4	38.9	0.9	0.2	0.4	4.7	11.5	43.4	40.4
30.20–30.30	9.5	–	8.4	2.2	1.3	2.9	7.3	45.8	37.8	1.2	0.4	1.1	3.5	10.2	45.8	40.5
30.30–30.40	10.3	–	8.4	3.2	1.9	3.4	15.6	45.4	29.4	0.7	0.1	0.3	5.1	19.0	45.4	30.5
30.40–30.50	7.8	–	8.5	2.9	2.7	2.8	12.2	45.3	32.6	1.1	0.2	0.2	5.6	15.0	45.3	34.1
30.50–30.85	9.0	–	8.5	1.7	1.8	1.1	11.3	46.6	35.9	1.0	0.2	0.4	3.5	12.4	46.6	37.5
30.85–31.00	15.5	–	8.5	2.6	0.4	3.4	17.2	27.0	46.2	2.1	0.4	0.7	3.0	20.6	27.0	49.4
31.00–31.10	4.7	0.43	8.1	21.6	6.7	8.5	17.4	31.0	12.5	1.6	0.3	0.4	28.3	25.9	31.0	14.8
31.10–31.20	4.7	0.43	8.2	23.3	6.7	8.5	19.2	28.9	10.9	2.0	0.3	0.2	30.0	27;7	28.9	13.4
31.20–31.28	10.8	0.43	8.3	22.4	12.5	10.3	17.8	23.6	10.5	2.0	0.4	0.5	34.9	28.1	23.6	13.4
31.28–31.40	13.8	0.65	8.4	27.7	8.7	9.1	17.9	23.6	10.6	1.8	0.3	0.3	36.4	27.0	23.6	13.0
31.40–31.50	16.8	0.54	8.3	27.7	9.4	10.4	17.9	22.9	9.7	1.6	0.2	0.2	37.1	28.3	22.9	11.7
31.50–31.60	14.6	0.65	8.4	29.2	10.2	8.8	16.7	23.9	8.7	1.9	0.5	0.1	39.4	25.5	23.9	11.2
31.60–31.66	14.2	0.65	8.3	29.6	10.0	9.2	17.4	24.3	7.1	1.8	0.4	0.2	39.6	26.6	24.3	9.5

Photo 30. View of the Paks brickyard exposure (Photo by J. BALOGH)

The data present an overview of the studied exposure. Clays are mainly represented by fossil soils, their clay content is 30–40%. Silt category is typical of the transitory horizons of soils.

Loess fraction is represented in the profile with the highest, 35–50 wt % down to 18 m (except for the sand horizon between 12–13.5 m). Its carbonic chalk content varies between 8–32%, i.e. it has somewhat lower values compared with the loesses of the Carpathian Basin (15–35%).

Sand fraction is above 20% all along the profile, with the exception of paleosols of MB and PD type, where it drops below 20%. The sand content is higher within the horizon between 12–13.5 m and at the bottom of the profile (29–31 m) above the thickening sandstone bench and in its cavities, indicating important denudational events.

Based on paleopedological features the lithostratigraphic subdivision of horizons was accomplished through the comparison of the fossil soils in the profiles Paks 1971, 1977 *(Fig. 17)*, (PÉCSI, M.–SCHWEITZER, F. 1977) formed in the Carpathian Basin (*Photo 30*) and those of the section Susak 1997 typical of the northern Adriatic region (*Photo 2).*

This comparison was carried out for the following paleosols: BD (Basaharc Double), BA (Basaharc Lower), MB (Mende Base) and PD (Paks Double) (*Fig. 18*).

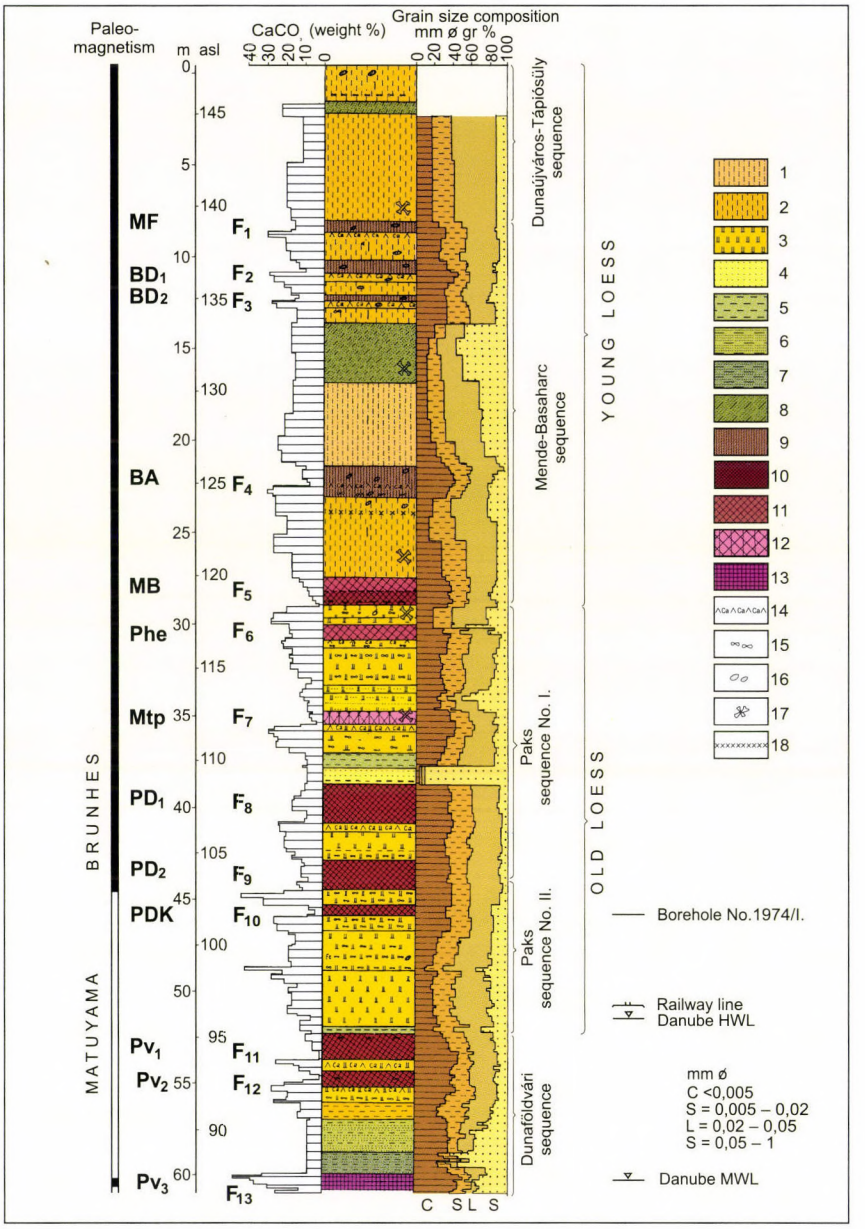

Fig. 17. Fig. Paks 1977 North profile (PÉCSI, M., SZEBÉNYI, E. *et al.* 1978). – 1 = sandy loess; 2 = stratified loess; 3 = old loess; 4 = fluvial sand; 5 = silt, gleyed silt; 6 = silty sand; 7 = sandy silt; 8 = sandy slope loess; 9 = steppe soil, chernozem, chestnut soil; 10 = lessivated brown forest soil; 11 = reddish brown fossil soil; 12 = hydromorphous soil; 13 = red clay; 14 = $CaCO_3$ accumulation; 15 = loess doll; 16 = krotovina; 17 = microfauna; 18 = tephra

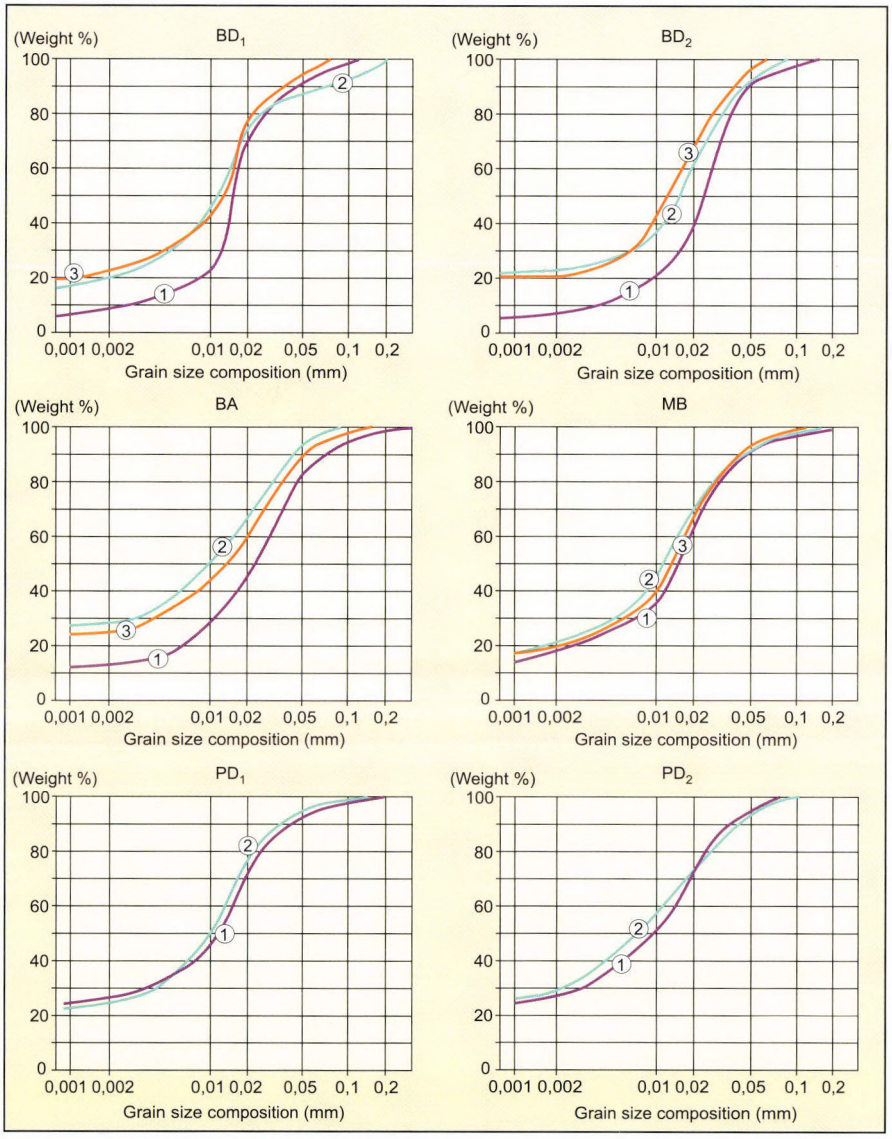

Fig. 18. Comparison between paleosols of Susak and Paks profiles by their granulometric composition (M. DI GLERIA 1998). – Basaharc Double: **BD**$_1$ = 1 Susak (1997): 16,50–16,52 m; 2 Paks (1977): 10,65–10,85 m; 3 Paks (1971): 8,80–9,00 m; **BD**$_2$ = 1 Susak (1997): 17,02–17,16 m; 2 Paks (1977): 12,60–12,75 m; 3 Paks (1971): 10,80–11,0 m; Basaharc Lower: **BA** = 1 Susak (1997): 18,10–18,40 m; 2 Paks (1977): 22,05–22,20 m; 3 Paks (1971): 17,40–17,60 m; Mende Base: **MB** = 1 Susak (1997) 22,85–23,00 m; 2 Paks (1977): 28,20–28,35 m; 3 Paks (1971): 24,35–24,60 m; Paks Double: **PD**$_1$ = 1 Susak (1997): 31,10–31,20 m; 2 Paks (1977): 39,35–39,65 m; **PD**$_2$ = 1 Susak (1997): 31,50–31,60 m; 2 Paks (1977): 43,35–43,55 m

Photo 31. PD red fossil soil at the bottom of the Paks brickyard exposure (Photo by J. BALOGH)

Photo 32. Paks MB reddish brown fossil soil (Photo by J. BALOGH)

Photo 33. Paks BA chernozem fossil soil (Photo by J. BALOGH)

PD (5YR5/8 according to the Munsell-scale, *Photo 31*) was compared with the SAV (Susak Lower Red) tropical-subtropical soil (5YR4/8) found at the bottom of the section (*Photo 41*). MB reddish brown (7,5YR4/4) soil of Parabraunerde type (*Photo 32*) met in several exposures of the Carpathian Basin was related to the reddish brown soil of Mediterranean type (7,5YR5/4, *Photo 22*) overlying sandstone bench. Chernozem-like soils of BA (10YR6/3, *Photo 27*) and BD (10YR6/4, *Photo 49*) from the Susak profile were compared with fossil soils of analogous stratigraphic position at Paks: BA (10YR4/3, *Photo 33*) and BD_{1-2} (10YR4/4, *Photo 34*).

A comparison of particle size distribution of the selected paleosols found in the two exposures was made through integral curves in a system of coordinates with logarithmic ordinates.

Photo 34. Paks BD_1–BD_2 fossil soil horizons (Photo by J. BALOGH)

Of chernozem-like paleosols (BD_1, BD_2, BA) compared, those found in Susak differ with a lower clay content. Differences between the curves might refer to variations in pedogenesis, to be attributed probably to characteristic features of multi-layered soils formed in the dell.

Granulometric curves for the reddish brown soils of MB type show sheer analogies, evidencing to a similar genesis.

The paleosol SAV (Susak Lower Red) – based on paleopedological features – seems to be comparable with the PD soil in the Paks section. The Brunhes–Matuyama paleomagnetic boundary (730 000 yr) was found in this horizon in the Carpathian Basin. Curves of the two red paleosols, both of subtropical origin, nearly coincide and suggest analogous pedogenesis, promoting chronological comparisons.

6. MINERALOGICAL AND GEOCHEMICAL ANALYSES OF SEDIMENTARY FORMATIONS: METHODS

6.1. Material and methods

100 gs of air dried sediment samples were dried in oven at 100–105 °C for 3 hours. 10 gs of granular sediment were averaged, then homogenised and pulverised in the Fritsch-type agate mill to less than 0.06 mm grain size. Samples were not sieved or treated chemically beforehand, and went through the same preparation processes. The prepared samples were used at analytical and chemical measurements. Thermal analyses were done on air-dried sediment samples.

6.2. Thermal analysis

Measurements on the 62 samples were carried out with the PAULIK, F.–PAULIK, J.–ERDEY, F.-type MOM Derivatograph-PC system.

The simultaneous analysis method introduced by PAULIK, F.-PAULIK, J. (1963) allowed to register three thermoanalytical curves with the heating of only one sample.

The three curves are:

– differential thermoanalytical curve (DTA)

– derivative thermogravimetric curve (DTG)

– thermogravimetric curve (TG).

With the help of the first one the endothermic and exothermic processes can be traced back, while the two latter enable to carry out weight measurements.

Sample were analysed under conditions and using computing system:

– temperature interval: 25–1000 °C

– heating rate: 10 °C/min

– weight of sample: ~ 1 g, the volume of the examined sample was identical to that of the Al_2O_3 (used as inert)

– specimen holder: No. II Pt-crucible (Ø = 13.0 mm)

– atmosphere: air, without sipping.

Discussion of results were made according to FÖLDVÁRINÉ VOGL, M. (1958), LANGIER-KUZNIAROVA, (1967), LIPTAY, G. (1971–1976), MACKENZIE, R.C. (1962, 1970) and SMYKATZ-KLOSS, W. (1964).

The method of the thermoanalytical laboratory of MÁFI was applied, namely colour changes between the natural sample and the heated (to 1000 °C) one.

Ferrous samples due to oxidation change their colour to red, for example siderite turns to dark purple, and humic samples appear grey in colour (FÖLDVÁRI M. 1980). Goethite becomes red after heating to 1000 °C. Samples rich in humic fraction first turn to black and then, after heating them to 1000 °C, they lighten.

6.3. Evolved gas analysis by quadrupol mass spectrometer (EGA-QMS)

The main point in the attached system is that gas products released during thermic decay are put through the mass spectrometer by double pressure-decrease with a heatable, molecular lattice-equipped capillary system (BERECZ, I et al.1983, SZÖŐR, Gy.and BOHÁTKA, S. 1985). Beside the thermo-analytical curves (DTA, DTG, TG) we can obtain whole mass spectra, or signed with peak-pointer, we can detect atomic mass (QMS-EGA).

Measurements could be carried out with variable programmed heating, atmosphere (carrying gas), in static or dynamic environment.

High vacuum system of quadrupol mass spectrometer can be cooled with liquid nitrogen, it serves with water-cooling oiltrap and oil-diffusive pump. Background pressure is smaller than 1×10^{-1} mbar, its sensitivity is 4×10^{-4} A/mbar, measured with Faraday-detector.

Speed of gas flowing in the 1.2 m long heatable capillar system is 0.5 cm^3/s, reaction time is 50 ms, mass spectrum currently is 10–100 a.t.e. The IBM XT/AT computer control allows setting the system parameters, retrieval of the main parameters, and also quick data collection, elaboration and building up a database.

The software makes it possible to measure continuously 8 ions with different atomic mass simultaneously under various electrometer-amplification. Spectra are drawn with graphics of high resolution.

This method was only applied at sample examination to detect evolved thermogas.

6.4. X-ray analysis

Partly to have control measurements, but also to compare the different instrumental analytical procedures mineralogical identification of several typical sediment samples was carried out by x-ray analysis, as well. Measurements and data evaluation were carried out by P. KOVÁCS-PÁLFFY at the X-ray Analytical Laboratory of MÁFI.

Instrumental and measurement parameters: Philips PW 1710 diffractometer, Cu anticathode, graphite monochromator, 30 mA tubeflow, 40 kV.

6.5. Chemical analyses

Thermoanalytical serial measurements proved that samples contained high proportion of carbonate, thus the so called Scheibler carbonate content was determined for all samples, and also the Ca^{2+} and Mg^{2+} ion content by complexometric titration, from the results the mass and gramme-molecule % quantity of $CaCO_3$ and $MgCO_3$ were calculated.

6.5.1. Determination of carbonate content using Scheibler calcimeter

Sample preparation took place according to the methods mentioned above at thermic analysis. 5–6 g of pulverised samples was dried in oven at 100–105 °C till weight stability (for about 3 hours). The dried samples were cooled and kept in exsiccator until the measurements. 0.1–1 g of samples, according to the estimated CO_2 content, weighted at 0.1 g accuracy.

Distraction of carbonates took place with 20 cm^3 10% cc. hydrochloric acid, shaking several times. Reaction was let to take place for 15 minutes, after bubbling stopped the reaction was regarded to be over.

Then the volume of the developed CO_2 gas and the temperature in the laboratory were read. Data on atmospheric pressure (daily average) were provided by the Department of Meteorology, University of Debrecen.

With the help of these data, and knowing the sample weight the CO_2 volume was converted to $CaCO_3$ using the appropriate table. On principle the Scheibler-calcimetry is only for determining $CaCO_3$ content, but here the CO_2 content given in $CaCO_3$ % include all types of carbonates consisting the sample that decay alongside gas development in 10% cc. hydrochloric acid at room temperature (KÉZDY, Á. 1961).

The $MgCO_3$, $Ca,Mg(CO_3)_2$, $FeCO_3$, and $MnCO_3$ mineral phases only partly dissolve in cold 10% hydrochloric acid, total and quick decay of them can be achieved by heating.

6.5.2. Ca and Mg identification by complexometric titration

1–7 g (according to the predicted Ca and Mg content) of the samples dried till weight-stability and pulverised were measured. These quantities were put into Erlenmeyer flasks, then 30–50 ml distilled water, and 10 % cc. hydrochloric acid was added until bubbling stopped.

Then the solutions were diluted with distilled water to about 70 ml, and warmed in boiling water for about an hour. Acidity of solutions were checked by universal indicator paper. After cooling the samples they were poured together with solid fraction into 200 ml volumetric flask and distilled water was added up to the sign.

a) Ca determination:

10 ml of the samples was piped into a 200 ml Erlenmeyer flask and diluted to 100 ml, pH was set 12 with 5 ml 10% cc. NaOH. To mask the available disturbing ions (mainly Fe^{2+}, Fe^{3+}, Al^{3+}, Mn^{2+}) 5 ml 1:4 diluted tri-ethanol-amine and a pinch of KCN were used.

The solutions were titrated with 0.05 gramme-molecule EDTA measuring solution by Patton-Reeder indicator. The factor of EDTA was determined with 0.05 gramme-molecule $ZnCl_2$ solution.

b) Simultaneous determination of Ca and Mg:

10 ml of samples was piped into a 200 ml Erlenmeyer flask and diluted to 100 ml with distilled water. PH of solutions was set to 10 with 10 ml puffer-10 solution (mixture of NH_4Cl and NH_4OH). As mask agent we used the same compounds as for the determination of Ca.

We titrated the solutions with 0.05 gramme-molecule EDTA measuring solution by eriochrome-black T-indicator.

Knowing the joint quantity of Ca-Mg, the Mg quantity could be calculated by detracting the quantity of Ca (SAJÓ, I. 1973).

6.6. Other complementary studies

6.6.1. Microscopic studies

In the lower part of the profile two layers of special diagenetic features, namely rhyzolites were observed, and in a thick, benchy appearance calcareous sandstone concretions occurred. Of them thin sections were prepared and examined under NIKON Microphot-SA polarisation microscope, and documented.

6.6.2. Microprobe examinations

Sand fraction of each sample was examined under microscope for two purposes:

– to identify whether, if any, extraterrestrial material (spherulites, micrometeorites) is present there,

– to separate quartz grains, the shape analysis of which is intended to be performed in the future.

These X-ray analytical (SEM-EDAX) examinations were carried out using scanning electron microscope.

The scanning-EDX-instrument was an AMRAY 1831 type. Photos were taken with a BSE detector. EDX parameters: SiLi detector, 10 μm Be window, usually 20 kV accelerator voltage, 150 eV energy resolution. Samples were coated with graphite.

6.6.3. Stable isotope examinations

In order to gather some more information $\delta^{13}C$ and $\delta^{18}O$ stable isotopic measurements were also carried out at the ATOMKI, Debrecen. Results were provided by E. HERTELENDI, senior research fellow.

7. MINERALOGICAL AND GEOCHEMICAL ANALYSES: RESULTS

7.1. Evidence from thermic and X-ray diffraction analyses

Of the 62 serial examinations the most important ones are presented, as they are the typical analyses (*Figs 19–28*).

The above thermoanalytical curves show clearly the special processes of thermal decay of the different mineral samples, and also the mineral phases detectable by these examinations. The so called thermogravimetric parameters can be determined as well, from which four important constituents can be calculated, namely total clay mineral content, carbonate content, amorphous phase and organic material. The mineralogical composition results of X-ray analyses were also indicated on the graphics of derivatographical analysis reported here.

Four thermoanalytical parameters were separated in these analyses which had been facilitated by the small amount of the measured sample and the plate-form of the specimen-holder. The releasing gas was detected by QMS-EGA method.

Interpretation of parameters:

H_2O(a) m% = weakly bound H_2O and OH-content of amorphous polysilicates and alumina, and that of clay minerals. Endothermic material loss.

Org m% = decay of organic material, with release of H_2O, CO_2 and organic matter. Generally, exothermic processes in changing temperature.

H_2O(s) m% = decay of lattice configuration of phyllosilicates (clay minerals and chlorites), release of the so called structural OH and H_2O during endothermic reaction.

CO_2 m% = CO_2 releasing from thermal dissociation of carbonates.

Two types of CO_2 release can be observed: parameter CO_2(1) suggest either thermodissociation of dolomite $MgCO_3$ or that of amorphous/aphaniphyric $CaCO_3$. Parameter CO_2(1) can be attached to thermodissociation of $CaCO_3$ as at calcite as calcite+dolomite.

H_2O(p) m% = $Ca(OH)_2$, releasing portlandite, endothermic reaction.

H_2O(g) m% = Fe(OOH), release of water from goethite, endothermic reaction.

We can conclude to four important constituents from the thermogravimetric m% values. H_2O(a) alone suggests amorphous polysilicates and the presence of alumina. Carbonates can be calculated with CO_2 Δ m% × 2,27, clay minerals – H_2O(s) Δ m% × 9,5; while organic C (Corg) – Org Δ m% × 2,5 (SZÖŐR GY. 1992).

Quantitative results of thermic analyses are shown in *Table 5*.

The change and specialities in vertical of the whole of clay and carbonate minerals, as well as amorphous material and organic C content of the profile are shown by *Figs 29 and 30*.

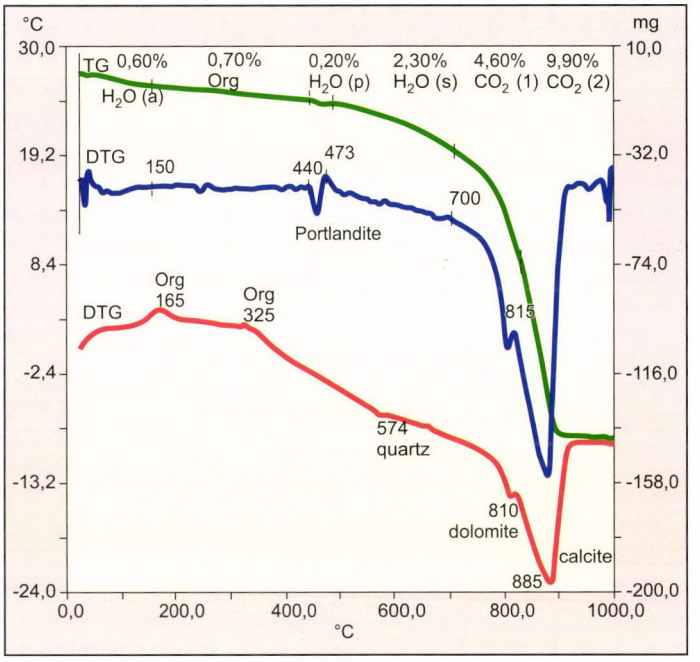

Fig.19. Thermoanalytical studies of young sandy loess from the upper part of the Susak profile. X-ray analysis defined the following minerals:illite-montmorillonite 1%, muscovite 9%, chlorite 7%, quartz 30%, plagioclase feldspar 11%, calcite 25%, dolomite 15%, amorphous 2%

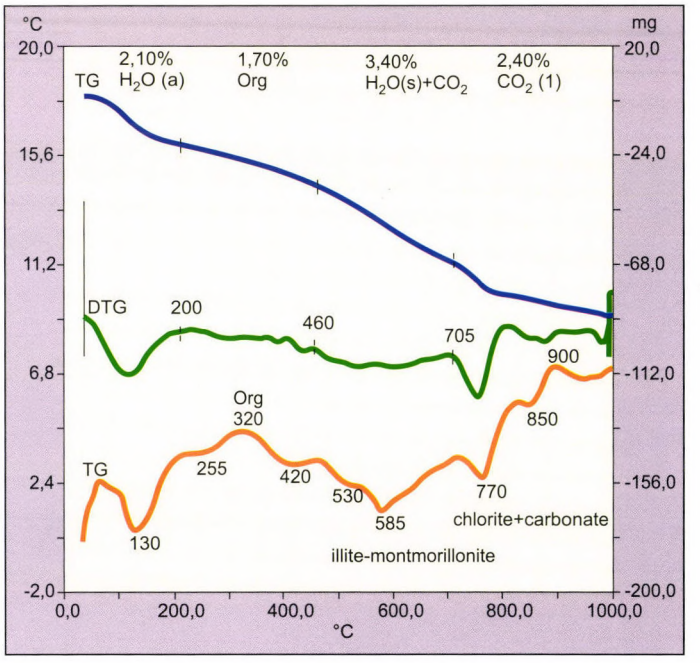

Fig. 20. Thermoanalytical studies of the upper tephra layer of the Susak profile. X-ray analysis defined the following minerals: montmorillonite 1%, illite-montmorillonite 3%, muscovite 34%, chlorite 14%, quartz 28%, amphibole 1%, plagioclase feldspar 7%, K-feldspar 1%, calcite 5%, dolomite 4%, amorphous 2%

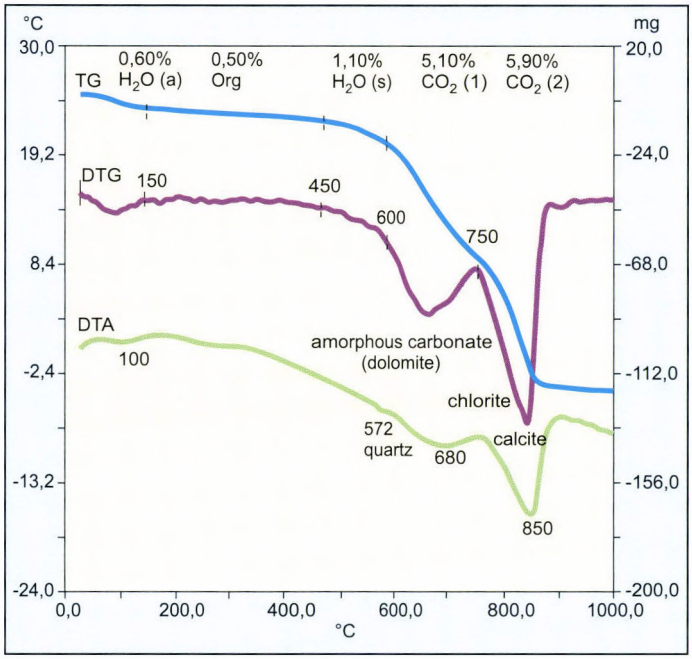

Fig. 21. Thermoanalytical studies of the carbonate layer of the paleosol (11.5 m) of the Susak profile. X-ray analysis defined the following minerals: montmorillo-nite 1%, illite-montmo-rillonite 3%, muscovite 13%, chlorite 11%, quartz 35%, amphibole 1%, plagioclase feldspar 10%, calcite 9%, dolomite 12%, pyrite 3%, amorphous 2%

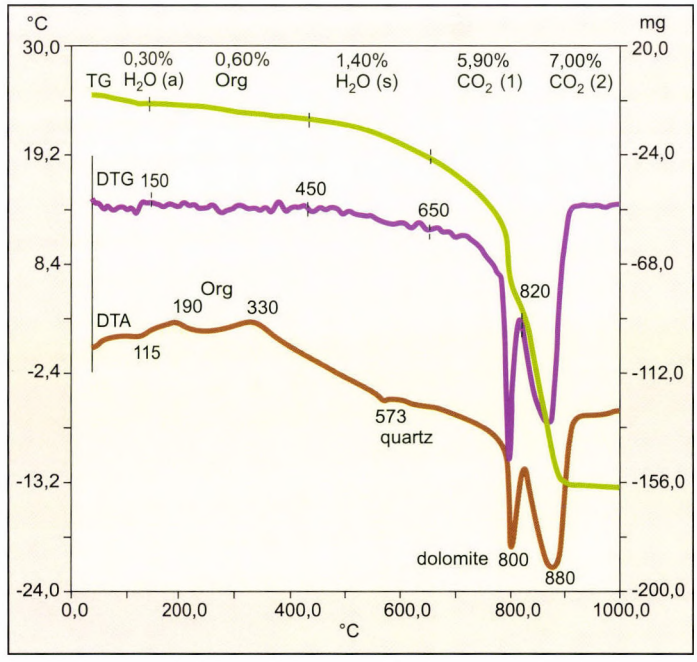

Fig. 22. Thermoanalytical studies of paleosol (18 m) of the Susak profile. X-ray analysis defined the following minerals: montmorillo-nite 1%, illite-montmo-rillonite 2%, muscovite 17%, chlorite 7%, quartz 28%, amphibole 1%, plagioclase feldspar 10%, calcite 9%, dolomi-te 25%

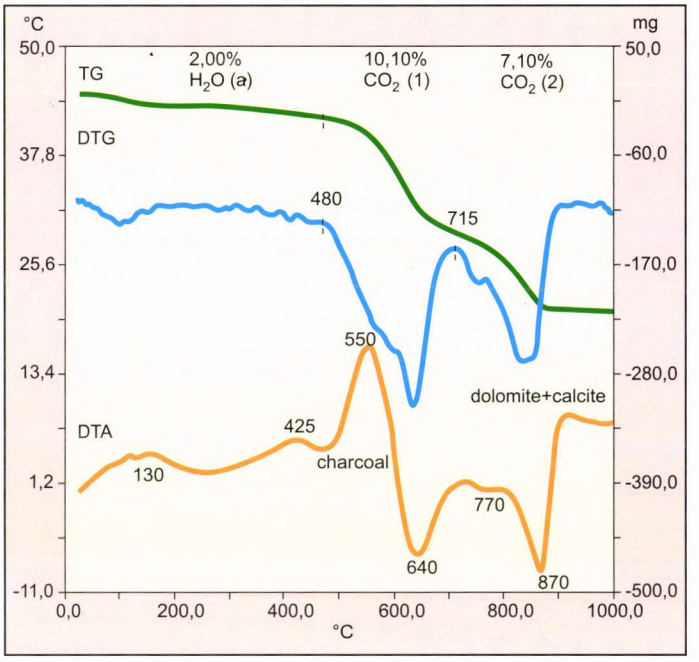

Fig. 23. Thermoanalytical studies of fired layer, containing charcoal from the Susak profile. X-ray analysis defined the following minerals: montmorillonite 1%, illite-montmorillonite 1%, muscovite 14%, chlorite 6%, quartz 27%, amphibole 1%, plagioclase feldspar 11%, K-feldspar 2%, calcite 10%, dolomite 26%, amorphous 1%

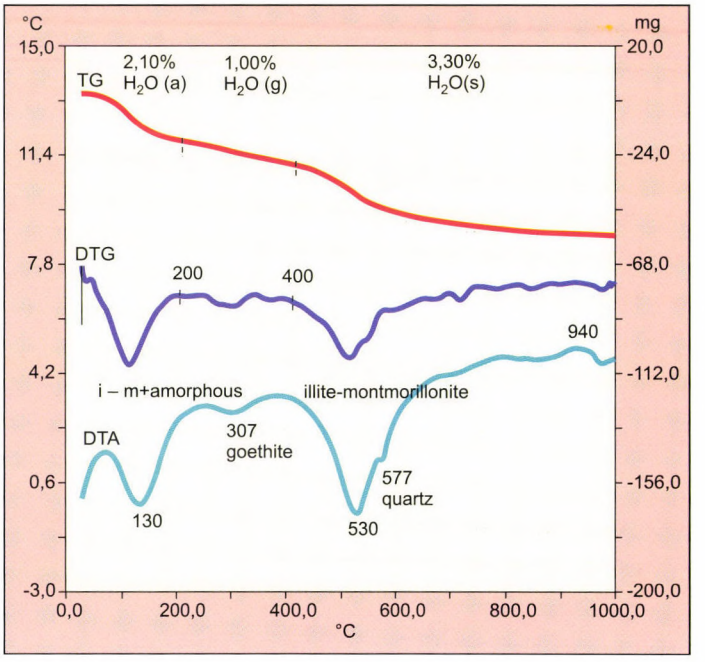

Fig. 24. Thermoanalytical studies of diagenetically altered old loess from the Susak profile. X-ray analysis defined the following minerals: montmorillonite 2%, illite-montmorillonite 4%, illite 14%, chlorite 3%, quartz 42%, plagioclase feldspar 15%, K-feldspar 4%, calcite 3%, pyrite 2%, amorphous 6%

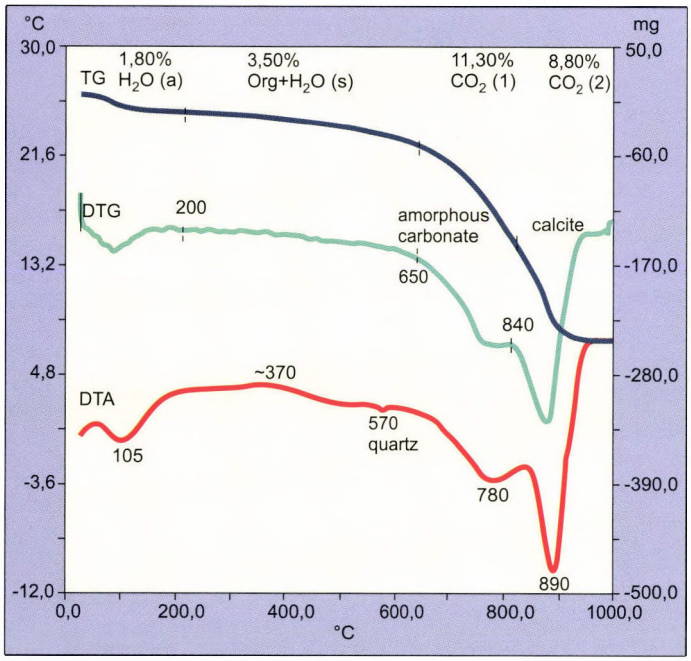

Fig. 25. Thermoanalytical studies of rhyzolith from diagenetically altered old loess from the Susak profile (Croatia). X-ray analysis defined the following minerals: montmorillonite 1%, illite-montmorillonite 1%, muscovite 6%, chlorite 3%, quartz 29%, plagioclase feldspar 10%, K-feldspar 3%, calcite 43%, goethite 2%, amorphous 2%

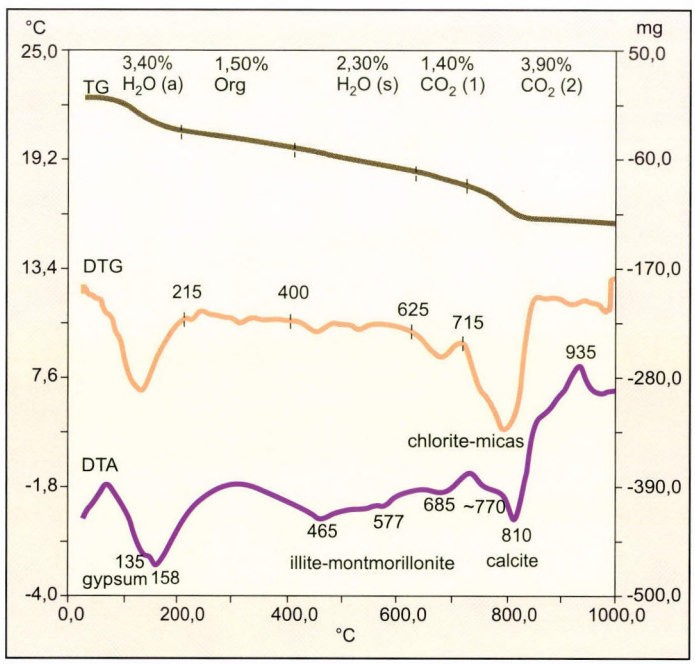

Fig. 26. Thermoanalytical studies of the lower (grey) tephra layer of the Susak profile. X-ray analysis defined the following minerals: illite-montmorillonite 3%, muscovite 19%, chlorite 10%, quartz 29%, amphibole 2%, plagioclase feldspar 17%, calcite 9%, dolomite 7%, gyps 1%, amorphous 2%

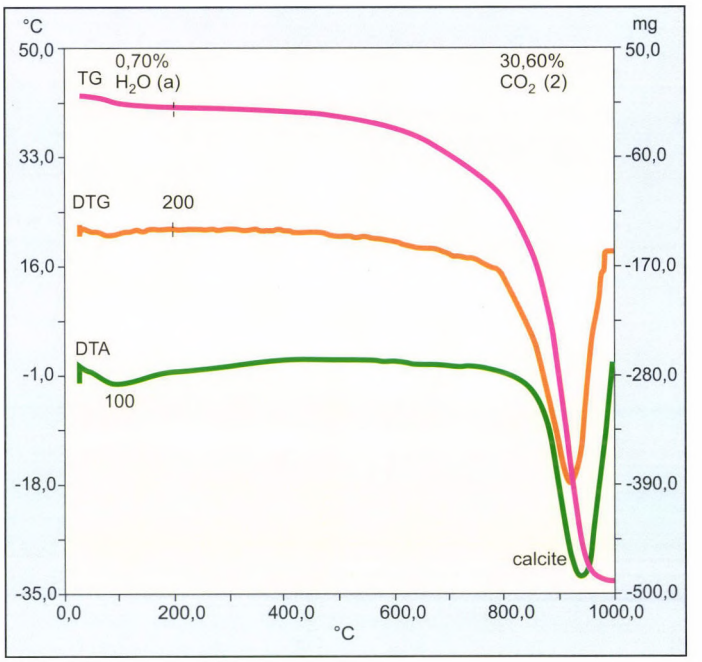

Fig. 27. Thermoanalytical studies of bedded diagenetic carbonate concretion above the lower reddish clay of the Susak profile

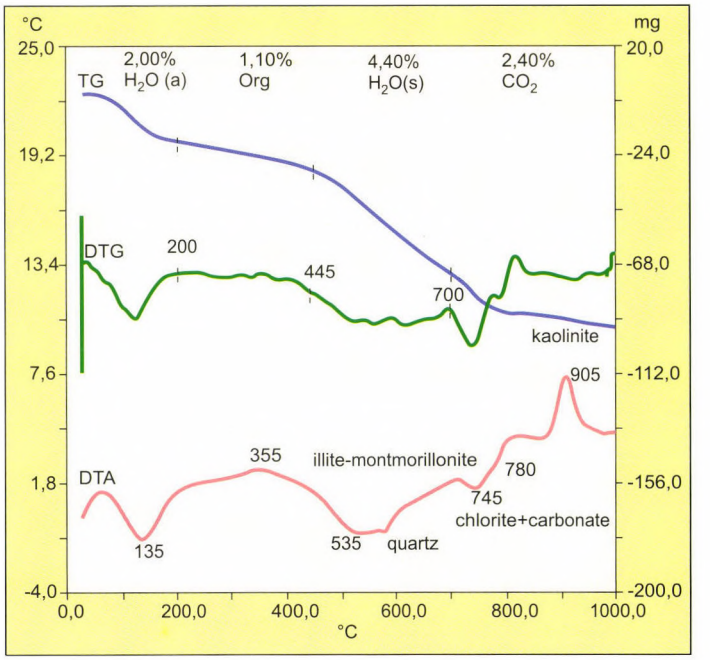

Fig. 28. Thermoanalytical studies of red clay overlying Cretaceous limestone from the Susak profile. X-ray analysis defined the following minerals: montmo-rillonite 2%, illite-montmorillonite 2%, muscovite 20%, kao-linite 1%, chlorite 9%, quartz 29%, amphibole 2%, plagioclase feldspar 15%, K-feld-spar 3%, calcite 11%, dolomite 2%, pyrite 1%, amorphous 3%

Table 5. Determination of main constituents of carbonates in the Quaternary sediments of Susak by the thermoanalytical method

Depth [m]	TG parameter values [m/m%]				Mineralogical composition [%]				
	H_2O (a)	Org	H_2O (s)	CO_2 (1)	CO_2 (2)	Amorphous material	C Org	Clay mineral	Total carbonate
0.50	0.68	0.71	2.47	4.41	9.96	1.36	1.78	23.47	32.62
1.20	0.61	0.37	1.29	4.68	8.28	1.22	0.93	12.26	29.42
1.35	0.69	0.41	1.63	4.78	8.48	1.38	1.03	15.49	30.10
1.85	0.31	0.44	1.45	4.09	8.06	0.62	1.10	13.78	27.58
2.10	0.60	0.21	1.24	4.08	8.16	1.20	0.53	11.78	27.78
2.45	0.59	0.45	1.54	4.09	7.46	1.18	1.13	14.63	26.22
2.85	0.67	0.29	1.38	3.77	6.95	1.34	0.73	13.11	24.33
3.10	0.56	0.38	1.39	3.71	6.81	1.12	0.95	13.21	23.88
3.55	0.53	0.34	0.89	3.33	6.76	1.06	0.85	8.46	22.90
4.40	0.61	0.35	1.12	3.31	7.93	1.22	0.88	10.64	25.51
6.15	0.62	0.44	0.97	4.19	7.07	1.24	1.10	9.22	25.56
6.25	0.50	0.50	1.38	3.98	7.80	1.00	1.25	13.11	26.74
6.65	0.48	0.46	1.34	4.01	7.97	0.96	1.15	12.73	27.19
6.80	0.36	0.28	1.10	4.45	8.49	0.72	0.70	10.45	29.37
9.82	0.65	0.50	1.50	2.57	4.92	1.30	1.25	14.25	17.00
11.00	0.68	0.31	1.77	1.24	4.85	1.36	0.78	16.82	13.82
11.30	0.57	0.33	1.45	2.24	4.69	1.14	0.83	13.78	15.73
11.60	0.90	0.37	1.32	4.35	6.11	1.80	0.93	1.54	23.74
13.60	0.28	0.22	0.58	3.10	6.26	0.56	0.55	5.51	21.25
14.15	0.58	0.27	0.84	2.60	4.83	1.16	0.68	7.98	16.87
14.30	0.58	0.44	1.10	0.00	7.55	1.16	1.10	10.45	17.14
16.50	1.07	0.83	1.82	3.46	3.66	2.14	2.08	17.29	16.16
16.51	2.58	1.08	2.31	2.22	2.01	5.16	2.70	21.95	9.60
16.80	0.82	0.70	1.63	4.77	4.64	1.64	1.75	15.49	21.36
17.00	0.56	0.67	1.44	5.94	7.11	1.12	1.68	13.68	29.62
17.70	0.73	0.27	1.08	3.85	5.90	1.46	0.68	10.26	22.13
18.00	1.78	0.71	1.57	1.65	2.56	1.56	1.78	14.92	9.56
18.25	1.47	0.55	2.04	1.59	1.79	2.94	1.38	19.38	7.67
18.50	1.67	0.76	1.43	1.86	0.00	3.34	1.90	13.59	4.22
18.75	1.71	0.73	1.88	1.69	1.00	3.42	1.83	17.86	3.84
19.00	1.36	0.72	1.57	3.87	6.99	2.72	1.80	14.92	24.65
19.20	0.55	0.44	1.34	3.98	5.96	1.10	1.10	12.73	22.56
19.40	0.49	0.19	0.96	2.97	5.99	0.98	0.48	9.12	20.34
19.65	0.97	0.59	1.39	3.66	5.63	1.94	1.48	13.21	21.09
19.80	0.96	0.55	1.25	3.55	5.48	1.92	1.38	11.88	20.50
19.90	1.00	0.55	1.24	3.94	7.92	2.00	1.38	11.78	26.92
20.05	0.50	0.55	1.21	3.76	6.91	2.10	1.25	11.50	24.22
20.12	0.79	0.45	1.10	3.79	7.04	1.58	1.13	10.45	24.58
20.22	1.00	0.42	1.08	3.52	5.53	2.00	1.05	10.26	20.54
20.28	0.51	0.34	0.81	2.96	4.62	1.02	0.85	7.70	17.21

Table 5. (Continuation)

Depth [m]	TG parameter values [m/m%]				Mineralogical composition [%]				
	H_2O (a)	Org	H_2O (s)	CO_2 (1)	CO_2 (2)	Amorphous material	C_{org}	Clay mineral	Total carbonate
19.80	0.96	0.55	1.25	3.55	5.48	1.92	1.38	11.88	20.50
19.90	1.00	0.55	1.24	3.94	7.92	2.00	1.38	11.78	26.92
20.05	0.50	0.55	1.21	3.76	6.91	2.10	1.25	11.50	24.22
20.12	0.79	0.45	1.10	3.79	7.04	1.58	1.13	10.45	24.58
20.22	1.00	0.42	1.08	3.52	5.53	2.00	1.05	10.26	20.54
20.28	0.51	0.34	0.81	2.96	4.62	1.02	0.85	7.70	17.21
20.60	0.70	0.26	0.99	3.19	6.06	1.40	0.65	9.41	21.00
21.00	0.68	0.36	1.15	3.19	7.37	1.36	0.90	10.93	23.97
21.40	0.92	0.56	1.49	4.16	5.91	1.84	1.40	14.16	22.86
21.55	1.16	0.70	2.00	0.00	6.72	2.32	1.75	19.00	15.25
21.65	0.89	0.32	1.19	2.69	5.55	1.78	0.80	11.31	18.70
21.85	0.59	0.31	1.09	2.71	5.48	1.18	0.78	10.36	18.59
22.10	0.71	0.31	1.13	2.55	4.28	1.42	0.78	10.74	15.50
22.15	0.78	0.27	1.05	2.28	4.41	1.56	0.68	9.98	15.19
22.30	1.94	0.66	1.76	1.51	0.00	3.88	1.65	16.72	3.43
22.50	1.75	0.55	2.14	0.00	2.37	3.50	1.38	20.33	5.38
22.75	2.60	1.00	2.78	0.00	0.00	5.20	2.50	26.41	0.00
22.90	1.44	0.43	1.63	1.24	0.00	2.88	1.08	15.49	2.81
23.15	1.71	0.72	1.87	0.00	1.62	3.42	1.80	17.77	3.68
23.45	2.18	0.82	1.96	0.81	0.00	4.36	2.05	18.62	1.84
23.75	1.57	0.72	1.95	0.00	0.00	3.14	1.80	18.53	0.00
23.95	1.92	0.88	1.92	1.15	0.00	3.84	2.20	18.24	2.61
24.80	0.69	0.44	1.98	1.45	6.25	1.38	1.10	18.81	17.48
25.50	3.40	1.50	2.30	1.40	3.90	6.80	3.75	21.85	12.03
26.50	1.20	0.60	2.90	7.10	0.00	2.40	1.50	27.55	16.12
27.50	1.70	0.70	3.00	2.10	0.00	3.40	1.75	28.50	4.77
30.50	0.70	0.00	0.00	0.00	30.60	1.40	0.00	0.00	69.46
31.50	2.00	1.10	4.40	2.40	0.00	4.00	2.75	41.80	5.45

7.2. Results of chemical analyses

Chemical analyses were aimed at an exact determination of carbonate content, namely the variations of the total carbonate content by SCHEIBLER (*Table 5*) and those of complexometrically titrated $CaCO_3$ and $MgCO_3$ changes with depth (*Table 6*).

BLOHM M. introduced the nomenclature based on limit values of $MgCO_3$ content (1974) to identify Ca-Mg carbonate minerals. The x-ray diffraction examinations proved so far only calcite and dolomite as individual phases. In the thermic analyses, however, beside the typical twin dolomite peaks characteristic DTA curve running down attributed to protodolomites could be observable. $MgCO_3$ m% of the

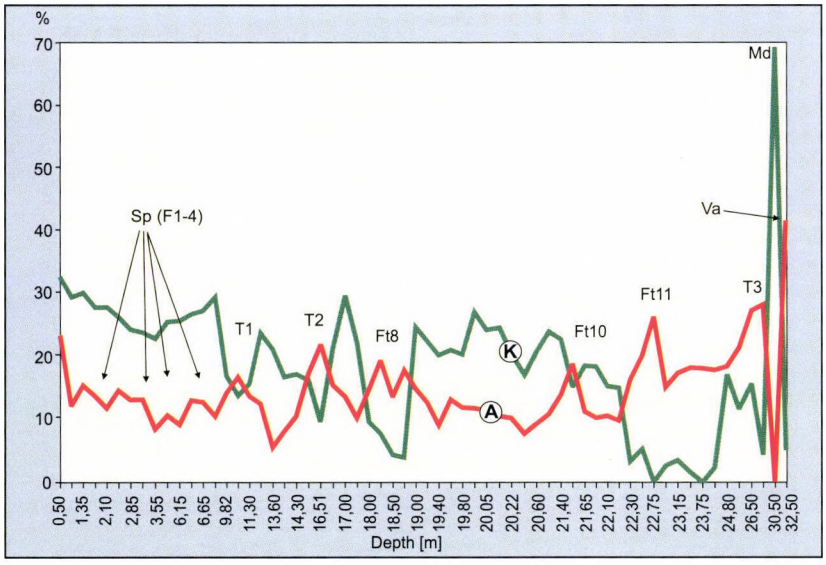

Fig.29 . Variations of mass changes in total carbonate and clay mineral content (TG, Δm%) with depth. – Sp = humified horizon; Ft = paleosol; Va = red clay; T = tephra; Md = diagenetic carbonate concretions; A = clay minerals; K = total carbonate content

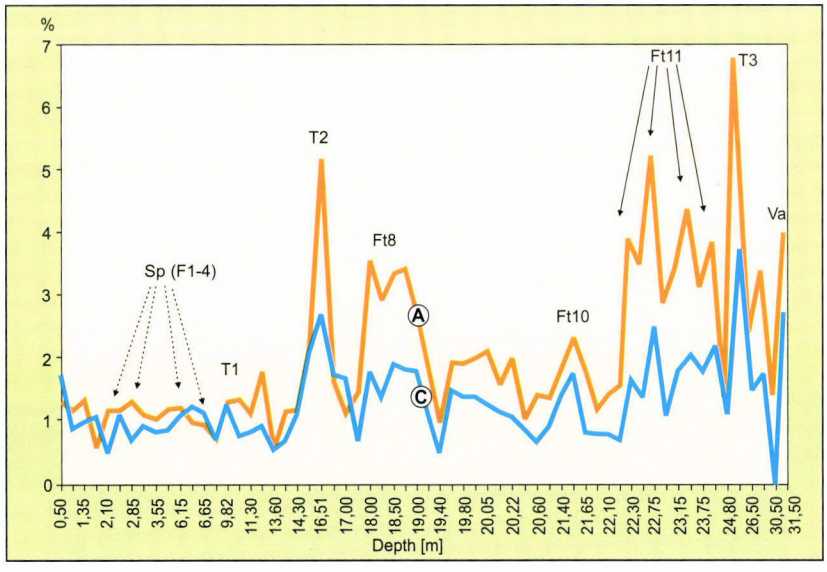

*Fig. 30. V*ariations of mass changes in amorphous and organic material content (TG, Δm%) with depth. – Sp = humified horizon; Ft = paleosol; Va = reddish clay; T = tephra; A = amorphous material; C = organic C content

Table 6. Determination of main constituents of carbonates in the Quaternary sediments by chemical method

Depth [m]	$CaC0_3$ [m/m %]	$MgC0_3$ [m/m %]	$CaC0_3$ [mol %]	$MgC0_3$ [mol %]	$\frac{CaCO_3}{MgCO_3}$ [mol]
0.50	20.65	12.37	58.57	41.43	1.41
1.20	20.65	9.16	65.08	34.92	1.86
1.35	21.74	10.08	64.18	35.82	1.79
1.85	20.65	7.79	69.49	30.51	2.28
2.10	21.74	6.87	72.88	27.12	2.69
2.45	20.65	6.87	71.93	28.07	2.56
2.55	18.48	6.87	69.81	30.19	2.31
3.10	19.02	6.42	71.70	28.30	2.53
3.55	17.39	5.96	71.43	28.57	2.50
4.40	19.02	7.79	67.86	32.14	2.11
6.15	17.94	7.79	66.67	33.33	2.00
6.25	20.11	6.42	72.73	27.27	2.67
6.65	20.11	7.79	68.97	31.03	2.22
6.80	21.74	8.71	67.19	32.81	2.05
9.82	13.58	5.50	67.50	32.50	2.08
11.00	11.96	5.04	66.67	33.33	2.00
11.30	11.96	5.04	66.67	33.33	2.00
11.60	15.22	10.08	55.56	44.44	1.25
13.60	15.22	7.79	62.50	37.50	1.67
14.15	11.96	5.96	63.16	36.84	1.71
14.30	13.59	5.96	65.85	34.15	1.93
16.50	10.87	6.87	57.89	42.11	1.37
16.51	7.06	5.50	54.85	45.15	1.21
16.80	12.50	5.04	67.57	32.43	2.08
17.00	18.48	9.62	61.67	38.33	1.61
17.70	13.04	5.04	68.42	31.58	2.17
18.00	10.87	1.37	88.00	12.00	7.33
18.25	7.06	5.50	51.85	48.15	1.08
18.50	5.43	1.37	78.57	21.43	3.67
18.75	4.89	1.83	69.23	30.77	2.25
19.00	19.02	6.42	71.70	28.30	2.53
19.20	17.94	6.42	70.59	29.41	2.40
19.40	15.76	5.04	72.09	27.91	2.58
19.65	16.30	5.96	70.21	29.79	2.36
19.80	15.76	3.66	77.50	22.50	3.44
19.90	21.20	5.96	75.00	25.00	3.00
20.05	18.48	5.96	72.55	27.45	2.64
20.12	17.39	7.79	66.04	33.96	1.94
20.22	13.58	6.42	64.29	35.71	1.80

Table 6. (Continuation)

Depth [m]	$CaC0_3$ [m/m %]	$MgC0_3$ [m/m %]	$CaC0_3$ [mol %]	$MgC0_3$ [mol %]	$\frac{CaCO_3}{MgCO_3}$ [mol]
20.28	10.87	5.96	61.11	38.89	1.57
20.60	14.13	5.50	68.29	31.71	2.15
21.00	16.85	6.42	69.39	30.61	2.27
21.40	16.85	5.50	72.34	27.66	2.62
21.55	13.04	3.21	76.47	23.53	3.25
21.65	14.67	5.50	69.05	30.95	2.23
21.85	11.96	6.87	60.00	40.00	1.50
22.10	9.78	5.96	58.82	41.18	1.43
22.15	10.33	5.04	63.34	36.66	1.73
22.30	2.17	1.37	57.14	42.86	1.33
22.50	5.43	0.46	91.67	8.33	11.00
22.75	0.54	0.92	33.33	66.67	5.50
22.90	2.17	1.37	57.14	42.86	1.33
23.15	2.72	2.29	50.00	50.00	1.00
23.45	1.63	1.37	50.00	50.00	1.00
23.75	0.54	0.92	33.33	66.67	0.50
23.95	2.17	2.29	44.44	55.56	0.80
24.80	13.04	5.96	65.00	35.00	1.86
25.50	12.42	2.63	80.65	19.35	4.17
26.50	14.30	4.84	72.50	27.50	2.64
27.50	5.99	0.79	95.59	14.29	6.00
30.50	64.78	2.50	85.71	4.41	21.68
31.50	8.37	1.21	85.00	15.00	5.67

different samples was plotted against depth on *Fig. 31*, and the calcite, magnetocalcite, protodolomite, dolomite and dolomite+magnezite areas were marked according to the Blohm limit values. Thus the carbonate facies of the Susak loess profile were supposed to be specified.

7.3. Results of preliminary stable isotope analyses

Regularities in isotopic composition of carbon and oxygen from terrestrial carbonate sediments, carbonates and diagenetic carbonate concretions were described by HUDSON J. D. (1977). In his work he unfold in detail the environmental factors, diagenetic and fossilisation parameters that can be the cause for the isotopic composition of the different sediments.

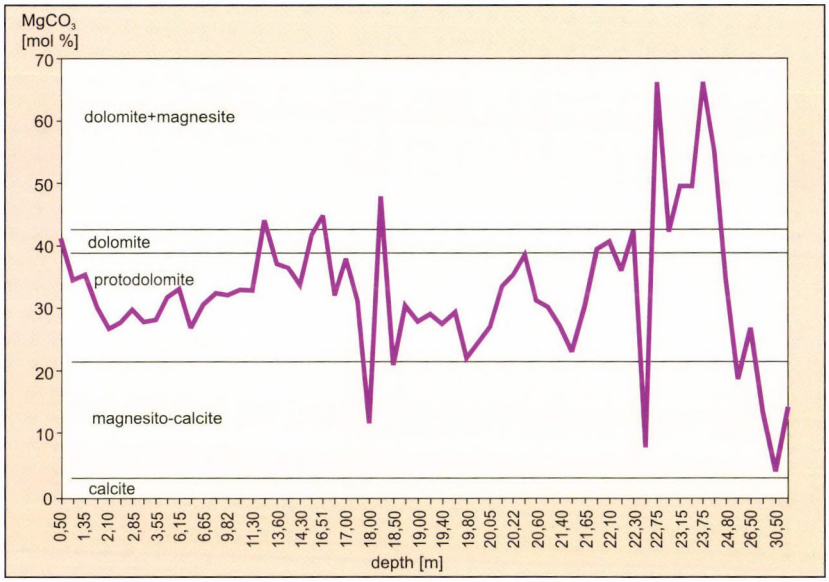

Fig. 31. Variations in $MgCO_3$ gramme-molecule % with depth, in order to name the typical carbonate facies

On the basis of these data some of the relevant formations of the Susak loess profile were compared to each other, such as reddish clays, paleosols, diagenetic carbonate concretions (rhyzolith and bed) and tephras.

Results are reported in *Table 7*, projection points of isotopic rates of $\delta^{13}C$ and $\delta^{18}O$ are shown in *Fig. 32*.

Before discussing the results it should be emphasised that reddish clays and diagenetic concretions in the lower part of the profile form a rather well defined group, they are separated from the paleosols and tephras which also can be differentiated.

$\delta^{13}C$ values range between 2 and 11‰ and $\delta^{18}O$ values between 4 and 6.5‰.

7.4. Microscopic and electron microscopic evidences

The reddish clay layer within the Susak loess profile is overlain by a thick limestone-like formation of which several thin sections were prepared and examined under polarizing microscope (RÓZSA, P. 1998). *Photos 35* and *36* show two textural views at 200× magnification and at crossed nicols.

These two pictures show unambiguously that the formation is porous and the main part of it is constituted by carbonate (calcite) matter *(Fig. 27)*.

The matrix is coloured at some parts of limonite spots. Most of the clastic grains are angular, subangular, often with undulatory extinction (metamorphic) quartz grains.

Table 7. Stable isotope examination of important Susak formations

Sample signature	Depth (m)	Formation	$\delta^{18}O$ (SMOV) (‰)	δ^{13} (PDB) (‰)
Su-1	32.50	red clay	–4.42	–10.3
Su-2	23.30	reddish brown soil	–6.58	–9.68
Su-3	9.80	tephra	–5.29	–8.91
Su-4	26.50	tephra	–6.31	–3.41
Su-5	31.50	reddish clay	–4.66	–10.92
Su-5k	30.50	diagenetic carbonate	–4.13	–9.81
Su-6	18.50	fossil soil	–5.02	–3.99
Su-7k	24.90	diagenetic carbonate	–3.94	–8.67
Su-8	21.30	fossil soil	–5.04	–1.56

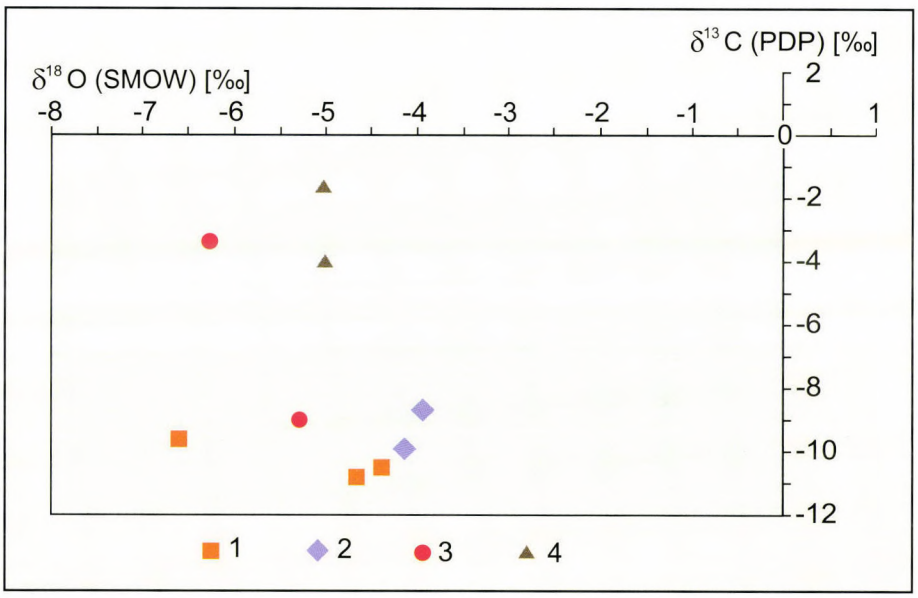

Fig. 32. Stable isotope examination of important Susak formations. – 1 = red clay, reddish clay; 2 = diagenetic carbonate; 3 = tephra; 4 = paleosol

It is rich in muscovite. It is noteworthy that plagioclase feldspar was found, although in much lower quantities. The specimen on *Photo 36* has a very nice shape indicating that it was affected by water for only a short time.

As a result it is presumed that the carbonate cementation is of fluviatile type, or it rather preserved a beach sand accumulation as a specific coastal diagenetic formation. Other sandy formations of the profile (*Fig. 4*) are eolian, as shown in the well abraded quartz grains belonging to category 5 according to PETITJOHN (SCHNEIDERHÖHN P. 1959).

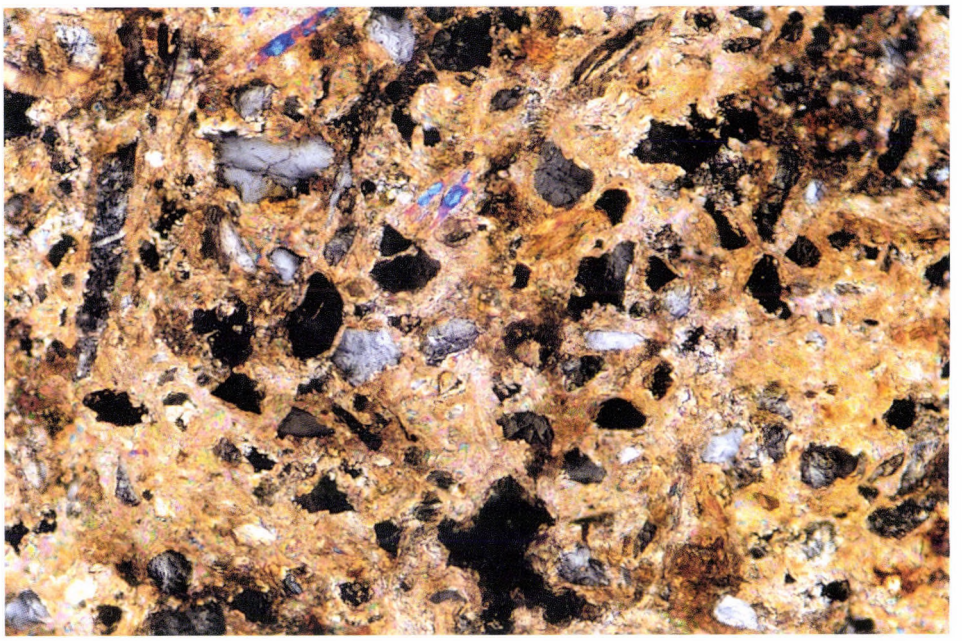

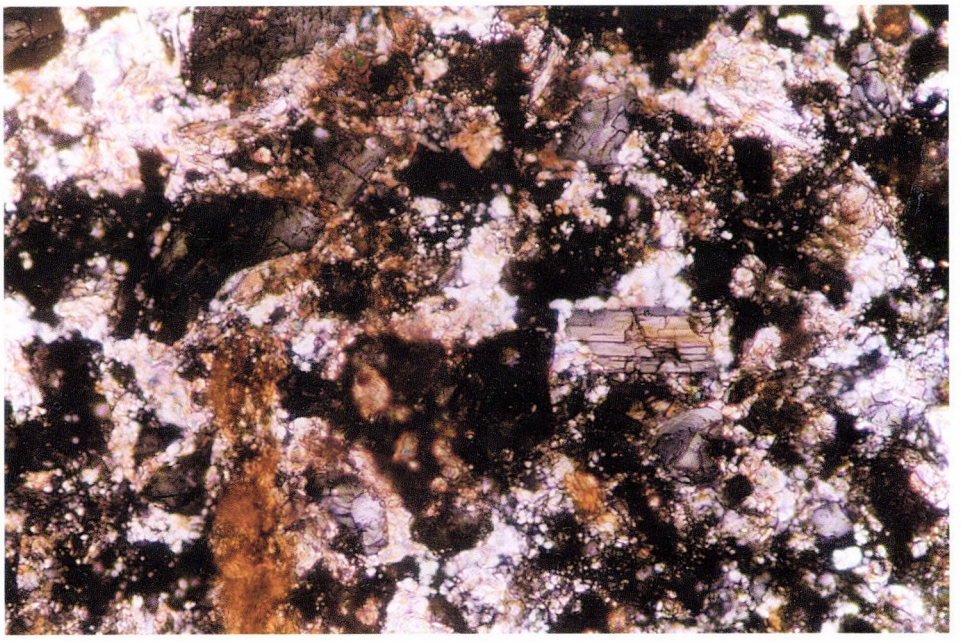

Photos 35 and *36.* Microscopic analysis of the horizontally bedded diagenetic formation on the top of the lower reddish clay layer of Susak loess profile. Crossed nicols, M 200×.

On Picture (*Photo 37*) a type specimen can be observed in a form of a quartz grain originating from layer between 12.50–12.60 m depth. On the surface of the grains the structural features of solution process after the deposition can be seen that prove the presence of intense diagenetic processes along the profile.

7.5. Evidence from microprobe (SEM-EDAX) examinations

Grains larger than 200 μm of the Susak loess profile were examined under binocular microscope and the globular ones, the so called spherulites were separated. These type of grains were found in two formations, in the reddish clay overlying the lower Cretaceous sequence (*Photo 38*), and in sandy loess at a depth between 23.85 and 24.05 m (*Photo 39*).

Spherula coming from the reddish clay is diagenetic in origin (besides ferrum, with high manganese, aluminium and silica content), and the old loess contains extraterrestrial objects (Fe-micrometeorites). They fail to occur in other parts of the profile.

In the course of the analysis principal attention was paid to the study of clay and carbonate minerals regarding their composition, and determination of organic and amorphous matter, and to description of their distribution and features in the different formations.

We think that comparisons of other mineral components of the Hungarian loess formations and the Susak profile hold further importance.

Results of mineralogical examinations on six various loess profiles of Hungary (PÉCSI, M. 1993) were published by PÉCSI-DONÁTH, É. (1979, 1987). Averaging these data the mineralogical spectra of Hungarian loesses were prepared. By courtesy of KOVÁCS-PÁLFFY, P. (MÁFI) available his average results from 25 x-ray diffraction measurements has been made *(Fig 33).*

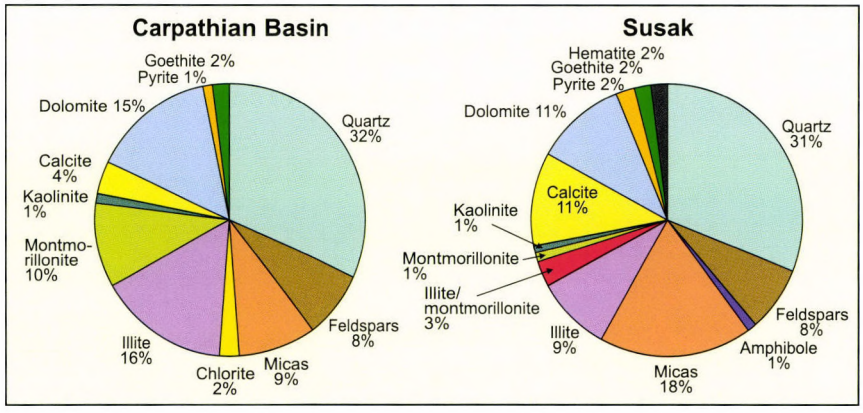

Fig. 33. Mineralogical composition of Susak loess profile and Paks loesses based on x-ray diffraction analyses (KOVÁCS-PÁLFFY P. 1998; PÉCSI-DONÁTH É. 1985)

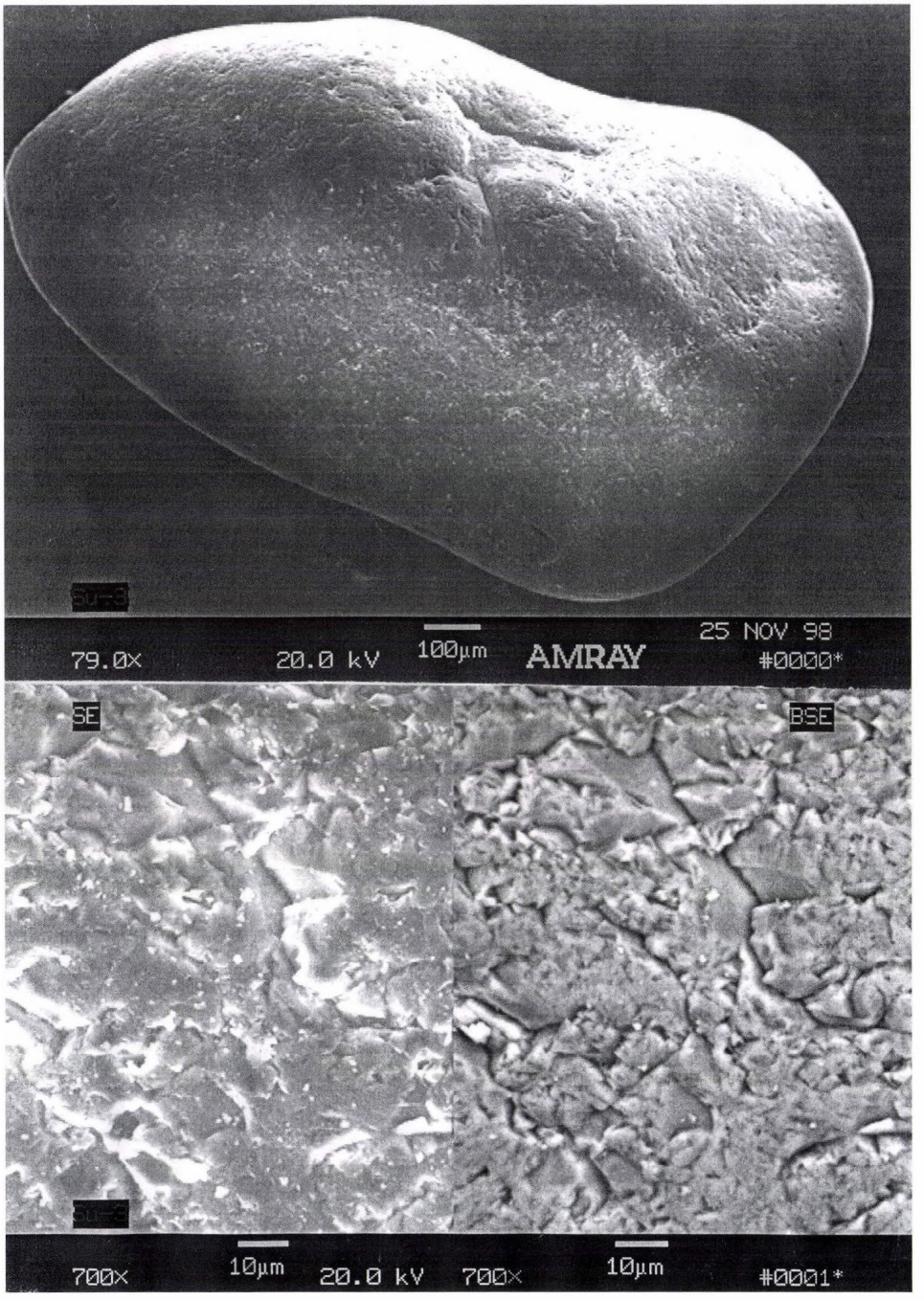

Photo 37. Abraded quartz grain from sand, with diagenetic solution features on its surface

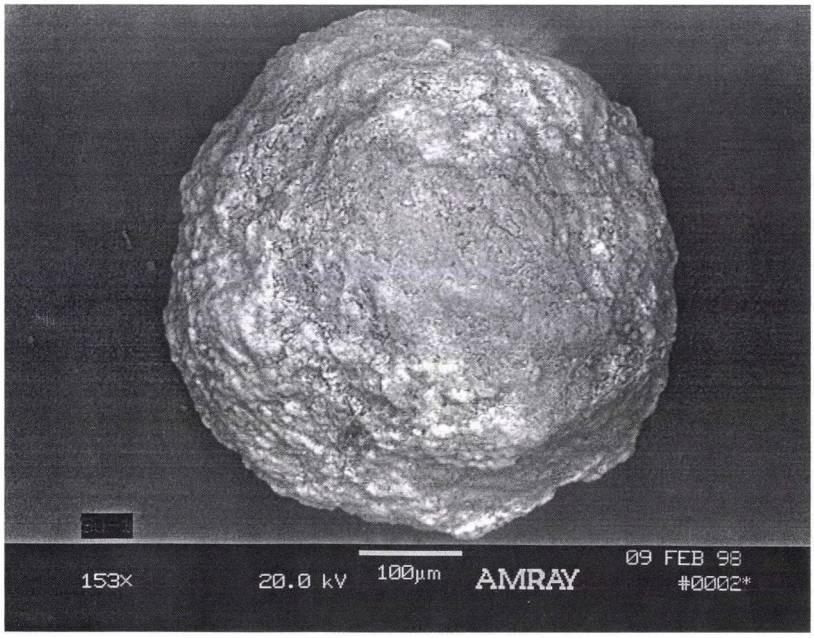

Photo 38. Diagenetic spherula from the red clay bed.

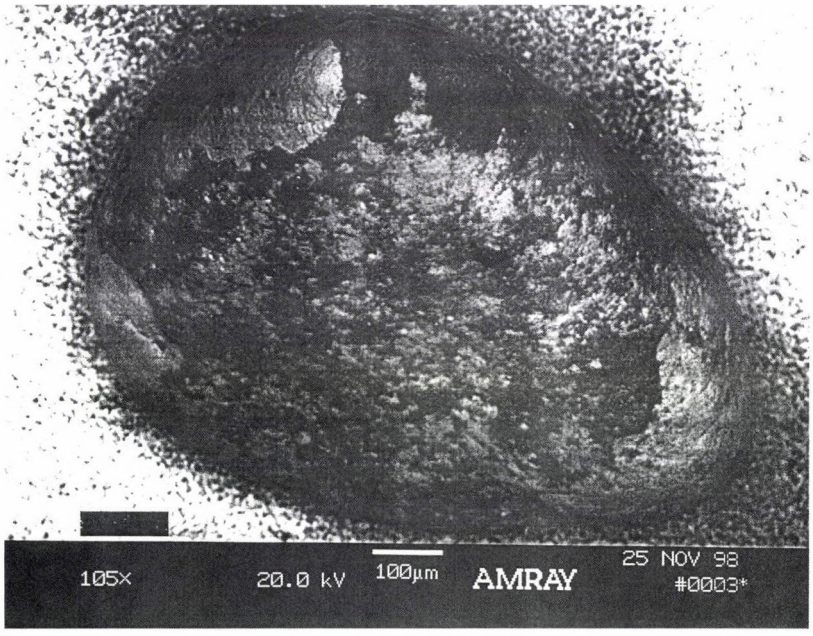

Photo 39. Micrometeorite from the Susak loess

Using the above data and those of our own, the followings can be concluded:

– Regarding clay mineral paragenesis, Susak formations can be described with chlorite and mixed illite-montmorillonite structures. Smectites are characteristic for tephras, whereas kaolinite is typical of the reddish clay only.

– It is typical of carbonate mineral paragenesis that both dolomite and calcite occur in the profile. Comparing to the Hungarian profiles, on Susak less dolomite occurs than calcite. Our analysis has revealed that the material cementing diagenetic concretions is calcite, whereas dolomite enrichment can be observed in two layers of the profile. On the basis of the results obtained by the thermic method most of the formations can be labelled as "protodolomite facies".

– According to the thermalanalyses, humified horizon, lying close to the surface contains less clay mineral than carbonates (otherwise they are similar to the parent rock). The former might be considered to be characteristic formations of the desert margin, as BRUINS H.J. and YAALON D.T. showed from the Negev desert (1979).

– Clay mineral content in paleosols and tephra horizons, as well as in the reddish clay bed is always higher than carbonate content.

– Amorphous matter shows enrichment in the lower sediments of the profile, reaching its maximum in tephras and paleosols. It changes with organic material (Corg) value.

– Diagenetic hematite, gypsum and portlandite appear as important indicator minerals. All of them are characteristic in the upper part of the profile, while gypsum is detectable near to the lower tephra layer as well.

– Charcoal remains can be found in two layers of the profile. According to the thermalanalysis they are result of forest or bush fires and not of decomposition under humid conditions.

– Morphometric analysis of quartz grains proves that sand from the bottom of the profile are marine (or perhaps fluviatile) in origin, other sediments are coarse grained, as a result of wind action.

– Considering the preliminary stable isotopic examinations and references (FRITZ P. et FONTES I.C.H. 1989; HUDSON J.D. 1977; MANZE U. et al. 1974) reddish clays in the lower part of the profile were formed under warm and humid climates, while the diagenetic carbonate concretions (rhyzolites, beds) in warm and arid environmental conditions. Paleosols could be formed during interglacials.

– Diagenetic spherules of red clay forming the bedrock allow us to conclude to warm and humid subtropical environment.

– Notable extraterrestrial event in the profile cannot be suggested.

Considering all of these data the geological view of the island can be modified as follows.

– Typical red clay overlying the Cretaceous so called rudist limestone facies forming the basement of the island must have developed more than 700,000 years BP. Comparing our thermoanalytical results with the results of SCHWEITZER, F. et SZÖŐR, GY. (1997), it can be stated that the Susak formations in a mineralogical-

geochemical point of view are very similar to the Hungarian Csarnótanum "typical red clay" formations (4.0–3.0 ma BP).

– Sand benches were settled in a tidal flat, but diagenetic carbonate concretions developed under the impact of atmospheric precipitation (meteoric diagenesis, HAAS J. 1998, p. 120).

– Carbonate concretions above reddish clay are chalich-type and the dolomitisation of the environment can also be observable, thus warm and arid climatic change can be suggested. This is also supported by the gypsum concretion around the lower tephra layer.

– It is probable that there is a sediment gap above these older formations.

– Paleosols and humified horizons differ from each other with regards to their formation processes. Paleosols can be attributed to warming periods with more humidity, while humified horizons developed under more arid climates. Gypsum and hematite in the upper part of the profile can also be attributed to that thermoxerotic phase. $Ca(OH)_2$ and portlandite in the upper part of the profile is the result of present day climate, characterised by an intense evaporation during summer.

8. MAGNETOSTRATIGRAPHIC INVESTIGATIONS

Quaternary loessial sequence in the Carpathian Basin and northern Adriatic Region has been studied by traditional lithostratigraphic and paleopedological methods and subdivided into two major series: the so called 'young' and 'old' loesses.

Paleomagnetic methods have been involved in chronological studies of loess series within these characteristic sediment sequences (Paks 1977, Slankamen 1977, Susak 1997).

The Brunhes–Matuyama paleomagnetic boundary and the Matuyama epoch were identified using paleopedological and paleomagnetic methods by the late 1970s.

Attempts have been made (by performing several hundred measurements) to trace the fluctuations within the Brunhes epoch, but only some of them could be fixed in certain localities (MÁRTON, P. Hódmezővásárhely 1979, BALOGH, J. Paks 1989, Mende 1989).

In the literature on paleomagnetism several events are described based on the lithostratigraphic subdivision of the young loess sequence. Of them the most important ones are the following: Blake (dated ca 100 000 yr. BP), Lachampe (35 000–40 000 yr. BP), Mono (27 000–29 000 yr. BP), Göteborg (12 000 yr. BP). There have been reported, however, several changes in paleomagnetism from different localities. Of the latter those confined to marker horizons were identified in lacustrine deposits. This is why it is not very likely that these short spells in a geological sense could be traced in sequences of autochtonous position.

When performing paleomagnetic investigations of loess samples, because of specific conditions of terrestrial landform evolution and probable presence of sedimentation gaps, there has been widely accepted that (in a lack of changes in inclination) paleomagnetic events can be deduced from the trend of magnetic values. Taking into account the rate of sedimentation of loess material (0.005–0.5 mm/yr; VELICHKO, A. 1973), in the case when short spells of reversed polarity (100–1000 yr) were considered, a separate evaluation of the measured magnetic data of each specimen seemed to be expedient.

The paleomagnetic polarity of fossil soils was analysed on samples collected by BOGNAR, A. and ZÁMBÓ, L. in 1993. The measurements were performed in the laboratory of the Department of Geophysics, Eötvös Loránd University (DG ELTE, Budapest) headed by P. MÁRTON. All the specimens showed normal polarity as it had been anticipated from the sporadic character of sampling.

The 1997 sampling was aimed at the identification of the Brunhes–Matuyama boundary while that of 1998 was purposed for revealing the Blake event.

Of the fossil soils found at Susak (*Photo 40*) the PD-type SAV (Susak Lower Red) paleosol (*Photo 41*) and the BD-type chernozem brown forest soil were selected for subsequent paleomagnetic analysis.

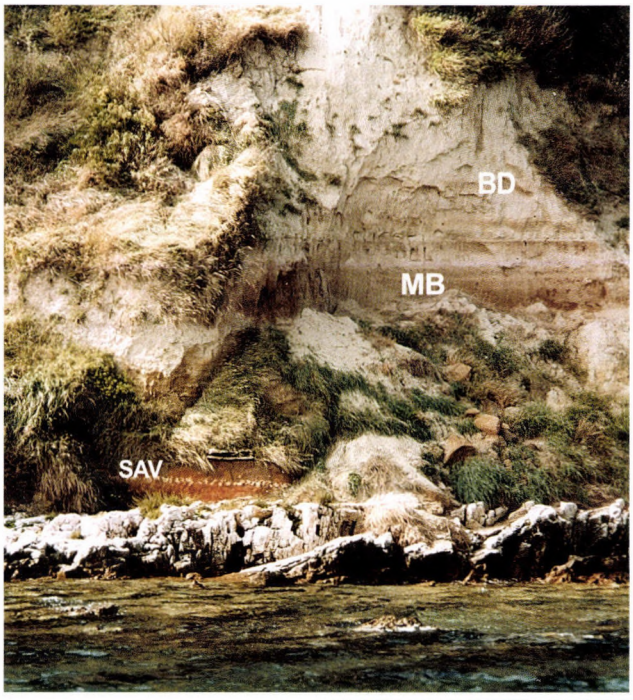

Photo 40. Geological position of BD, MB and SAV fossil soils at Susak (Photo by F. SCHWEITZER)

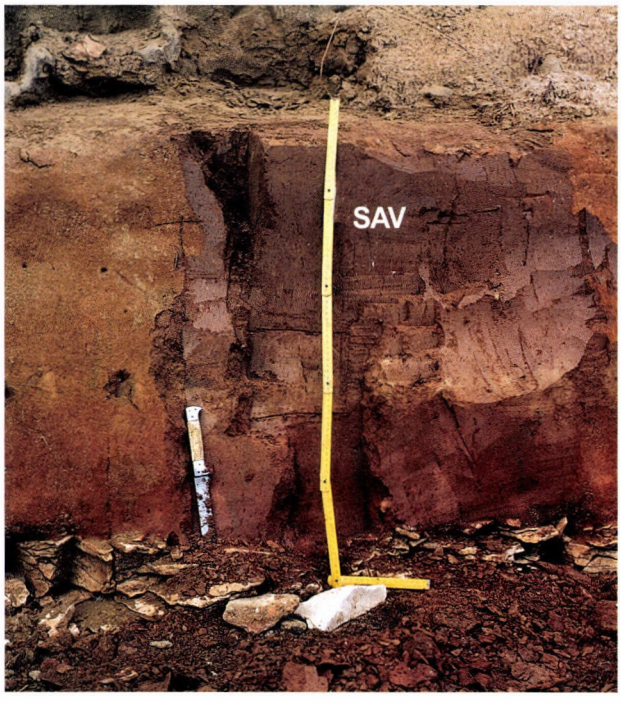

Photo 41. Profile of SAV fossil soil studied with the paleomagnetic method (Photo by J. BALOGH)

The measurements were carried out at the DG ELTE under the guidance of P. MÁRTON.

The stable magnetisation of the young sediments either is related to the period of sedimentation but it might be of chemical origin as well; sometimes it is the combination of the two.

Generally speaking, sands and clays contain geomagnetised grains, which align in the direction of the geomagnetic field contemporaneous to sedimentation thus endowing the deposits remanent magnetisation.

In an environment with low energy the declination of the former magnetic field usually is well reflected by the direction of magnetisation during sedimentation. The inclination however, owing to the compaction of the layers might be reduced considerably compared to that at the time of sedimentation. However, if there is time enough for the reorientation of the grains by the changed geomagnetic field after sedimentation, the inclination can be measured well.

From the paleosol SAV of 66 cm thickness, overlying the limestone on the sea level at the foot of the Susak profile, 7 pairs of monoliths had been taken for subsequent analyses. Because of the 'soft' magnetisation the specimens were held in shady place during the intervals between the measurements of magnetic orientation.

The temperature was increased in short steps taking care of samples of poor magnetisation.

Steps of glowing were as follows: 5–150–250–350–450–480–550–600 °C until the specimens lost their magnetic intensity.

Remanent magnetisation was determined using jK-2 rock generator. Susceptibility was measured by Kappa meter of KT-S type (Czech made).

8.1. Evaluation of paleomagnetic analyses

The measurements by BOGNAR A.–ZÁMBÓ L. and MÁRTON, P. within the marker paleosols showed normal magnetisation indicating that most part of the studied sediment sequence could be formed during the Brunhes epoch. Representing normal magnetisation of the present time, Brunhes comprises 730 000 years interrupted by shorter magnetostratigraphic intervals (events) of reversed anomalies (PÉCSI, M. 1996).

Another major unit within the magnetic time scale of the Quaternary was Matuyama of reversed polarity between 2 430 000–730 000 yr according to the time scale by Cox.

It contains several magnetostratigraphic intervals of normal polarity:

1. Jaramillo 950 000– 890 000 yr
2. Gilsa 1 620 000–1 610 000 yr
3. Olduvai 1 640 000–1 630 000 yr
4. Reunion I 1 980 000–1 950 000 yr
5. Reunion II 2 130 000–2 110 000 yr

Paleomagnetic measurements have been aimed at the correlation of the Susak 1997 profile with the magnetostratigraphic time scale of the Carpathian Basin and the Adriatic Region.

Paleosol SAV was chosen for a detailed magnetic analysis, for due to its geological position, paleopedological and lithological features of the soil, the Brunhes-Matuyama boundary was supposed to be found within this sediment sequence.

During the measurements of NRM (normal remanent magnetisation) inclination change of polarity did not take place. It is well known, however, that sediments formed during epochs of reversed polarity might acquire normal polarity in a later phase of rock diagenesis. So magnetisation of normal polarity of a certain layer does not exclude its formation during an epoch of reversed polarity. Initial polarity is reached through magnetic cleanings.

This could be observed when carrying out analyses of the samples taken from the middle part of SAV fossil soil (*Fig. 34*).

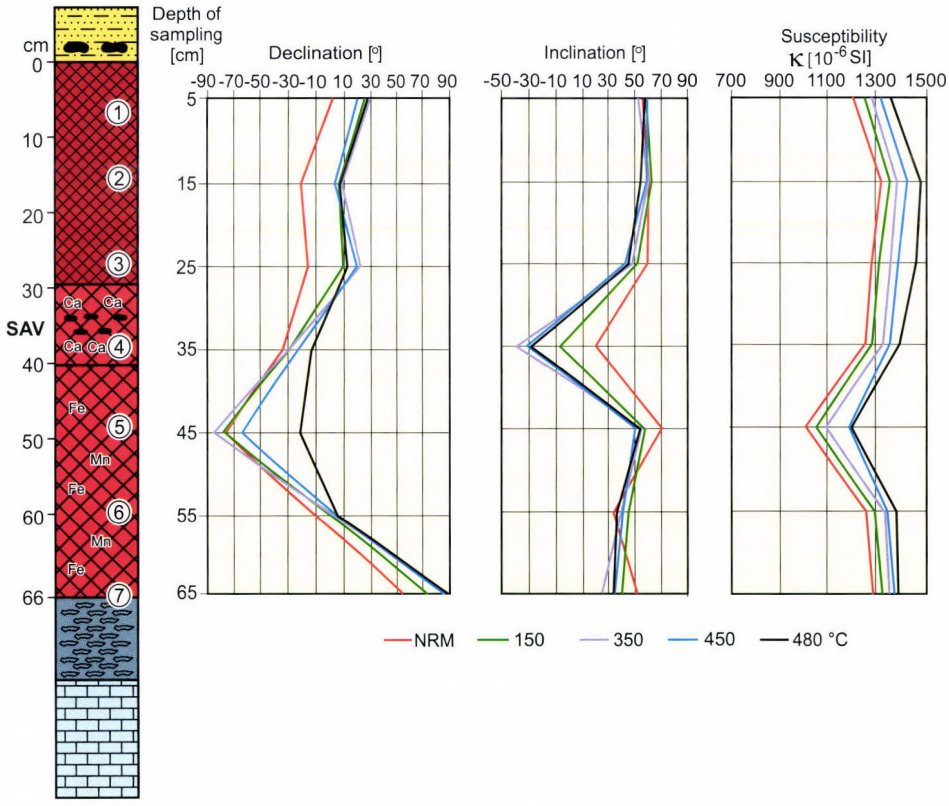

Fig. 34. Paleomagnetic values of SAV (Susak Lower Red) fossil soil in various stages of thermal demagnetisation cleaning (①–⑦ = Paleomagnetic samples) (J. Balogh 2002)

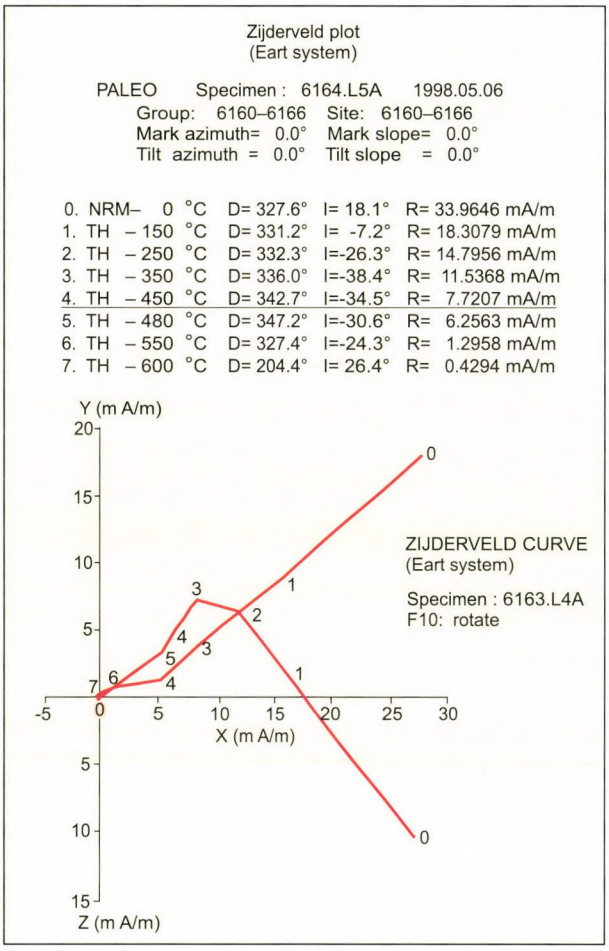

Fig. 35. Orthogonal demagnetisation diagram and results of paleomagnetic analyses of SAV N4 specimen (0–7: phases of thermal demagnetisation)

In the course of measurements of NRM specimen N4 indicated normal magnetisation, then after heating up to 150 °C, inclination was measured and calculated –7.2°, after further cleaning it had been stabilised at about –30°. A characteristic value of paleomagnetism of the given phase is –30.6° (*Fig. 35*). Specimen N4 lost its magnetic intensity at glowing up to 600 °C (*Fig. 36*).

Specimens 1, 2, 3, 5, 7 showed normal magnetisation both during the measurements of NRM and after cleaning through glowing, with measured and calculated data between +30° and +60° values.

In the terrestrial Quaternary sediments the occurrence of unambiguous reversed polarity for only a single sample within a series of measurements is a frequent case. This is explained by specific landform evolution, redeposition of sediments, processes of illuviation and denudation.

In the series of declination measurements specimen N5 showed positive inclination with simultaneous negative declination, i.e. –67° (complementary of 293°). Measurement of initial declination resulted in –84° (complementary of 276°).

Taking into account that N4 has negative values both for inclination and declination (–12.8° and –32.4° i.e. complementary 347.2° and 327.6°), declination shows a tendency to grow in absolute value for the 'two' samples underlying each other. This suggests the *occurrence of a paleomagnetic event in this layer* (*Fig. 37*).

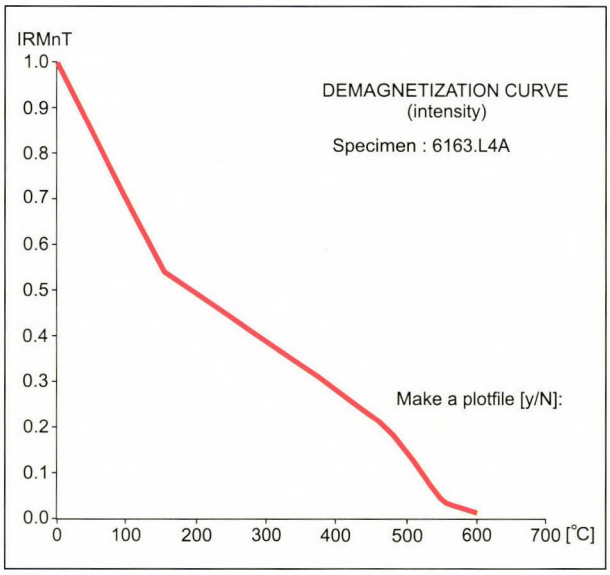

Fig. 36. Steps of thermal demagnetisation of SAV N4 specimen and changes of magnetic intensity by phases of cleaning

A change for negative inclination in the case of specimen N4, its reversed polarity and a high negative value of specimen N5 might serve a detection of a magnetostratigraphic horizon at a depth between 35 and 45 cm.

8.2. Susceptibility measurements

In each phase of measurements within SAV, magnetic susceptibilities (inner magnetism) were also measured. Their dominant values based on the anticipated presence of magnetite mineral serving for the measurements of stable magnetisation.

NRM susceptibility was measured in the field all along the Susak profile (*Fig. 38*).

For the fossil soils 1000–1200 k (x10^{-6} SI), while for loess layers 500–800 k (x10^{-6} SI) values were obtained.

Sandy loess sequences have about 1000 k (x10^{-6} SI) in the uppermost 3–4 m and between 7–11 m, which can be attributed to the presence of semipedolites. There are sands with remarkably high susceptibility between 12 and 13.5 m (1000–1200 k (x10^{-6} SI) whereas the sandstone bench (29–31 m) represents the lowest value within the profile, i.e. 400 k (x10^{-6} SI).

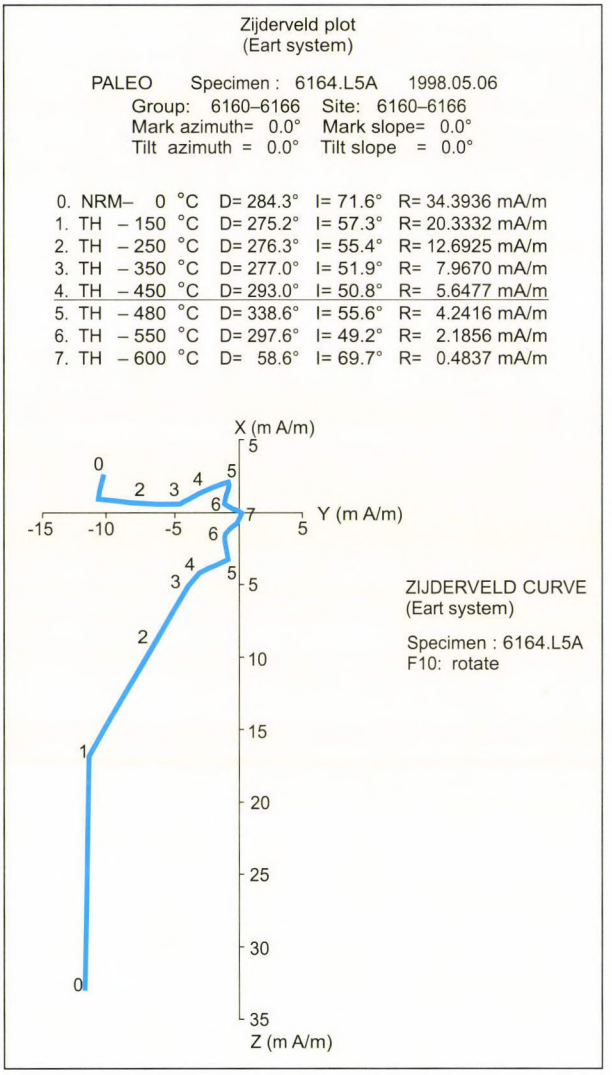

Fig. 37. Orthogonal demagnetisation diagram and results of paleomagnetic analyses of SAV N5 specimen (0–7: phases of thermal demagnetisation)

The fossil susceptibility of MF type at 11.5–11.9 m is lower than the value typical of paleosols but similar anomalies have been found in several Hungarian profiles e.g. in Paks 1971, 1977 *(Fig. 17)*.

Tephra horizons have spectacularly high values: 1400 k ($x10^{-6}$ SI).

Measurements of inner magnetisation are suitable for the differentiation between loesses and slightly humous horizons and magnetic anomalies.

For the application of magnetic susceptibility data in loess stratigraphy a method was elaborated by KUKLA, G. and AN, ZHISHENG (1988) for the Chinese loesses, subsequently used by HELLER, F. and LIU, TUNGSHENG.

The renewed Paks 1977 type locality was studied lithostratigraphically and magnetostratigraphically by HELLER, F. together with PÉCSI, M. and colleagues. The susceptibility throughout the Paks profile (1995) is shown for the sake of comparison with the chronostratigraphic subdivi-sion of the Susak profile (*Fig. 39*).

Comparison of the two susceptibility curves has made obvious a lower inner magnetisation of the paleosols of MB type than that of paleosols of BD_1, BD_2 and BA (chernozem) type.

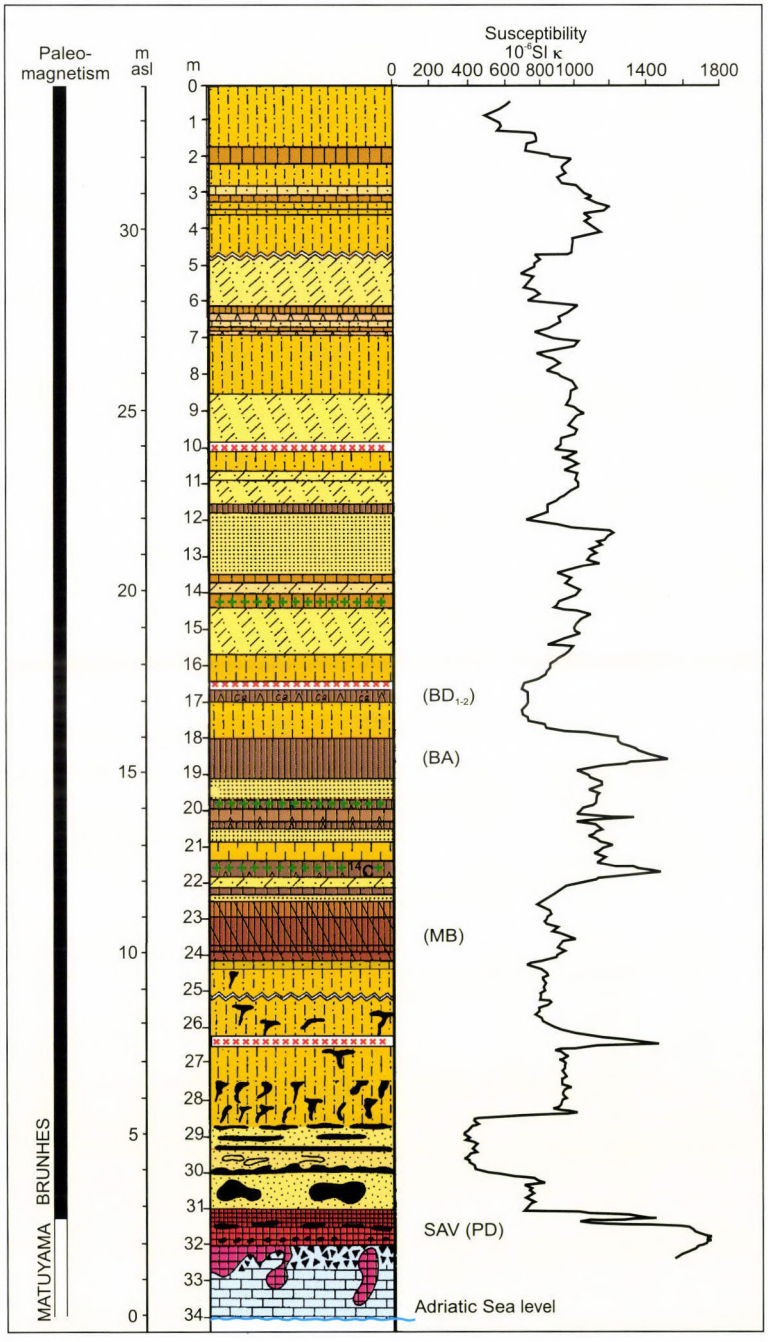

Fig. 38. Values of magnetic susceptibility along the Susak profile (J. BALOGH 2002)

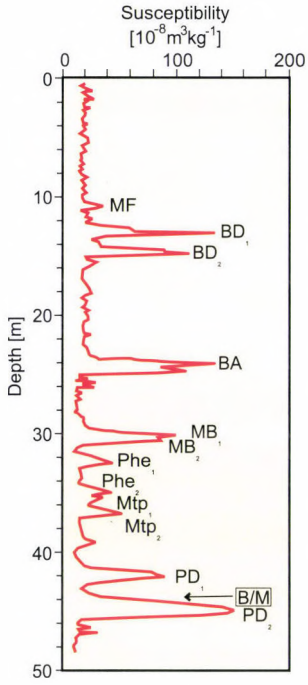

Fig. 39. Values of magnetic susceptibility along the Paks North (1977) profile (HELLER, F. 1995)

At the same time, within the sequence comprising Brunhes–Matuyama boundary the susceptibility value is on the increase and changes considerably within a short interval. This might be an indication of double soil formation. The trend of increase and decrease is very similar to values of inner magnetisation measured in the SAV paleosol.

8.3. Magnetostratigraphic subdivision

Along Susak profile down to 31 m depth the whole Quaternary sequence is regarded to belong to the Brunhes paleomagnetic epoch on the basis of a small number of specimens of positive magnetisation, lithological features and of the mollusc species identified.

There could not be recovered any short negative intervals within the epoch (*Fig. 38*).

In some loess sequences in the Carpathian Basin (e.g. at Paks) with interbedding paleosols, which litostratigraphically and paleopedologically are similar to chernozem-like fossil soils at Susak, paleomagnetic events might occur (*Fig. 40*). Of them BD_{1-2} chernozem-like brown soil horizon can also be traced in the key sections

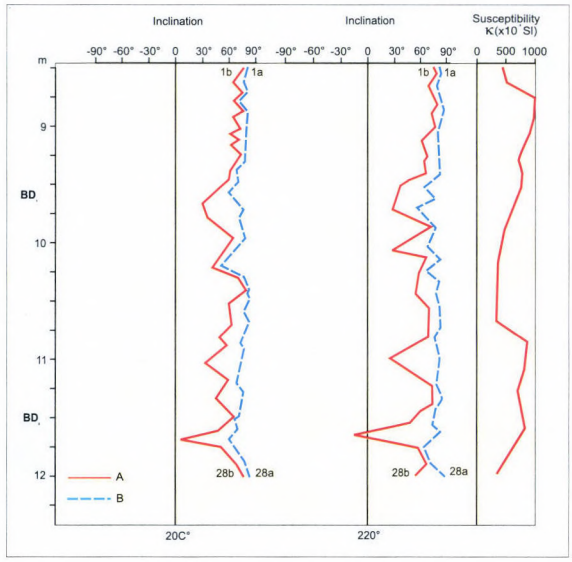

Fig. 40. Results of paleomagnetic analyses of BD_{1-2} fossil soils from the Paks (1971) profile (J. BALOGH 1997)

of northern Adriatic Region. During paleomagnetic analyses of the samples collected at Susak it was expected that the Blake event would be recognised, but fossil chernozems showed an exclusive normal polarity. However, further studies with the involvement of new specimens might reveal a paleomagnetic event in this fossil soil.

Litostratigraphic and chronostratigraphic evaluation of double paleosols still remains a controversial issue. If individual soil horizons constituting paleosol complexes are conceived as those formed in subsequent interglacials, there might be a difference about one hundred thousand years in their age. In this case a considerable erosional hiatus is presumed. Another interpretation suggests that soil formation was interrupted for a short time and then it continued in a way of similar pedogenesis in the mineral matter accumulated during this interval. In the Susak exposure sediments of this kind are BD_{1-2} chernozem-like fossil soil of eroded profile and SAV fossil soil.

Negative inclinations found in SAV paleosol suggest initial magnetisation of the Matuyama epoch with reversed polarity. Measurements in PD paleosol from the Paks profile used for comparison showed similar magnetisation. The apparent similarities based on the comparison of susceptibility curves make it probable the presence of the Brunhes/Matuyama boundary within the paleosol layer.

Taking into account the poor thickness of sediments with reversed polarity and their specific geographical setting, and the bedding of a thick sandstone bench and sand layer, however, a substantial denudation might be assumed which resulted in a sharp sedimentation gap (*Photo 41*). Between the soil of MB type and SAV there might be a hiatus of several hundred thousand, perhaps a million years.

With regard to the magnetic time scale by Cox it is possible that the uppermost horizon of the SAV paleosol represents an event of normal polarity Gilsa between 1 610 000 and 1 620 000 yr BP, the intercalated middle layer belongs to a reversed interval of Matuyama between 1 620 000 and 1 630 000 yr BP, and the lowermost red soil horizon represents an event of normal polarity Olduvai 1 630 000 and 1 640 000 yr BP.

9. QUARTERMALACOLOGICAL EXAMINATIONS

9.1. Taxonomy

More than 23,000 specimen of 20 species appeared in the samples. We came across only terrestrial Molluscs in 90 samples covering the whole profile (*Table 8*). On the basis of our examinations on the recent fauna none of these species exist on the island, and even in the Mediterranean they can be found presently in the transition zone of lower regions and alpine regions of high mountains exclusively (SOÓS, 1943). It means that this fauna became extinct locally at the end of the Pleistocene, or has withdrawn to the higher regions of the Dinarides. The fossil fauna consists of typical loessy elements (*Pupilla muscorum, Succinea oblonga,* etc.) together with shade-loving Mollusc species (*Macrogastra ventricosa, Macrogastra plicatula, Cochlodina laminata).*

Table 8. Mollusc fauna and its palaeoecological groups from Susak loess profile. The Mollusc fauna was grouped by papers of LOŽEK (1964), MEIER (1985), KROLOPP–SÜMEGI (1995)

Species / Paleoecological group	Paleoclimatological indicator group	Paleohumidity indicator group	Paleovegetation indicator group
Succinea oblonga	Cold-resistant	Higrophilous	Open vegetation loving
Cochlicopa lubrica	Mesophilous	Mesophilous	Ecoton habitat preferring
Cochlicopa lubricella	Thermophilous	Xerophilous	Open vegetation loving
Pupilla muscorum	Mesophilous	Mesophilous	Open vegetation loving
Pupilla triplicata	Thermophilous	Xerophilous	Open vegetation loving
Vallonia costata	Mesophilous	Mesophilous	Ecoton habitat preferring
Chondrula tridens	Thermophilous	Xerophilous	Open vegetation loving
Punctum pygmaeum	Mesophilous	Mesophilous	Ecoton habitat preferring
Discus ruderatus	Cold-resistant	Higrophilous	Shade-loving
Vitrea crystallina	Mesophilous	Higrophilous	Ecoton habitat preferring
Nesovitrea hammonis	Mesophilous	Higrophilous	Ecoton habitat preferring
Limacidae	Mesophilous	Higrophilous	Ecoton habitat preferring
Euconlus fulvus	Mesophilous	Higrophilous	Ecoton habitat preferring
Cochlodina laminata	Thermophilous	Higrophilous	Shade-loving
Macrogastra ventricosa	Thermophilous	Higrophilous	Shade-loving
Macrogastra plicatula	Thermophilous	Higrophilous	Shade-loving
Clausilia pumila	Thermophilous	Higrophilous	Shade-loving
Bradybaena fruticum	Thermophilous	Higrophilous	Ecoton habitat preferring
Trichia hispida	Cold-resistant	Higrophilous	Open vegetation loving
Arianta arbustorum	Cold-resistant	Higrophilous	Shade-loving

They appear extremely rarely in loessy sediments, and have been found so far only in the southern subregions of the Carpathian Basin (environs of Mecsek Mountains, southern Bačka, northern part of the Fruška Gora and environs of the Iron Gate). They were absent in other parts of the Central European loess area (HUM and SÜMEGI 2000, SÜMEGI *et al.* 1998). This peculiar feature of findings has great importance from a biogeographical standpoint (*Fig. 41*).

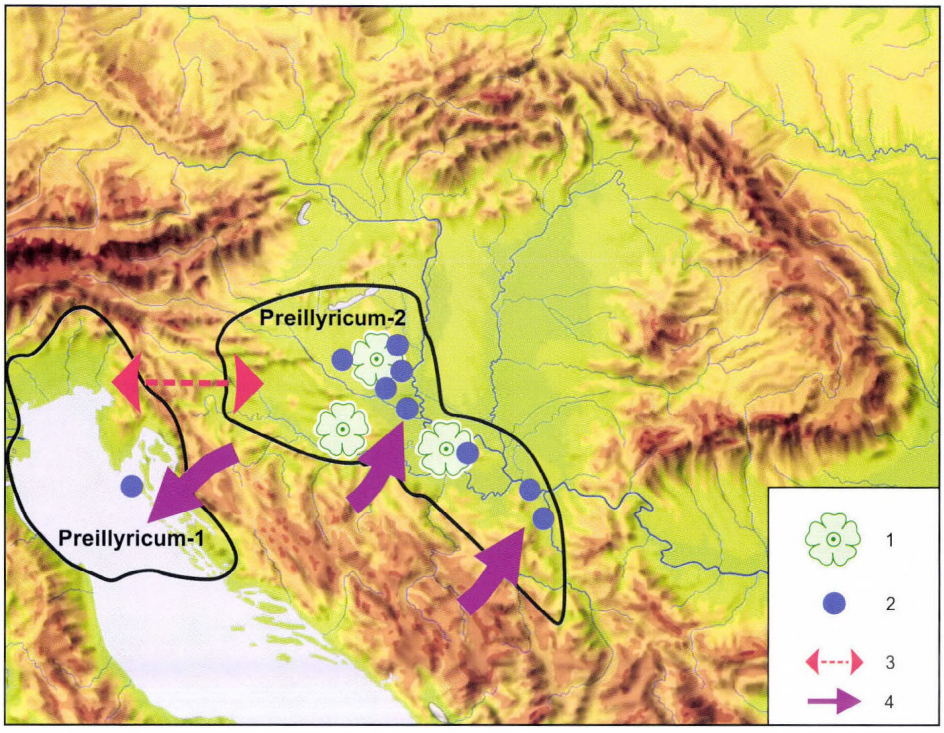

Fig. 41. Mollusc fauna related paleobiogeographical links between the Carpathian Basin and the North Adriatic at the end of the Pleistocene (base map compiled by ZENTAI, L. 1996). – 1 = Illyricum forest refugia spots (e.g. Mecsek) in the Preillyric area; 2 = *Cochlodina laminata, Macrogastra ventricosa, M. latestriata* sites; 3 = possible faunal transition between the two Preillyric areas; 4 = directions of Illyric floral/faunal effects

9.2. Taphonomy

Loessial sediments contained rich fauna, while from sands and fossil soils no Mollusc shells have been recovered. According to the formation of wind-blown sand we cannot expect *in situ* embedded Mollusc shells, as under contemporary extremely dry and warm climate no Molluscs lived in the area. As far as fossil soils are regarded, they must have contained rich Mollusc fauna, but their shells have been dissolved due to cabonate leaching processes (braunisation) syngenetic or postgenetic to soil formation. The carbonate-disposition as a consequence of the braunisation process is clearly observable in the bottom horizon of the lower reddish brown fossil soil.

Many chocolate brown paleosols are found in the middle part of the profile. Not only braunisation but redeposition from the former upper surfaces and postgenetic

resedimentation also occurred during the diagenesis of these soils. These two latter processes could contribute to the destruction of Mollusc shells.

All these processes contribute to the formation of malacologically sterile layers, which express stratigraphical and paleoecological significance of the profile. Mollusc shells are not present in the horizontally developed, sometimes a meter thick layers with concretions overlying the bedrock.

9.3. Paleoecology

No cryophilous elements appeared in the fauna. This points to the basic difference between the Susak loess area and the loess regions of Central and Western Europe where cryophilous Boreo-Alpine or northern Asian fauna can be detected in masses in the similar layers, moreover, in almost every kind of loess and loess-like sediments.

Rate of cold resistant species is high, just like the rate of species with wide range of tolerance. Thermophilous (demanding mild climate) species appeared with the highest rate in the upper part of the sequence (end of Pleistocene) and in the middle part of the section. To a surprise, xerophilous (dry-tolerant) species appear only during the periods of intense warming. The mean temperature of the warmest month (paleo-July temperature) of the contemporary growing season was about 15–17°C, according to the malaco-thermometer method (SÜMEGI, P. 1989, 1996). This value differs greatly from the present day July mean temperature (by about 10°C). However, the breeding season of snails in the Mediterranean now is winter, because they are inactive during summer owing to the drought (anabiosis). So the temperature difference between the Susak breeding seasons during the Pleistocene and present day is only a few degrees. Thus the region could serve as a refugium during Pleistocene coolings regarding the malacological breeding season. This is reflected in the composition of malacofauna, by the lack of cryophilous species, and by the presence of original species.

Ecotone species (living in the transition zone between open and closed vegetation) dominated throughout the profile, although forest species were also present, and their ratio sometimes reached quite a high level. According to these data, during sediment accumulation a more or less open, forest steppe environment existed. At the same time, a continuous presence of forest species points to the role of Susak as an area of refuge during the Pleistocene. All these data prove that the vegetation of the area differs from the general view about the classical steppe vegetation of loess regions. Above all its vegetation cover was thicker than previously thought. A sudden rise in the dominance of forest-species (in terms of percentage values) in some layers shows that a rapid reforestation took place in the area when the climate turned milder. Rate of steppe areas, according to the percentage appearance of open vegetation demanding species, never exceeded 50%. At the same time, there were stages

when rate of species demanding thicker vegetation cover exceeded 90%. It is similar to the composition of the malacofauna in the southern part of the Carpathian Basin (WILLIS et al. 2000).

9.4. Biostratigraphy

The malacologically evaluable part of the profile has proven to be of Würmian age, and can be classified into the *Bithynia leachi - Trichia hispida* biozone described by E. KROLOPP (1983). This is supported by the presence of *Trichia hispida* in masses throughout the profile.

On the basis of *Cochlodina laminata* appearing in the lower loess layers in large quantities they can be put in lower Würm by comparing to the southern Hungarian profiles. This corresponds to the *Clausilia pumila* subzone (KROLOPP, E. 1983). This classification is also supported by the abundance of *Clausilia pumila.*

Mollusc fauna of the layers between 9–12 m, consisting of sandy loess and loessy sand suggest an interstadial phase. This stage could be mostly classified into the *Helicopsis striata Oppel* subzone (KROLOPP, E. 1983), but the denominator species has not come to light. Thus this biostratigraphic correlation remains questionable, although we think it is reasonable to put this part of the profile into Middle Würmian.

The upper part of the profile was classified as upper Würmian, belonging to the *Semilimax kotulai* subzone (KROLOPP, E. 1983) according to the dominance of cold-resistant species and rate variations proving cyclic climatic changes in this part of the profile.

9.5. Paleobiogeography

On the basis of its malacofauna, the Susak loess profile shows similarity to the loess and loess-like sediments of the northern foreland of the Dinarides (Mecsek, Fruška Gora, Bačka, Villányi Mountains). This area, like a dynamic zone encompassing the Dinarides (Illyricum), could function as a fluctuation zone according to the investigations of Z. VARGA (1981) on recent areal dynamics. That means it could be a zone with different elements alternating periodically depending on the climatic fluctuations. This fluctuational or slackening zone thus can be interpreted as a Würmian Preillyricum and it can be enlarged to comprise the Susak loess area, as well as the south-western foreland of the Dinarides. In our opinion, such a dynamic paleobiogeographic region was formed along both sides of the Dinarides (the Preillyricum), where forest species (Illyric) formed sporadic refugial area (Palaeoillyric), like small oases (WILLIS *et al.* 2000; SÜMEGI *et al.* 1998), during the cold phases of the Pleistocene. From these relic areas (microrefugia) spreaded the forest fauna (*Cochlodina laminata, Clausilia pumila, Macrogastra ventricosa, M.*

plicatula) under milder climates. On the basis of Mollusc finds such kind of microrefugia was formed in the Susak loess area, where shade-loving species consisting the fluctuational zone lived permanently, it was dynamic, but pulsing within a small area, and this refugium followed mosaic vegetational rearrangement. These paleobiogeographical suggestions are proved by data on vertebrate fauna during the Upper Pleistocene (SALA 1998) and by cyclic changes in the ratio of forest resident Paleoillyric elements in the uppermost layer of the Susak loess profile.

9.6. A short description of Susak I malacological profile

(The Bay of Bok, *Figs 42 and 43)*

0–40 cm: slightly pedified horizon with roots, with a considerable amount of Mollusc remnants (of at present extinct species) (Layer 1).The 0 m horizon corresponds to an altitude of 24.5 m a.s.l.

40–680 cm: sandy loess, light brownish-yellow, with high content of alternating silt and locally sand fractions. F. SCHWEITZER identified an incipient ochre-red tephra horizon at a depth of 475–480 cm. This layer contains substantial Mollusc remnants, now extinct in the area. (Layer 2).

680–700 cm: light brown incipient soil horizon locally with red patches; 4–5 north of the sampling strip falling apart, forming two weakly developed soil horizons. This horizon granulometrically is abundant in silt and contains negligible clay. In this paleosol tiny pieces of charcoal, and Mollusc shells occur (Layer 3).

700–900 cm: greyish-yellow fine sand (airborne). It is malacologically sterile (Layer 4).

900–1180 cm: alternating yellowish-brown sandy loess and greyish-yellow loessy sand are descernible. Upward it has a dark brown tint with sporadic appearance of ash dots and mangenese precipitations. It contains abundant Mollusc shells (Layer 5).

1180–1300 cm: dark brown clayey silt and silty clay with manganese patches and tiny, elongated precipitations resembling root system. In the field F. SCHWEITZER identified this as paleosol horizon and pointed out a tephra layer of patchy development within. It is malacologically sterile (Layer 6).

1300–1400 cm: greyish-yellow loessy sand, malacologically sterile (Layer 7)

1400–1500 cm: dark brown clayey silt, paleosol, malacologically sterile (Layer 8)

1500–1580 cm: greyish-yellow sandy loess, malacologically sterile (Layer 9)

1580–1640 cm: brownish-yellow clayey silt, loess horizon, with abundant Mollusc shells. (Layer 10)

1640–1800 cm: paleosol horizon, reddish-brown when wet and brick red when dry. It is malacologically sterile. (Layer 11).

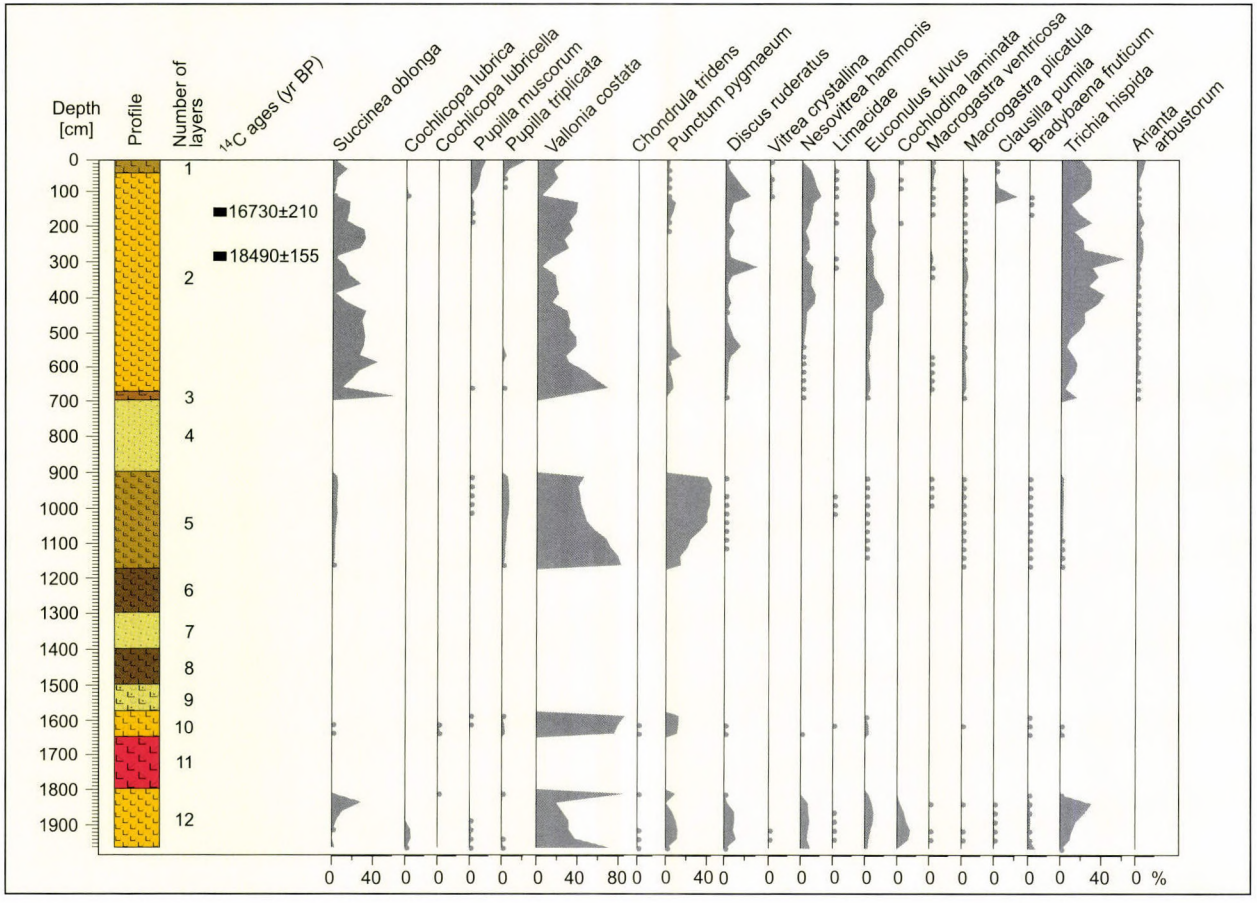

Fig. 42. Dominance changes of the Mollusc species from the loess sequence at Susak island (dots indicate fauna occurrence less than 2%)

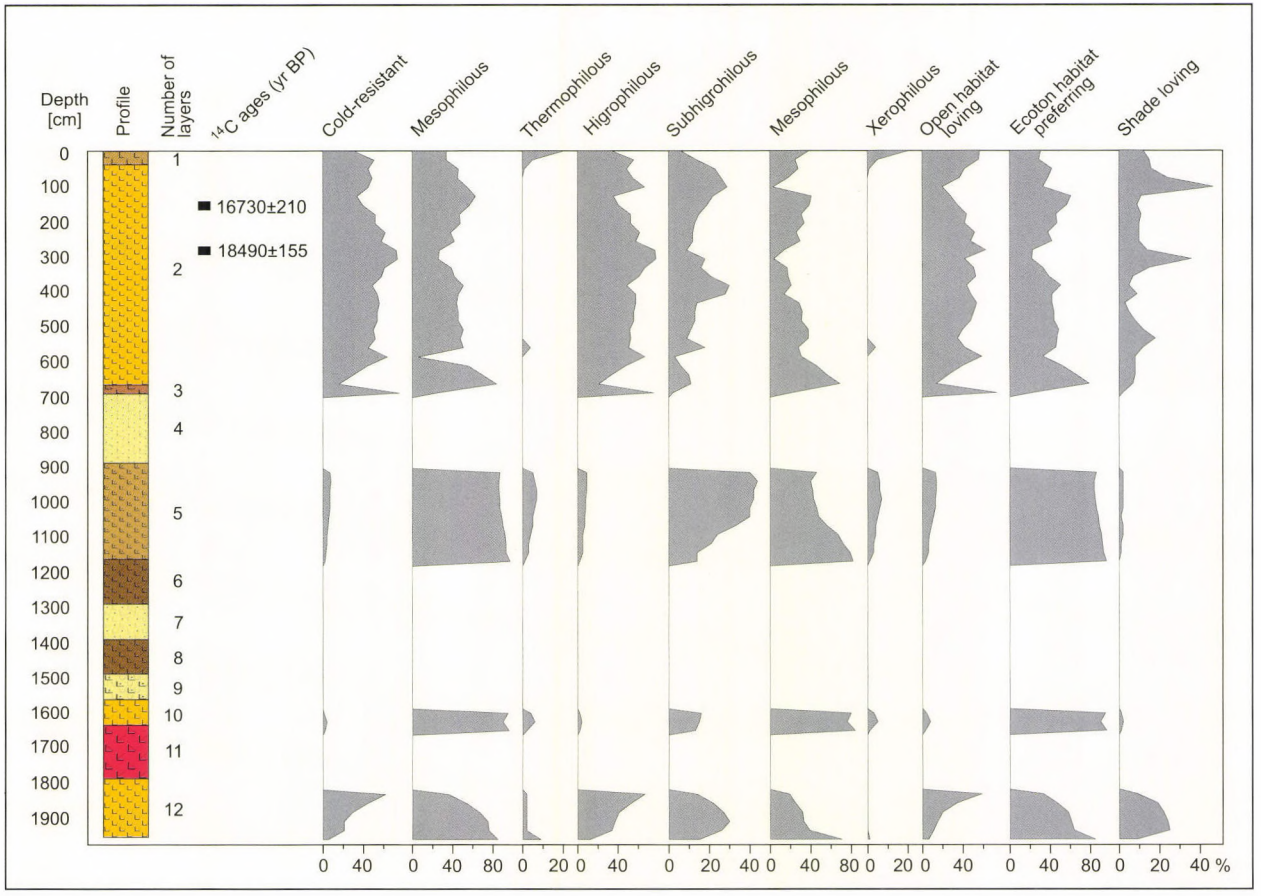

Fig. 43. Dominance changes of the different palaeoecological groups of Mollusc species from the loess sequence at Susak Island

1800–1960 cm: brownish-yellow silty layer, loessy horizon. It contains substantial amount of Mollusc fauna. There are carbonate concretions of vertical arrangement with a thickness of 10 cm or so. Mollusc shells are found locally in the carbonate concretions. Probably the lime solved out by leaching (braunisation) from the upper paleosol layer. (Layer 12, closing the malacological profile – it is not shown in the figure.)

1960–2220 cm: a hard layer of sandstone bench character, with concretions of horizontal arrangement. Malacologically sterile. This layer is the bottom of the profile, although between the Cretaceous limestone considered the lowermost level and the sandstone bench there is a clayey horizon of 20 cm thickness of uncertain formation. It proved to be malacologically sterile as well. No Mollusc shells were found. (This layer is not shown in the figure.)

10. ANTHRACOLOGICAL EXAMINATIONS

In the course of a complex paleoecological examination of a loess profile charcoal examinations – the so called anthracology – holds a great importance for in most cases this is the sole opportunity to reconstruct past vegetation. Charcoal is well preserved in dry sediments, whereas pollen, widely used to reconstruct vegetation, do not survive in loess. In most of the cases no proper wet environment, e.g. a lake (from the bottom sediment of which pollen could be recovered) can be found close to the studied profile. The local past vegetation can be identified from charcoal samples, which is a further advantage to palinology, as *in situ* charcoal is the remain of buried trees. Its disadvantage is that charcoal allows to identify arboreal vegetation elements only. Nevertheless, its presence holds information about past arboreal cenoses at the site.

Generally charcoal is used only for carrying out radiocarbon measurements, but if the latter is preceded by anthracological analysis, the time of extinction of the reconstructed vegetation can be specified.

Anthracological analyses on charcoal collected from Susak loess profile are reported below.

10.1. Material and methods

The Susak loess series contained macroscopic charcoal remains in two layers. Along the main profile a layer lying 21.40–21.65 m below the surface a fossil soil abounds in small charcoal particles (*Fig. 4*). Along the profile at Bay of Kalučica is thought to have been a fireplace (*Fig. 2, Photo 42*), with numerous larger charcoal pieces.

Samples were sieved through 0.5 mm mesh size, then left to dry at room temperature. This is necessary because charcoal moulder easily when wet. Thus samples were enabled to carry out xylotomy based species identification on them. Using the list of the determined species and on the basis of recent species ecology it was attempted to suggest the climatological and ecological conditions of the time period in concern. Paleoecological data were obtained using the principle of actualism.

The fraction coarser than 2 mm was examined only, because smaller particles do not always contain all of the diagnostic characteristics.

The samples were sorted under stereo-microscope with maximum magnification of 80×. This resulted in charcoal groups of homoxyls and heteroxyls on the basis of transversal section examinations. Regarding homoxyl types, their presence, and if so, types and distribution of resin canals were also determined. Identification took place under reflected-light microscope with magnification around 400–600× on three ana-

Photo 42. Traces of a fireplace in the section of Bay of Kalučica. Radiocarbon age is 31,830 ± 720 yr BP (Photo by F. SCHWEITZER)

tomical planes (STIEBER 1967), namely on transversal, longitudinal radial and longitudinal tangential planes, at the Geographical Research Institute of HAS. The keys of SCHWEINGRUBER (1978, 1990) were used. As to the documentation, photos of the species were taken by the author with Hitachi type natural scanning electron microscope at the Department of Plant Anatomy, Eötvös Lóránd University. This instrument was also used for the identification of species. As no chemical treatment had to be applied, radiocarbon measurements could be carried out on the samples.

The botanical nomenclature by SIMON (1992) was used, with regard to Quaternary LOWE and WALKER (1997) were followed.

Only qualitative results are reported here as no systematic sampling allowing quantitative representations took place.

Anthracological examinations included sieving of samples, then identification of charcoal on the basis of xylotomy. During this kind of examination no chemical treatment is applied, thus samples could have been dated with radiocarbon measurements.

Radiocarbon measurements were carried out at Nuclear Research Centre of HAS. Preparation of charcoal for radiocarbon dating was made according to Csongor *et al.* (1982). Measurements were performed according to HERTELENDI *et al.* (1987, 1989). Errors were taken into account in congruence with HERTELENDI (1990).

10.2. Results

Characteristic features of charcoal remains suggest that they are the result of fires, not compression. Xylotomical features sometimes remained unidentifiable, compact coal matter consisted of some parts of the samples (*Photos 43a,b,c*). In other cases big bubbles occurred on the surfaces (*Photos 44a,b*). These bubbles are also resulted from firing (MENDOZA-ANAYA *et al.* 2000). These results are corroborated by the thermonalytical investigation carried out by SZÖŐR (see in this volume), for 550 °C firing temperature indicates forest fire (MacDONALD 1991). The bubbles for the first sight suggested that remains of broad leaved trees are found. Only the careful examinations pointed out that the bubbles represent no vessel elements but are the results of firing.

Both the rate of sedimentation and charcoal confirmed forest firing (CARCAILLET and THINON 1996).

The concentrated (lens type) occurrence of charcoal in the upper zone refers to a fireplace.

In both samples charcoal belongs to *Pinus sylvestris* group of tree species (*Photos 45a,b; 46a,b,c; 47a,b,c*). They may belong to *P. sylvestris* (common pine), *P. mugo* (mountain pine) or *P. nigra* (black pine). These three species could be hardly differentiated on the basis of their xylotomy.

Radiocarbon ages determined can be seen in *Table 9*.

10.3. Discussion

Charcoal samples originating from two layers of Susak loess profile were examined. Remains proved to be from individuals of *Pinus sylvestris* type trees, diploxylon. That means that they can either be *Pinus mugo* (mountain pine), *Pinus nigra* (black pine) or *Pinus sylvestris* (common pine), although the occurrence of the first is nearly improbable, as now it grows in the Carpathians at altitudes of 1300–2000 m above sea level (GENCSI and VANCSURA 1997). Thus it is not probable to have appeared during glaciations in an area with warmer climate than Hungary (as it was not the member of the Hungarian upper Pleistocene flora, and appeared only in traces).

Black pine is a Mediterranean mountainous species. It has a wide-range ecological tolerance, being a xerophilous species, regardless of the soil composition. It could live at the site during the time period in concern. However, BOGNÁR *et al.* reported in 1983 that on the basis of pollen examinations *Pinus sylvestris* (common or Scots pine) existed on the island during the Pleistocene from that group of trees. Thus all data confirm the presence of the latter type of tree in the anthracological profile. As a comparison, in the southern part of Hungary from the same time interval (around 32,000–31,000 BP) also *Pinus sylvestris* (common pine) had been recovered (WILLIS *et al.* 2000; SÜMEGI and RUDNER 2001; RUDNER and SÜMEGI 2001).

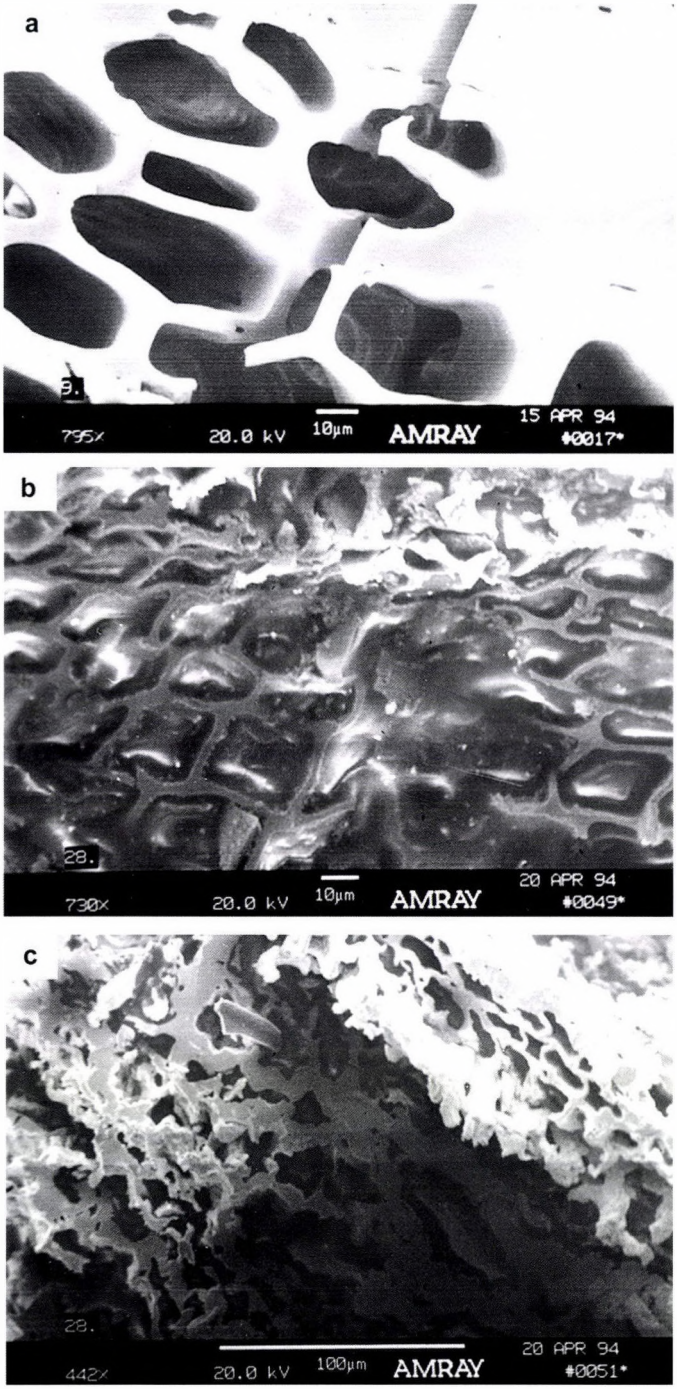

Photos 43a,b,c. Scanning electron-micrographs of fired charcoal

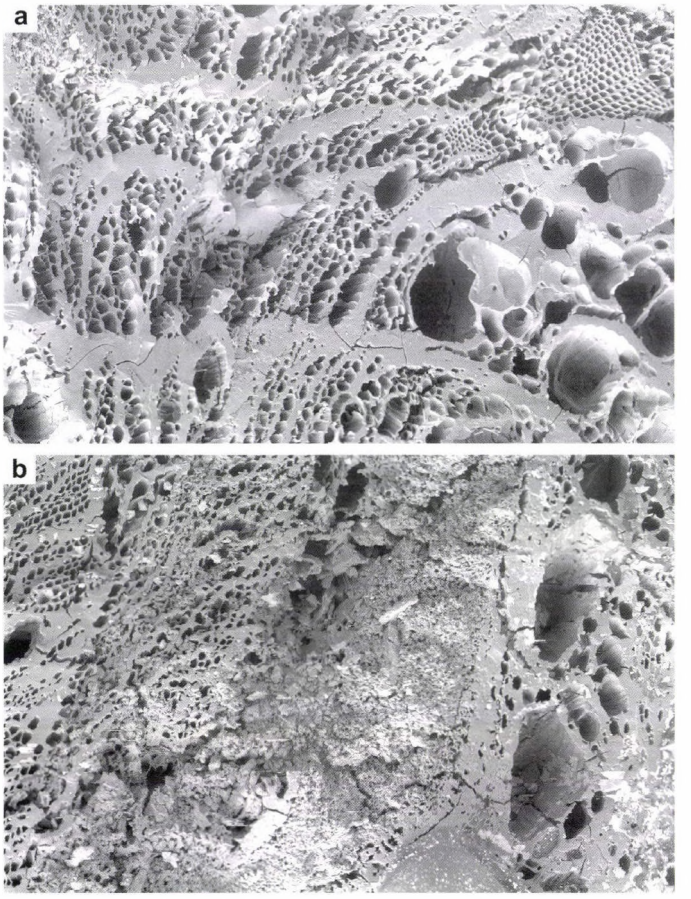

Photos 44a,b. Charcoal belonging to *Pinus sylvestris*. Fired, with big bubbles which can be thought a vessel under smaller magnification. Actually, these bubbles resulted from firing (Mendoza Anaya *et al.* 2000).

On the basis of its microscopic features charcoal seems to be the result of fire, as Szöőr has confirmed using thermal analysis (see in this volume). Firing could occur as the self-inflammation of forest, as pines contain much resin, which is highly flammable, and in a relatively dry climate spontaneous forest fires occur. Besides, early man is conceivable to have caused forest fires. In the case of the younger sample, charcoal of open hearths was found put by early man.

Regarding the Hungarian loess profiles of the same age, paleosols bearing type of charcoal developed presumably under interstadial conditions, thus similar ones might have prevailed in Susak island when these two layers of the profile were formed. During interglacials vegetation demanding warmer conditions were dominant even in

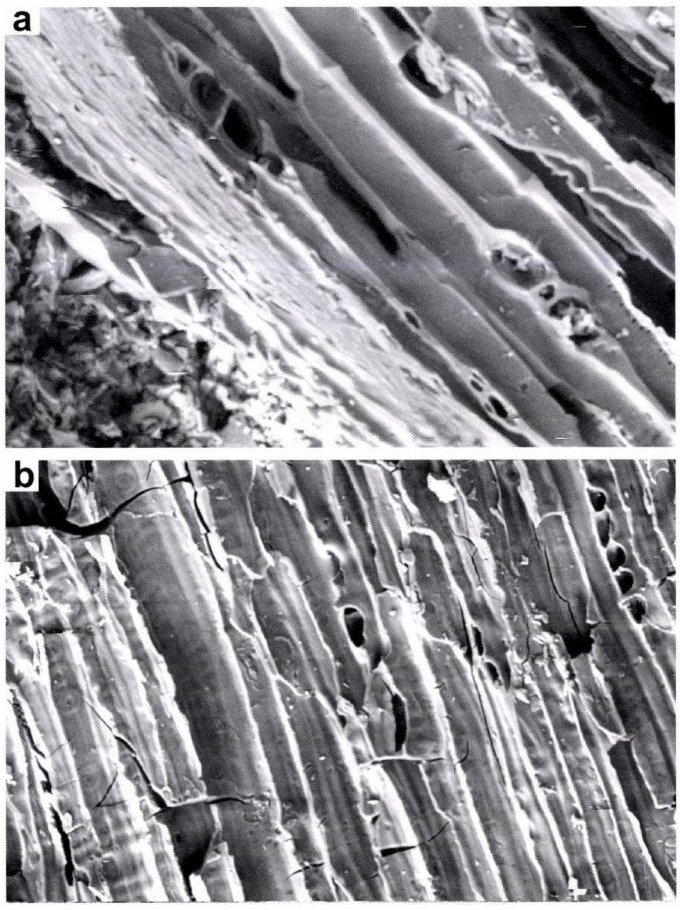

Photos 45a,b. Pinus sylvestris charcoal remains, in longitudinal tangential surface view. (SEM photos)

Hungary which is a cooler area now than Susak must have been in the Pleistocene (STIEBER 1968). So remains of a fired forest vegetation of boreal type were identified having developed under interstadial conditions. Early humans used pines of these forests to set fire.

On the basis of radiocarbon data the upper, younger layer developed during the Denekamp interstadial (32,000–28,000 BP, Behre 1989) was described from Northern Europe. This phase was traced in the Carpathian basin from many sites, forming a main biostratigraphical marker, although with somewhat younger ^{14}C data, but very likely the same period was reconstructed using various kinds of paleoecological methods (SÜMEGI 1996, SÜMEGI and RUDNER 2001, RUDNER and SÜMEGI 2001). Thus this biostratigraphic unit can be extended in southern directions, on the basis of the Susak paleoecological studies.

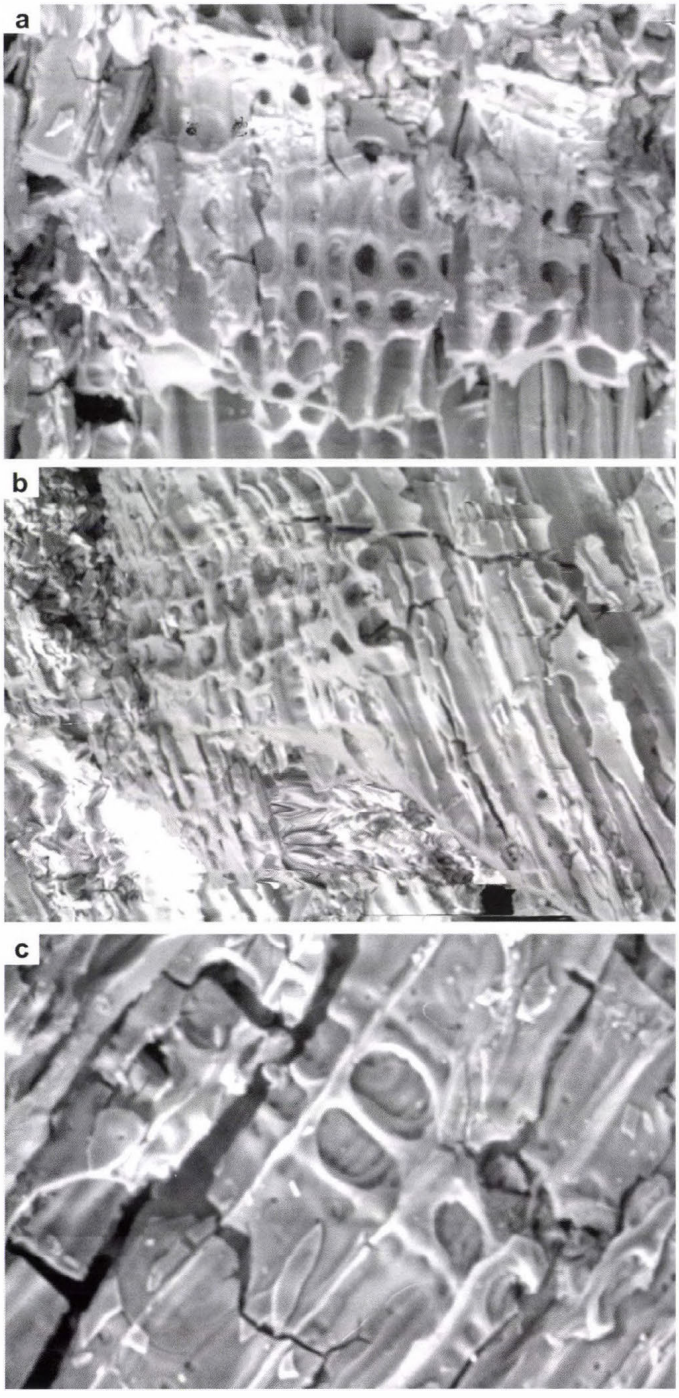

Photos 46a,b,c. Pinus sylvestris charcoal remains, in longitudinal radial surface view. (SEM photos)

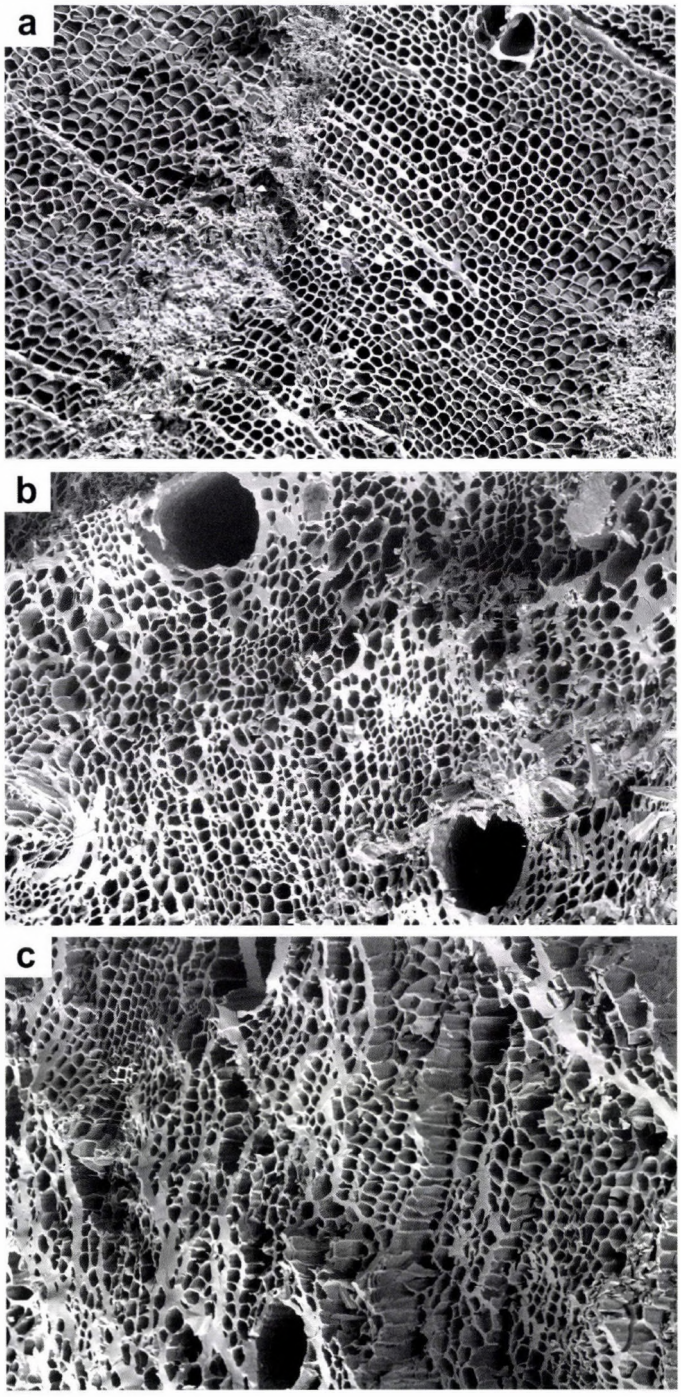

Photos 47a,b,c. Pinus sylvestris charcoal remains, in transversal surface view. (SEM photos)

Table 9. Radiocarbon datings of two charcoal samples

Laboratory code	Sample name	$\delta^{13}C$(PDB)	Conventional radiocarbon age (yr BP)
deb-6694	Susak 1998 charcoal 21.40–21.65 m	-25.18	> 35 000
deb-6679	Susak 3. charcoal	-25.48	31 830 ± 720

Regarding the lower layer, it is likely to have been formed also under interstadial conditions, as it contained similar anthracomass, but it is not clear if this horizon developed during the Upper, Middle or Lower Pleistocene.

11. ARCHEOLOGICAL FINDINGS

From the Susak exposure (Bay of Bok) three worked artefacts have been recovered at an altitude 18.0 m a.s.l. *(Fig. 3, Photo 48).*

A specific feature of these finds is that limestone served as the raw material of implements. In prehistoric times a basic requirement to rocks used for the fabrication of tools was a homogeneous structure with isotropic splitting which granted long durability.

The use of limestones, especially their intensely recrystallized varieties (such as marble) for making implements was widespread both in a spatial and temporal sense but nowhere it acquired a massive scale. However, when trying to associate this utilisation with a particular age, it is to be confined to lower and middle Paleolithic rather than upper Paleolithic, when blade industry was already applied.

Each of the three Paleolithic artefacts recovered from the BD_{1-2} paleosol horizons *(Photos 49* and *50)* was a flake broken off of a larger stone or a worked flake *(Photo 48)*. The raw material was a piece or block of stone) larger in size than the average abrasional gravels. There could not be observed a worked platform and a marked bulb of percussion in any case. This refers to a technology not younger than middle Paleolothic. The support of two implements *(Photo 48A,B)* is trapeze or trap-

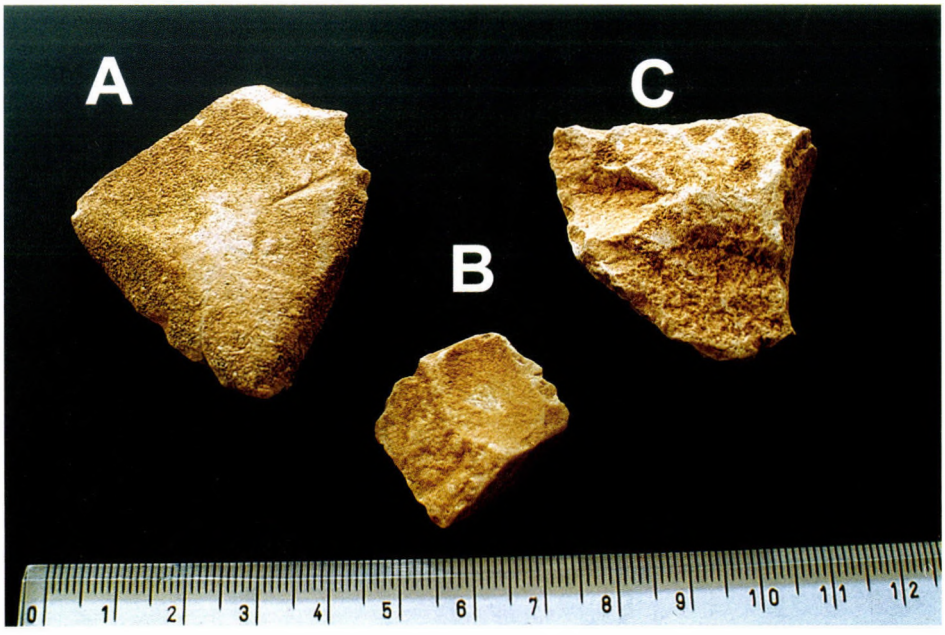

Photo 48. Worked Paleolithic artefacts recovered from Susak (Photo by F. SCHWEITZER)

Photo 49. Susak key section with Paleolithic site in the BD_{1-2} fossil chernozem soil (Photo by F. SCHWEITZER)

Photo 50. Position of Paleolithic artefacts in BD_{1-2} fossil chernozem soil (Photo by F. SCHWEITZER)

ezoid while that of the third implement is a blade-shaped flake. Edge finish of 1b artefact, a convex transverse scraper, however, is a product of retouche, which is not considered typical of middle Paleolithic industry.

– Non-retouched trapezoid flake. Its ventral and dorsal sides and edges are equally weathered. Raw material: limestone. Size: width – 4 cm; thickness – 0.7 cm (*Photo 48A*).

– Convex transverse scraper made of trapezoid shaped flake. Its platform is smooth, bulb of percussion is missing. Dorsal surface of the weathered piece is partly covered by the crust of original raw material. Raw material: limestone. Size: width – 2 cm; thickness – 0.5 cm (*Photo 48B*).

– Blade-shaped broken flake. Its proximal end is broken off. There is a blade-shaped crest running along the dorsal side. Left of this the original crust of raw material. Raw material: limestone. Size: width – 4.8 cm; thickness – 1.3 cm (*Photo 48C*).

This mini collection is a valuable contribution to the Paleolithic in the Mediterranean Basin.

CONCLUSIONS AND DISPUTED PROBLEMS

Susak Island belongs to the archipelago in the Kvarner Bay (northern part of the Adriatic). The island covers an area of 3.76 square km, its highest point is 98 m above sea level. A well develop step divides the island to a higher level (60–98 m a.s.l.) and a lower level (30–50 m a.s.l.). Susak is built of loess and loess-like sediments, thickness of which vary between 50–80 m depending on the position of the karstified surface of limestone of the so called rudist facies.

In the course of geochemical and sedimentological analyses special attention was devoted to studies on paragenesis of clay minerals and carbonate minerals, identification of amorphous material and organic matter and their characteristics by the individual formations.

– With regard to *clay mineral paragenesis*, there is a prevalence of chlorites and mixed illite–montmorillonite structures within the sedimentary formations on Susak Island. Smectites are common in tephras, whereas an abundance of kaolinite is typical only of the red clay at the bottom of loess profiles.

– *Paragenesis of carbonate minerals* can be characterised with a simultaneous occurrence of dolomite and calcite. Contrary to loesses in the Carpathian Basin the amount of dolomite remains below that of calcite. Analyses call attention to calcite as the material cementing diagenetic precipitations, whereas enrichment in dolomite is typical of two horizons of the Susak profile. An overwhelming part of sediments can be termed as 'protodolomite facies' by the thermal analysis.

– According to thermal analysis of the *humified horizons* near the surface, the amount of clay minerals is less than carbonate minerals and almost equals to that in parent material. This regularity is typical of formations along desert margin as it was established by BRUIJNS, H.J. and YAALON, D.T. (1979).

– *Amorphous matter* shows an enrichment in sediments toward the lower part of the profile but it reaches maximum in tephras and paleosols; its change is parallel with the content of *organic matter* (C_{org}).

– Diagenetic hematite, portlandite and gypsum emerge as important *indicator minerals*. These minerals prevail in the upper part of the profile. Gypsum is confined to the lower tephra layer.

– *Charcoal remains* including traces of fireplaces could be observed in two levels along the profile. Thermal analysis identified them as consequences of forest and bush fires or induced by humans and not as a result of biodegradation in moist environment.

– Morphometric investigations of *quartz grains* testified to marine (or fluviatile) origin of sands overlying SAV reddish clay downward the profile. In other parts coarse-grained sand is apparently the result of eolian accumulation.

– Interpretation of preliminary *stable isotopic analyses* suggests that *red clay* in karstic pits of the limestone at the bottom of the profile and the superimposing *reddish clays* could develop under warm and humid climates, whereas *diagenetic calcareous concretions* (rhyzoliths, benches) indicate warm and arid conditions of formation. *Paleosols* could have formed during interglacials.

– Diagenetic spherules of the lowermost red clay suggest warm and humid subtropical environment.

– Traces of any relevant extra-terrestrial event cannot be found along the profile.

Taking into consideration the above results, our knowledge of the geology and geomorphology of Susak Island can be modified in the followings.

– Overlying Cretaceous rudist limestone there are 10–30 cm thick layers of limestone debris (material of which was transported by torrents and subsequently cemented), sometimes with ventifact occurrences. This formation is covered with typical red clay of Csarnotan type. Its relative age is probably to be correlated with Messinian Salinity Crisis, but the solution of this question needs further investigations.

– Comparing the results of thermoanalytic analyses with the concept evolved by F. SCHWEITZER and Gy. SZÖŐR (1997) it can be stated that the Susak complex is very similar to 'typical red clays' of Hungarian Csarnotan (4–3 million yr BP). *The overlying reddish clays (SAV) might be much older than 700,000 years BP.*

– *Cemented sands of 0.5–1.5 m thickness* had deposited over a tidal plain but calcareous diagenetic concretions formed upon the impact of atmospheric precipitation (meteoric diagenesis, HAAS, J. 1998)

– Carbonate concretions above the red clay are of chaliche character and there are traces of dolomitisation of the environment, which probably indicates climate turning warmer and drier. Such a period could be associated in the northern Mediterranean and in the Carpathian Basin with Hungarian Kislangian fauna characterised by the presence of camel and ostrich. This hypothesis is corroborated with gypsum appearing close to the lower tephra horizon. Sands and sandstones void of Mollusc fauna also indicate arid climate conditions. *In some places of the island there is a sedimentation gap within the lower part of the loess sequence. Even prior to the formation of the soil of MB-type, 100–200 m wide valleys dissected the paleosurface. This cut was so deep that all sediments including red clay, reddish clays (SAV), cemented sand, together with the old grey tephra had been removed down to the rudist limestone. This ancient depression (erosional valley, derasional trough or marine bay) was subsequently filled up with younger loess and loess-like sediments during the Middle and Late Pleistocene, which constitute the island at present.*

– Fossil soils and humified horizons differ basically, as far as their formation is concerned. *In the upper part of the loess sequence sandy skeletal soils and chernozem-like soils are interbedded. In the middle part forest soils occur, whereas in the lower part reddish soils appear.* The formation of fossil soils can be attributed to warm

and humid periods. Gypsum and hematite upward the profile are associated with a drier spell. Portlandite ($Ca(OH)_2$) found in the upper part of the profile is due to an intense evaporation during summers under more recent climates.

Investigations into chernozem-type paleosols within the Susak profile show that soils in the upper 21 m of the section slightly differ from those of similar genesis in the Carpathian Basin. In the Susak profile there are several thin horizons of chernozem dating of which requires further analyses. *Chernozem-like soils in the Carpathian Basin are younger than 250–300 thousand yr BP. Humified skeletal soils are 16–18 thousand yr old (an interstadial of W_3). Chernozem soil of MF_1-type probably formed 26–30 thousand years ago (W_{2-3}). Time of the formation of MF_2 is probably 85–105 thousand yr BP. BD_1 and BD_2 soils of 120–150 thousand years might have formed during R–W interglacial. The lowermost chernozem-like soil is BA and put to 200–230 thousand yr and formed probably during R_1–R_2 interstadial* (PÉCSI, M. 1998).

On the basis of its physical and genetic characteristics a reddish-brown forest soil occurring at a depth of 23–24 m along the profile strongly resemble Hungarian paleosols of MB type, which were considered previously as R–W interglacial soil, but have lately been interpreted as 300–350 thousand year old soils (PÉCSI, M.1998).

Paleosol SAV (Susak Lower Red) bears characteristic features of subtropical–mediterranean soils showing similarity with the soil complex of PD-type within the Paks profile and its chronological problems are also identical.

For a deeper understanding of the Susak layers the traditional *sedimentological parameters* (K, S_k, So, M_d) were studied together with *granulometric parameters* newly introduced in Hungary: FG (fineness grade) adopted from Germany and K_d index (degree of weathering) adopted from China. These parameters have been considered as environmental indicators. Information can be derived from *Fig. 15* and *Table 3*.

In the course of data interpretation a wealth of information could be obtained on climate changes during the past two million years: extremes of warming and cooling by layers were fixed, lithological units, periods of and gaps in sedimentation identified, boundaries of layers drawn, *in situ* and redeposited sediments distinguished, circumstances of formation cleared.

Using the above methods 31 horizons were identified along the Susak 1997 profile.

I. *11 paleosol layers*:

– 1 double, sometimes triple reddish clay,

– 1 double reddish brown soil labelled Susak soil of MB-type,

– 6 chocolate brown chernozem-type soils, in some cases with fire places resembling paleolithic sites i.e. horizons with charcoal remains,

– 3 weak humified horizons with a thickness of 20–40 cm, containing gypsum.

II. *4 sand layers*:
– 1 coarse grained sand,
– 2 fine grained sands superimposing young loess,
– 1 fine grained sand superimposing reddish clay.
III. *13 layers of loess and loess-like deposits*:
– 11 loess layers,
– 2 loess-like layers.
IV. *3 tephra horizons*:
– upper tephra horizon: a reddish brown layer in loess with fine sand, redeposited in several places,
– middle tephra horizon: a yellow layer overlying a chocolate brown fossil soil,
– lower tephra horizon: a grey layer overlying silty sand.

Paleomagnetic measurements were aimed at correlating Susak 1997 profile with the magnetostratigraphic time scale of the Carpathian Basin and with that of the Adriatic region.

SAV paleosol (Susak Lower Red) was chosen for a detailed paleomagnetic analysis. Its physical and chemical composition and colour showed strong similarities with PD_1 and PD_2 reddish soils at Paks and Dunaföldvár in the Carpathian Basin. Based on geological, paleopedological and lithological properties, identification of the Brunhes–Matuyama paleomagnetic boundary in this horizon seemed very probable and analyses have appeared to yield reversed polarity here.

A further study could perhaps solve the problem if the specimen with an ambiguously reversed polarity really represents Brunhes–Matuyama boundary or, due to a considerable gap in sedimentation, it rather indicates a paleomagnetic event within the latter epoch.

Malacological investigations revealed 23,000 fossils of 20 species contained by the samples. There is a mix of typical elements of loess fauna (*Pupilla muscorum*, *Succinea oblonga* etc.) with Mollusc species hitherto found in loesses very rarely (*Macrogastra ventricosa*, *Macrogastra plicatula*, *Cochlodina laminata*) and exclusively in the southern loess regions of the Carpathian Basin (Mecsek region, southern Baèka, Iron Gate area). This is a remarkable feature from the biogeographical viewpoint.

Mollusc fauna did not contain any cold tolerant elements at all. This points to a basic difference between the Susak loess and the central and west European loesses where a large amount of boreal-alpine or northern Asian species were recovered from profiles of similar age in general and from loess layers in particular.

From the profile of the Susak loess-paleosol sequence human *artefacts* have been recovered. Recrystallised limestones served as raw material of implements. Based on the technology of elaboration the artefacts cannot be younger than the second half of middle Paleolithic. They represent a modest contribution to the Paleolithic of the Mediterranean.

REFERENCES

AN, Z.–WEI, L.–LU, Y.–WANG, N.–HE, X.–DING, S. 1979. Magnetostratigrahy of the core S–5 and the transgression in the Beijing area during the early Matuyama Epoch. – Geochimica. *4.* pp. 343–346.

AN, Z.–WEI, L. 1980. The fifth layer paleosol in the Lishi Loess and their paleoclimatic significance. – Acta Pedologica Sinicam. *17.* pp. 1–10.

ANDELKOVIĆ, M. 1988. Geologija Jugosavije. Građevinska knjiga. Beograd

ANDÓ J.–KIS K.–MÁRTON P. 1976. Fiatal üledékek mágnesezettségének vizsgálata. Kézirat. Bp., ELTE Geofizikai Tanszék, 42 p.

ARIAS, C.–AZZAROLI, A.–BIGAZZI, G.–BONADONNA, F. 1980. Magnetostratigraphy and Pliocene–Pleistocene boundary. – Quaternary Research. *13. 1.* pp. 65–74.

AZZAROLI, A.–DE GIULI, C.–FICCARELLI, G.–TORRE, D. 1982. Table of the Stratigraphic Distribution of Terrestrial Mammalian Faunas in Italy form the Pliocene to the Early Middle Pleistocene. – Geografia Fisica e Dinamica Quaternaria. *5.* pp. 55–58.

BACSÁK, GY. 1942. Die Wirkung der skandinavischen Vereisung auf die Periglazialzone. Bp., 86 p.

BALOGH, J. 1997. The Blake paleomagnetic event, in the Basaharc Double paleosol complex of loess profiles Paks, Mende and Basaharc, Hungary. – In: BREMER, H.–LÓCZY, D. (eds.): Geomorphology and changing environments in Central Europe. Berlin-Stuttgart, Gebrüder Borntraeger. pp. 85–93. (Zeitschrift für Geomorphologie. Supplementband. 110.)

BALOGH J. 2000. A Brunhes paleomágneses időszak változásainak vizsgálata a Paks, Mende, Basaharc feltárások BD fosszilis talajaiban. – In: FÁBIÁN SZ. A.–TÓTH J. (szerk.): Geokronológia és domborzatfejlődés. Pécs. – Pécsi Tudományegyetem Természettudományi Kar. pp. 15–22.

BEHRE, K.-E. 1989. Biostratigraphy of the last glacial period in Europe. – Quaternary Science Reviews. *8.* pp. 25–44.

BERECZ, I.–BOHÁTKA, S.–LANGER, G.–SZÖŐR, GY. 1983. Quadrupole mass spectrometer coupled to derivatograph. – International Journal of Mass Spectormetry and Ion Physics. *47.* pp. 273–276.

BLASKOVIĆ, V. 1957. Gospodarski-geografske oznake. – In: Otok Susak. Zagreb (Dela JAZU Knj. 49.)

BLOHM, M. 1974. Sedimentpetrographische Untersuchungen am Neusidler See (Österreich). Inaugural Dissertation zur Erlangung der Doktorwürde der Naturwissenschaftlichen Gesamtfakultat. Heidelberg, 72 p.

BOGNAR, A. 1979. Distribution properties and types loess and loess like sediments in Croatia. – Acta Geologica Academiae Scientiarium Hungaricae. *22.* 1–4. pp. 267–286.

BOGNAR, A. 1987. Reljef i geomorfolške osobine Jugoslavije. Veliki geografski atlas Jugoslavije. Zagreb, SN Liber.

BOGNAR, A. 1998. The "Loess Islands" of the Kvarner region, natural history of the Rijeka region. Rijeka, Natural History Museum Rijeka. pp. 303–322.

BOGNAR, A.–KLEIN, V.–TONČIĆ-GREGL, R.–ŠERCELJ, A.–MAGDALENIĆ, Z.–CULIBERG, I. M. 1983 Kvartarne naslage otoka Suska i Baške na otoku Krku i njihovo geomorfološko značenje u tumačenju morfološke evolucije Kvarnerskog prostora. – Geografski Glasnik. *45.* pp. 7–32.

BOGNAR, A.–KLEIN, V.–TONČIĆ-GREG, I. A.–ŠERCELJ, A.–MAGDALENIC, Z.–CULIBERG, M. 1989. Geomorphological and Quaternary-Geological Properties of the Island "Susak". – Geographical Papers. 7. Zagreb, pp. 7–24.

BOGNÁR, A.–PREGOLOVIÆ, E.–KLEIN, V.–KRUŠLIN, ˝.–MESIÆ, I.–ŒARKOTIŒLAT, M.–HROMATKO, B. 1994. Regionalverbreitete Paleoklesschichten NW-Kroatiens und ihre geomorphologische Bedeutung für die Erklärung der Morphogenese des Reliefs und der neotektonischen Bewegung. – Acta Geogr. Croatia, 29. pp. 7–18.

BOGNÁR, A.–ZÁMBÓ L. 1992. Some New Data of the loess genesis on Susak Island. – In: BOGNAR, A. (ed.): Proceedings of the International Symposium "Geomorphology and Sea". University of Zagreb, Croatia. pp. 65–72.

BOMER, B. 1978. Le bassin de l'Ebre et ses bordures montagneuses; étude géomorphologique. – Unpublished thesis, Université de Caen, 662 p.

BORHIDI A. 199? Kiegészítések a botanikai nomenklaturához. Kézirat.

BROSCHE, K. U.–MOLLE, H. G. 1975. Morphologische Untersuchungen im Nordöstlichen Matmata Vorland (Sudtunisien). – Eiszeitalter und Gegenwart 26. pp. 218–240.

BRUINS, H. J.–YAALON, D. H. 1979. Stratigraphy of the Netivot Section in the Desert Loess of the Negev (Israel). – Acta Geologica Academiae Scientiarium Hungaricae. 22. 1–4. pp. 161–171.

BRUNNACKER, K. 1969a. Affleurements de loess dans les régions nord-méditerranéennes. – Revue de Géographie physique et Géologie dynamique, 2 (11), 3, pp. 325–334.

BRUNNACKER, K. 1969b. Observations en Espagne et en Grèce. – In: La stratigraphie de loess d'Europe. Bulletin. Association Française pour l'étude du Quaternaire. Supplement, pp. 67–69.

BRUNNACKER, K –LOSEK, V. 1969. Lössorkanmen in Südost-Spanien. – Zeitschrift für Geomprhologie, NF, 13, pp. 297–316.

CARCAILLET, C.–THINON, M. 1996. Pedoanthracological contribution to the study of the evolution of the upper treeline in the Maurienne Valley (North French Alps): methodology and preliminary data. – Rev. Palaeobot. Palyn. 91. pp. 399–416.

CASTALDINI, D.–GASPERI, G.–PANIZZA, M. 1988. Tectonic evolution of the Modena Appennine margin in the middle pleicsotcene–holocene. – IGU, Guidebook for the excursions in the Toscana, Emilia and Veneto regions. Modena, Istituto di Geologia Universitá di Modena. pp. 83–87.

COLTORTI, M.–DRAMIS, F.–GENTILI, B.–PAMBIANCHI, G. 1979. The loess of the Central-Eastern Po valley. In: Proc. 15th. Meeting. Geomorphological Survey Mapping. Istituto di Geologia, Universitá degli Studi, Modena. pp. 205–212..

COUDÉ–GAUSSEN, G. 1991. The loess and loess-like deposits along the sides of the Western Mediterranean Sea: genetic and paleoclimatic significance. – Quaternary International. 5. pp. 1–8.

COUDÉ–GAUSSEN, G.–ROGNON, P. 1988b. Caractérisation sédimentologique et conditions paléoclimatiques de la mi°e en place de loess au Nord du Sahara à partir de l'exemple du Sud-tunisien. – Bulletin. Société géologique de France. 8. 6. pp. 1081–1090.

COX, A. 1968. Geomagnetic polarity intervals. – Journal of Geophysical Research. 73. pp. 32–47.

CREMASCHI, M. 1974. Manufatti del Paleolitico medio-inferiore provenienti da Monte Nettó di Brescia e loro aspetti con i depositi quaternari del colle. – Natura Bresciana. 11. pp. 41–57.

CREMASCHI, M. 1978. Unitá litostratigrafiche e pedostratigrafiche nei terreni quaternari pedeappenninici; loess e paleosuoli tra il fiume Taro ed il torrente Sollaro. – Geografia Fisica e Dinamica Quaternaria. 1. pp. 4–22.

CREMASCHI, M. 1979. The loess of the Central-Eastern Po valley. – Proc. 15th. Meeting. Geomorphological Survey Mapping. Modena, Istituto di Geologia, Universitá degli Studi. pp. 103–115.

CREMASCHI, M. 1987a. Loess deposits of the Plain of the Po and of the adjoining Adriatic Basin (Northern Italy). – In: PÉCSI, M.–FRENCH, H. M. (eds.): Loess and Periglacial Phenomena. Bp., Akad. Kiadó, pp. 125–140. (Studies in Geography in Hungary 20.)

CREMASCHI, M. 1987b. Paleosols and vetusols in the central Po Plain (Northern Italy); a study in Quaternary geology and soil development. – Thesis, University of Amsterdam, ed. Unicoploi, Milano, 306 p.

CREMASCHI, M. 1988. The loess in Northern and Central Italy: A Loess Basin between the Alps and the Mediterranean Region. September–October 1988. – In: Guide Book, Preliminary edition. INQUA Commission on Paleogeography, C. N. R., Milano, Centro di Studi Stratigraphica et Petrographica Alpi Centro. 176 p.

CREMASCHI, M. 1991. Stratigraphy and Paleoenvironmental significance of the loess deposits on Susak Island (Dalmatian Archipelago). – Quaternary International. *51.* pp. 97–106.

CREMASCHI, M. 1991. The loess in Northern and Central Italy: a loess basin between the Alps and the Mediterran Region. Milano, INQUA Commission of Loess. Quaderni di Geodinamica Alpina e Quarternaria.

CREMASCHI, M.–PERETTO, C. 1977. Il paleolitico dell'Emilia e Romagna. – Atti 19° Riun. Scient. I. I. P. P. Emilia Romagna (1975), pp. 15–78.

CREMASCHI, M.–GASPERI, G.–LOSACCO, S.–TOSATTI, G.–ZAROTTI, L. 1979. The loess of the Central-Eastern Po valley. – Proc. 15th. Meeting. Geomorphological Survey Mapping. Modena, Istituto di Geologia, Universitá degli Studi. pp. 255–267.

CREMASCHI, M.–GUERRESCHI, A.–LEONARDI, P.–PERETTO, C.–SALA, B. 1978. L'arte mobiliare del Riparo Tagliente. – Arte Preistorica nell'Italia settentrionale. Verona. pp. 35–40.

CSONGOR, É.–SZABÓ, I.–HERTELENDI, E. 1982. Preparation of counting gas of proportional counters for radiocarbon dating. – Radiochemical Letters. *55.* pp. 303–310.

DE BRUIJN, H. 1983. Remains of the mole-sat Microspalaxodessanus Topashevski, from Karaburum (Greece, Macedonia) and the family spalacidae. – Kan. Ned. Akad. V. Wetenschappen, Proc. *87.* 4. pp. 417–427.

DE GIULI et al. 1987. Paleogeography and mammal faune in the Apulo-Dalmatic Area. Giorn. Geol. Bologna. 48. (1) (in press)

DÉBÉNATH, A.–DIBBLE, H. L. 1994. Handbook of Paleolithic Typology. Volume One. Lower and Middle Paleolothic of Europe. Philadelphia. University Museum. University of Pennsylvania.

DUBAR, M. 1979. Les caractères sédimentologiques des terrasses fluviatiles et leur couverture lumoneuse en Moyenne Durance. – Bulletin. Association Française pour l'Étude du Quaternaire. *60.* 3. pp. 109–120.

EMILIANI, C. 1955. Pleistocene temperatures. – Journal of Geology. *63.* pp. 538–578.

EVANS, P. 1972. The Present Status of the Determination in the Quaternary (with Special Reference to the Period between 70 000 and 1 000 000 years ago) 24th IGS. – Section 12. – Quaternary Geology. pp. 16–21.

FOLK, R. L.–WARD, W. C. 1957. Brazos River bar: a study in the significance of grain size paramters. – Journal of Sedimentary Petrology, *27.* pp. 3–26.

FÖLDVÁRI M. 1980. Magánközlés.

FÖLDVÁRINÉ-VOGL, M. 1958. The role of differential thermal analysis in mineralogy and geological prospecting. – Acta Geologica Academiae Scientiarum Hungaricae. *5. 1.* pp. 1–102.

FRAENZLE, O. 1969. Les loess rissiens et wurmiens de l'Italie du Nord. La stratigrafie des loess d'Europe. – Bulletin Association. Française et. Quaternaire. Supplement. pp. 93–97.
FRITZ, P.–FONTES, J. CH. (eds.) 1989. Handbook of Environmental Isotope Geochemistry. Vol. *3.* The Marine Environment, A. Amsterdam–Oxford–New York–Tokyo, Elsevier, pp. 1–428.
GASPERI, G. 1988. Geological sketch in the Northern Appennines. Joint Meeting on Geomorphological Hazards. Firenze–Modena–Padova 1988. – Guidebook for the excursions in the Toscana, Emilia and Veneto regions. pp. 78–80.
GAZZI, P.–ZUFFA, GG.–GANDOLFI. G.–PAGANELLI, L. 1973. Provenienza e dispersione litoranea delle sabbie delle speagge adriatiche fra le foci dell' Isonzo e del Foglia. – Memorie della Societá Geologica Italiana. *12.* pp. 1–37.
GENCSI, L.–VANCSURA, R. 1997. Dendrológia. Bp., Mezőgazda Kiadó, 728 p.
HAAS J. 1998. Karbonátszedimentológia. Bp., ELTE Eötvös Kiadó, 147 p.
HÁMOR, G.–RAVASZ-BARANYAI, L.–HALMAI, J.–BALOGH, K.–ÁRVA-SÓS, E. 1987. Dating of miocene acid and intermediate volcanic activity in Hungary. – MÁFI Évkönyve *70.* pp. 149–154.
HELLER, F.–MEILI, B.–WANG, J.–LI, H.–LIU, T. 1987. Magnetization and sedimentation history of loess in the Central Loess Plateau of China. – In: LIU, T. (ed.): Aspects of loess research. China. Beijing, Ocean Press. pp. 147–163.
HERTELENDI, E. 1990 Sources of random error in the Debrecen radiocarbon laboratory. – Radiocarbon. *32.* 3. pp. 283–287.
HERTELENDI. E.–CSONGOR, É.–ZÁBORSZKY, L.–MOLNÁR, I.–GÁL, I.–GYŐRFFY, M. NAGY. S. 1989. Counting system for high precision C-14 dating. – Radiocarbon. *34.* pp. 399–408.
HERTELENDI, E.–GÁL, J.–PAÁL, A.–FEKETE, S.–GYŐRFFY, M.–GÁL, I.–KERTÉSZ, ZS.–NAGY, S. 1987. WAND, U.–STRAUCH, G. (eds.): Stable isotope mass spectrometer. Fourth working meeting isotopes in nature. Akademie der Wissenschaften der DDR Zentralinstitut fr Isotopen und Strahlenforschung, Leipzig *1,* pp. 323–.
HEY, R. W. 1972. The Quaternary and Palaeolithic of northern Libya. – Quaternaria. 6. pp. 435–449.
HUDSOW, J. D. 1977. Stables isotopes and limestone lithification. – Journ. Geol. Soc. *133.* pp. 637–660.
HUM, L.–SÜMEGI, P. 2000. Cyclic Climatic Records in Loess-Palaeosol Sequences in Southeastern Transdanubia (Hungary) on the Basis of Sedimentological, Geochemical and Malacological Examination. Geolines. *11.* pp. 99–101.
INIZAN, M. L.–REDURON–BALLINGER, M.–ROCHE, H.–TIXIER, J. 1999. Technology and Terminology of Krapped Stone. Nanterre, CREP.
JÁNOSSY, D. 1972. Middle Pliocene Microvertebrate Fauna from the Osztramos Loc. 1. – Ann. Hist.-nat. Mus. Nat. Hung. *64.* pp. 27–52.
JÁNOSSY D. 1979. A magyarországi pleisztocén tagolása gerinces faunák alapján. Bp., Akad. Kiadó, 207 p.
KÉZDI Á. 1961. Talajmechanikai prakticum. Bp., Tankönyvkiadó, 208 p.
KLIMES-SZMIK A. 1962. A talajok fizikai tulajdonságainak vizsgálata. A talaj szemcseösszetétele. – In: BALLENEGER, R.–di Gleria M. (szerk.): Talaj- és trágyavizsgálati módszerek. Bp., Mezőgazdasági Kiadó, pp. 83–92.
KORDOS L. 1988. A spalax nemzetség (Rodentia) európai megjelenése és a plio–pleisztocén határkérdés. – MÁFI Évi Jelentése 1986-ról. pp. 469–491.
KOVÁCS-PÁLFFY P. 1998. A Susak-szigeti üledékminták röntgenvizsgálata. – MÁFI. Röntgenlabor (kéziratban).
KRETZOI M. 1954. Jelentés a kislángi kalabriai (villafrankai) fauna feltárásáról. – MÁFI Évi Jelentése az 1953. évről. I. pp. 213–265.

KRETZOI M. 1969. A magyarországi quarter és pliocén szárazföldi sztratigráfiájának vázlata. – Földrajzi Közlemények. 17. (93.). *2.* pp. 197–204.

KRETZOI, M.–MÁRTON, P.–PÉCSI, M.–SCHWEITZER, F.–VÖRÖS, I. 1982. Pliocene–Pleistocene piedmont correlative sediments in Hungary (based on lithological, geomorphological, paleontological and paleomagnetic analyses of the exposures in the opencast mine at Gyöngyösvisonta). In: Pécsi M. (ed.): Quaternary Studies in Hungary. Bp., Geogr. Res. Inst HAS. pp. 43–73. (Elmélet-módszer-gyakorlat 24.)

KROLOPP, E. 1983. Biostratigraphic division Hungarian Pleistocene Formations according to their Mollusc fauna. – Acta Geologica Academiae Scientiarium Hungaricae. *26.* 1–2. pp. 62–89.

LANGIER-KUZNIAROWA, A. 1967. Termogramy mineralow ilastich. Warszawa, Wydawnictwa Geologiczne.

LEROI-GOURHAN, A. 1998. Dictionaire de la Préhistoire. Paris, Presses Universitaires de France.

LIPTAY, G. 1971–1976. Atlas of thermoanalytical curves. Vol. 1–5. Bp., Akad. Kiadó.

LIU, T. et al. 1966. The Composition and Texture of Loess. Beijing, Science Press.

LIU, T. et al. 1985. The Loess Deposits of China. Beijing, Science Press.

LIU, Y. and AN, Z. 1979. The guest for series of nature environmental changes during the Brunhes Epoch. Tongbao, Kexue. *24.* pp 221–224.

LIU, Y.–AN, Z. 1981. Pleistocene climatic cycles and variation of $CaCO_3$ contents in a loess profile. – Sci. Geol. Sinica. *2.* pp. 122–131.

LOWE, J.J.–WALKER, M.J.C. 1997 Reconstructing Quaternary Environments. Essex, Addison Wesley Longman Ltd.

LU, YANGCHOU-AN ZHISHENG 1981. Pleistocene climatic cycles and variation of $CaCO_3$ contents in a loess profile. Sci. Geol. Sinica *2.* pp. 122–131.

MACDONALD, G. M.–LARSEN, C. P. S.–SZEICZ, J. M.–MOSER, K. A. 1991. The reconstruction of boreal forest fire history from lake sediments: a comparison of charcoal, pollen, sedimentological, and geochemical indices. – Quaternary Science Reviews. *10.* 1. pp. 53–71.

MACKENZIE, R. C. 1962. Scifax Differential Thermal Analysisi Data Index. London, Cleaver-Hume Press.

MACKENZIE, R. C. 1970. Differential Thermal Analysos. London–New York, Academic Press.

MANZE, U.–VOGEL, I. C.–STREITZ, R.–BRUNNACKER, K. 1974. Isotopenuntersuchungen zum Kalkumsatz im Löß. – Geologische Rundschau. *63.* pp. 885–897.

MARKOVIĆ–MARJANOVIĆ, J. 1966. Stratigrafija ljosa ostrova Susak i severnoj časti adriatičeskova morja. – Bjuletenj komisiji po izučeniju četvertičnovo perioda. No *31.* Moskva.

MARKOVIĆ–MARJANOVIĆ, J. 1969. Les profils de loess du Bassin pannonique. Région classique du loess de Yougoslavie. In: La stratigraphie des loess d'Europe. Bulletin. Association Française pour l'étude du Quaternaire. Supplement, pp. 165–170.

MÁRTON, P.–PÉCSI, M.–SZEBÉNYI, E.–WAGNER, M. 1979. Alluvial loess (infusion loess) on the Great Hungarian Plain – its lithological, pedological, stratigraphical and paleomagnetic analysis in the Hódmezővásárhely Brickyard exposure. – Acta Geologica Academiae Scientiarium Hungaricae. *22.* 1–4. pp. 539–555.

MELIK, A. 1952. Jugoslavija zemljopisni pregled. Zagreb, Školska knijiga. 463 p.

MENDOZA ANAYA, D.–CARAPIA MORALES, L.–RODRÍGUEZ LUGO, V.–TORRES MONTES, L.–FRANCO VELÁZQUEZ, F.–LEE WHITING, T. AS. 2000. Analysis by MEB, EDS and XRD of Samples of Wall Bricks, Slag and Minerals Belonging to Remains of a Possible Metal Smelting Furnace of the Colonial Period from Jalenton, Chiapas, Mexico. Absracts of 32nd Archaeometry Symposium, 201 p.

MILANKOVITSCH, M. 1930. Mathematische Klimalehre und astronomische Theorie der Klimaschwankungen. – In: KÖPPEN, W.–GEIGER, R. (eds.): Handbuch der Klimatologie I. Berlin, Gebr. Borntraeger. pp. 1–176.

MÜCHER, H. J.–SEVINK, J.–BERGKAMP, G. and JONEJANS, J. 1988. A pedological and micromorphological study on loessial mediterranean deposits near Gerona, NE-Spain. – In: Abstract, INQUA Commission on Loess – INQUA Commission on Paleogeography. Verona, C. N. R. Centro di Studii Stratigraphica et Petrographica Alpi Centro, Milano.

NIKIFOROVA, K. V.–KIND, N. V.–KRASNOV, I. I. 1984. Chronostratigraphic scale of the Quaternary. In: Quaternary geology and geomorphology. International Geological Congress, XXXVIIth Session, Section C. 03. Report of the Soviet geologists. Vol. 3. Moscow, Nauka. pp. 22–32.

OTOK SUSAK, 1957. Djela Jugoslavenske Akademije Znanosti i Umjetnosti, Knjiga 49, Zagreb.

PANIZZA, M. 1968. L'evoluzione geomorfologica ed idrografica del territorio di Pavullo nel Frignano (Appennino Modenese). – Atti. Soc. Nat. e Mat. di Modena, 99. 14 p.

PANIZZA, M.–PAPANI, G. 1979. The neotectonics of the Reggio-Emilia Appennines. The loess of the Central-Eastern Po valley. – Proc. 15th. Meeting. Geomorphological Survey Mapping. Istituto di Geologia, Universitá degli Studi, Modena. pp. 129–138.

PAULIK F.–PAULIK J. 1963. Termoanalízis. Bp., Műszaki Könyvkiadó. 280 p.

PÉCSI M. 1967 A löszfeltárások üledékeinek genetikai osztályozása a Kárpát-medencében. – Földrajzi Értesítő. 16. 1. pp. 1–18.

PÉCSI M. 1993. Negyedkor és löszkutatás. Bp., Akadémiai Kiadó. 375 p.

PÉCSI M. 1997. Lösz- és őstalajsorozatok és a negyedidőszaki ősföldrajzi változások kutatásának elvi, módszertani kérdései. In: Haas J. (szerk.): Fülöp József-emlékkönyv. Bp. Akad. K. 263–279.

PÉCSI M.– HELLER F.–SCHWEITZER F–BALOGH J.–DI GLÉRIA M.– HAVAS J. 1995. A new loess–paleosol sequence on terraced geomorphic surfaces. – Loess InForm 3. Bp., MTA FKI, pp. 63–79.

PÉCSI M.–RICHTER, G. 1996. Lösz. Berlin–Stuttgart, Gebrüder Borntraeger, 391 p.

PÉCSI M.–PÉCSINÉ DONÁTH É.–SZEBÉNYI E.–HAHN Gy.–SCHWEITZER F.–PEVZNER M. A. 1977. Magyarországi löszök fosszilis talajainak paleogeográfiai értékelése és tagolása. – Földrajzi Közlemények. 25. (101.) 1–3. pp. 128–137.

PÉCSI M.–PEVZNER, M. A 1974. Paleomagnetic measurements in the loess sequences at Paks and Dunaföldvár, Hungary. – Földr. Közl. 22 (98.) 3. pp. 215–219.

PÉCSI M. 1968. Loess: Fairbridge, R. W. ed. The Encyclopedia of Geomorphology. – Dowden, Hutchinson and Ross, Inc., Strassburg, pp. 674–678.

PÉCSI M. 1993. Quaternary and Loess Research. – Akadémiai Kiadó, Budapest, 375 p. (Hungar. with Engl. summary)

PÉCSI-DONÁTH É. 1979. Thermal investigation of the loesses and fossil soils of Paks. – Acta Geologica Academiae Scientiarium Hungaricae. *22*. 1–4. pp. 419–426.

PÉCSI-DONÁTH É. 1987. Mineralogical and granulometric analyses of the "old loess sequences" of Hungary. In: Pécsi M.–French, H. M. (eds.): Loess and periglacial phenomena. Symposium of mission for Periglacial Studies: Field and laboratory experimentatin. Normandy–Yersey–Brittany. Caen, August 1986. Bp., Akad. K., pp. 43–50.(Studies in Geography in Hungary 20.)

PEVZNER, M. A.–VANGENGEIM, E. A. 1985. On understanding the range and stratigraphic position of the Pannonian. In: Kretzoi M.–Pécsi M. (eds.) Problems of the Neogene and Quaternary. Bp., Akad. K. pp. 65–88. (Studies in Geography in Hungary 19.)

ROGLIÆ, J. 1949. Geomorfološka istra•ivanja na Kvarnerskim otocima i Zadarskom primorju, JAZU, Zagreb.

RÓNAI A. 1972. Negyedkori üledékképződés és éghajlattörténet az Alföld medencéjében. – MÁFI. Évkönyve 56. 1. Budapest. 421 p.

RÓNAI A. 1985. Az Alföld negyedidőszaki földtana. – Geologica Hungarica. Ser. Geol. 21. 445 p.
RÓNAI, A. 1985. Limnic and terrestrial sedimentation and the N/Q boundary in the Pannonian Basin. – In: KRETZOI, M.–PÉCSI, M. (eds.) Problems of the Neogene and Quaternary. Bp., Akad. Kiadó. pp. 21–49. (Studies in Geography in Hungary 19)
RÓZSA, P. 1998. Report on microscopic studies of concretions from Susak Island (Croatia). Dept. Min. Geol. Univ. Debrecen. Manuscript. (in Hungarian)
RUDNER, Z.E.–SÜMEGI, P. 2001. Recurring taiga forest-steppe habitats in the Carpathian Basin. – Quaternary International. *76–77.* pp. 177–189.
RUGGIERI, G.–SPROVIERI, R. 1977. A revision of Italian Pleistocene stratigraphy. – Geologia Romania. *16.* pp. 131–139.
SAJÓ I. 1973. Komplexometria. 3. jav. bőv. kiad. Bp., Műszaki Kiadó. 291 p.
SALA, B. 1990. Loess fauna in deposits of shelters and caves in the Veneto region and examples in the other region of Italy. – In: CREMASCHI, M. (ed.): The loess in Northern and Central Italy. Milano, INQUA Commission on Loess, pp. 139–149.
SCHNEIDERHÖHN, P. 1954. Eine vergleichende Studie der Methoden zur quantitativen Bestimmung von Abrundung und Form an Sand Körner. – Heidelberg Beitr. Miner. Petrogr. *4.* pp. 172–191.
SCHÖNHALS, E. 1955. Kennzahlen für den Feinheitsgrad des Lösses. – Eiszeitalter und Gegenwart. *6.* pp. 133–147.
SCHWEINGRUBER, F.H. 1978. Microscopic Wood Anatomy. Zürcher AG, CH-6301 Zug.
SCHWEINGRUBER, F.H. 1990. Anatomy of European Woods. Zürcher AG, CH-6301 Zug.
SCHWEITZER, F.–SZÖŐR, Gy. 1997. Geomorphological and stratigraphical significance of Pliocene red clay in Hungary. – In: BERMER, H.–LÓCZY D. (eds): Geomorphology and changing environments in Central Europe. Berlin, Stuttgart. Gebrüder Borntraeger. pp. 95–105. (Zeitschrift für Geomorphologie. Supplementband 110.)
SCHWEITZER, F. 1997. On late Miocene – early Pliocene desert climate in the Carpathian Basin. – In: BERMER, H.–LÓCZY D. (eds): Geomorphology and changing environments in Central Europe. Berlin, Stuttgart. Gebrüder Borntraeger. pp. 37–43. (Zeitschrift für Geomorphologie. Supplementband 110.)
SHACKLETON, N.J.–OPDYKE, N.D. 1973. Oxigen Isotope and Paleomagnetic Stratigraphy of Equatorial Pacific Core V28–238. Oxygen Isotope Temperature and Ice Volumes on a 105 Year and 106 Year Scale. – J. Quaternary Research. *3.* (1.). pp. 39–55.
SIEBERTZ, H. 1980. Die Bedeutung des Feinheitsgrades als geomorphologische Auswertungsmethode. – Eiszeitalter und Gegenwart, *32,* pp. 81–91.
SMITH, G. D. 1942. Illinois Loess, Variations in its Properties and Distribution. – Univ. Illinois Agricultural Experiment Station Bulletin, *490.* pp. 139–184.
SMYKATZ-KLOSS, W. 1964. Differential Thermo-Analysen von einigen Karbonat-Mineralen. – Beiträge zur Mineralogie und Petrographie *9.* pp. 481–502.
SOÓS L. 1943. A Kárpát-medence Mollusca-faunája. Bp., Akad. Kiadó.
STIEBER J. 1968 Anthrakotómia, kvarter kronológia és a hazai pleisztocén vegetáció. Akadémiai doktori értekezés. Bp., ELTE Növényszervezettani Tanszék, 395 p.
SÜMEGI P. 1989. Hajdúság felső-pleisztocén fejlődéstörténete finomrétegtani (üledékföldtani, őslénytani, geokémiai) vizsgálatok alapján. Egyetemi doktori értekezés, 96 p. Debrecen.
SÜMEGI P. 1997. Az ÉK-magyarországi löszterületek összehasonlító őskörnyezeti és sztratigráfiai értékelése. Kandidátusi értekezés, 120 p. Debrecen.
SÜMEGI P.–KROLOPP E. 1995. A magyarországi würm korú löszök képződésének paleoökológiai rekonstrukciója malakofauna alapján. – Földtani Közlöny. *125.* pp. 125–148.

SÜMEGI P.–KROLOPP E.–HERTELENDI E. 1998. A Ságvár-Lascaus interstadiális őskörnyezeti rekonstrukciója. – Acta Geographica, Geologica et Meteorologia Debrecina. *34.* pp. 151–166.

SÜMEGI, P.–RUDNER, Z. E. 2001. In situ charcoal fragments as remains of natural wild fires of Upper Würm in the Carpathian Basin. Quaternary International. *76–77.* pp. 165–176.

SZILÁRD J. 1983. Dunántúli és Duna–Tisza közi löszfeltárások új szempontú litológiai értékelése és tipizálása. – Földrajzi Értesítő. *32.* 1. pp. 109–165.

SZÖŐR, Gy. 1992. Termoanalitikai, kemofáciestani, paleobiogeokémiai megoldások. – MTA Doktori Értekezés. 139 p.

SZÖŐR, GY.–BOHÁTKA S. 1985. Derivatograph-QMS system in geochemical research. – Thermochimica Acta. *92.* pp. 395–398.

TRASK, D.P. 1931. Origin and Environment of Source Sediments of Petroleum. – Gulf Publish. Co. Houston, Texas.

VARGA Z. 1981. Elterjedési területek recens és történeti dinamikája. – Akadémiai Doktori Értekezés.

VELICHKO, A. A. 1990. Loess paleosol formations of the Russian plain. – Quaternary International. *7–8.* pp. 103–114.

WILLIS, K. J.–RUDNER, Z. E.–SÜMEGI, P. 2000. Full-glacial forests of Central and South Eastern Europe. – Quaternary Research. *53.* 2. pp. 203–213.

ZÁMBÓ, L. 1992. Factors Affecting Gully Development in Loess Areas, Hungary. – Taiyuan, China

Susak Island in the Adriatic Sea is a real attraction for geologists and geomorphologists. Our book makes the reader acquainted with its landform evolution over the past 5 million years. During most of the last one million year the surrounding area was part of the continent as the sea regressed from its northern basin. The latter was filled up with sediments by Po River and its tributaries. Winds had blown out fine-grained material of these muddy and sandy deposits and transported it to the island. From the falling dust loess was formed in a thickness of 50–98 m. This is how Susak Island was built up. Being like a chronicle of the Ice Age in the Adriatic, Susak loess sequence deserves attention of both science and public. With its conspicuous flora and fauna the island could be an ideal place for nature conservation of global significance.